Study on Enhancement of Vacuum Decay in Higher-Dimensional Theory

塚原, 壮平

Ph.D. Dissertation

Study on Enhancement of Vacuum Decay in Higher-Dimensional Theory

Sohei TSUKAHARA

Department of Physics
Graduate School of Science
Kyushu University

December, 2024

Abstract

String theory is widely regarded as a promising candidate for quantum gravity that naturally incorporates gravitational interactions. However, its vacuum structure is known to be extremely complicated. This complexity arises from the absence of a definitive guiding principle for compactifying extra dimensions in higher-dimensional theories. As a result, it has been suggested that an enormous number of vacua might emerge. In this scenario, transitions between vacua are expected to occur universally.

Many scenarios of vacuum decay are premised on the nucleation of bubbles in a homogeneous false vacuum. However, in nature, many examples are known where the presence of impurities catalyzes phase transitions. Similar phenomena have been observed in high-energy physics, where topological solitons or black holes can enhance phase transitions in the early universe. Since such impurities are expected to exist universally in realistic models involving symmetry breaking, examining the inhomogeneous nucleation of bubbles influenced by these impurities can be regarded as a more natural direction. Thus, when considering stringy vacuum decay in higher dimensions, there remains room to account for impurities and phenomena that can enhance decay. Such enhancement of decay is also intriguing from the perspective of formulating the mathematical conditions for effective theories coupled with gravity. In the bottom-up approach known as a Swampland program, various conjectures and constraints have been proposed based on empirical insights from grand unified theories and cosmology. Recent developments in the Swampland program suggest that dS vacua consistent with quantum gravity must, at least, be metastable and decay sufficiently quickly. Under this conjecture, most metastable vacua in low-energy effective theories are thought to be incompatible with quantum gravity. However, if contributions from impurities or singularities could enhance the instability of the system, it might be possible to construct UV-consistent de Sitter vacua within an effective theory. In light of these considerations, we discuss two objects, Dp-branes, and singular instantons, as potential objects for enhancing vacuum decay in higher-dimensional theories.

First, we discuss the enhancement of instability due to Dp-branes as a catalytic effect specific to string theory. Dp-branes are higher-dimensional objects in string theory, frequently utilized to construct metastable vacua. In this study, we construct a geometrically metastable vacuum by wrapping D5-branes and anti D5-branes on a higher-dimensional manifold with singularities. We also consider wrapping D3-branes in the internal space. These D3-branes dissolve into the domain wall D5-branes, forming bound states. We generalize the calculation method for the fluctuation operator and derive an exact 1-loop expression for the decay rate using the WKB approximation. Numerical calculations based on this expression confirm that, within a reliable parameter region for the approximation, increasing the number of D3-branes reduces the life-time of the metastable vacuum. Fur-

thermore, we approximated the life-time in the limit where the potential barrier vanishes by applying results for an anharmonic oscillator and compared this with constraints imposed by the trans-Planckian censorship conjecture, one of the Swampland conjectures. As a result, we found that under reasonable assumptions about the size of the compactification space, the critical life-time can satisfy the constraints from the conjecture when the string coupling is less than $\mathcal{O}(1)$.

The second theme is the enhancement of the decay rate due to singularities in instanton solutions. Higher-dimensional vacua with compactified dimensions possess a non-perturbative decay channel where a literal "bubble of nothing," devoid of spacetime degrees of freedom, expands. The instanton solution mediating this decay corresponds to a Euclidean higher-dimensional black hole solution, which is known to exhibit a conical singularity at the location corresponding to an event horizon of the original black hole solution. In ordinary discussions, we impose a proper condition on the periodicity of the imaginary time to ensure smoothness at the horizon, resulting in an instanton spacetime without such singularities. However, since the crucial physical quantity in vacuum decay physics is the decay rate, instanton solutions with singularities may also be admissible if their contribution to the decay rate remains finite. In this study, we examine the decay mediated by singular instantons in the simplest higher-dimensional vacuum, the five dimensional Kaluza-Klein vacuum, and derive the contribution of the conical singularity to the bounce action based on the conical deficit regularization. The contribution from the singularity is negative, acting to reduce the bounce action. Our analysis demonstrates that decay mediated by singular instantons can indeed have a higher decay rate, potentially making it the dominant decay process. Additionally, we reconstruct the bounce action using thermodynamic functions and discuss the thermodynamic interpretation of how singularities in instanton solutions enhance the decay.

This thesis is based on the following papers:

- S. Tsukahara, "*Life-time of metastable vacuum in string theory and trans-Planckian censorship conjecture*," JHEP 10 (2023) 109, arXiv:2305.00781[hep-th].
- Y. Ookouchi, R. Sato and S. Tsukahara, "*Decay of Kaluza-Klein Vacuum via Singular Instanton*," arXiv:2404.13917[hep-th].

In addition, appendix also includes the study based on the following paper:

- S. Tsukahara, "*On Stabilization of Magnetically Charged Brane Shell and Over-extremality*," arXiv:2408.08798[hep-th].

Acknowledgments

First, I would like to express my deepest gratitude to my academic supervisor, Prof. Yutaka Ookouchi. Through the Ph.D. course, he provided invaluable guidance and support, enabling me to devote myself wholeheartedly to my research. Without the daily discussions with him, it would have been challenging to bring my research to fruition. I would also like to thank my collaborator, Mr. Ryota Sato, for the daily discussions. Our regular discussions on the study of singular instantons significantly deepened my understanding of this topic. Additionally, I would like to express my special thanks to Dr. Yuri Okubo, who was a member of our research group. Although we did not collaborate directly, our daily discussions on physics served as a driving force in advancing my research.

I am also grateful to Prof. Hiroshi Suzuki and Prof. Yumi Kanno for the preliminary examinations. They provided many valuable comments on my research. I owe special thanks to Prof. Suzuki for serving on my advisory committee throughout the Ph.D. course. Furthermore, I would like to express my gratitude to Prof. Shotaro Naganuma, who also served on my advisory committee.

I deeply appreciate the advice I received from the faculty members of the laboratory, including Prof. Koji Harada, Prof. Kentaro Kojima, Prof. Kenichiro Nakazato, and Prof. Tokuro Fukui. Their broad knowledge of particle physics beyond elementary particle theory greatly inspired me and helped deepen my research. I am also grateful for their support in my daily life. I also thank my laboratory colleagues, Mr. Yin Qiang, Mr. Yuki Yamamoto, Mr. Ryuta Sugiyama, Mr. Yusuke Ikebe, Mr. Hayato Ogata, and Mr. Mahiro Yamasaki, for their daily discussions. I am also grateful to the former members of the laboratory, including Prof. Shuichiro Tao, Dr. Issei Koga, Mr. Shunsuke Taniwaki, Dr. Carolina Sayuri Takeda, and Mr. Yusuke Enomoto.

I would like to thank the Kyushu University Leading Human Resources Development Fellowship Program for its financial support. The program enabled me to fully dedicate myself to my studies throughout the Ph.D. course. I am particularly grateful to Prof. Kazuhiro Yamamoto for his advice on my research and career plans during the program's regular consultations.

Finally, I express my heartfelt gratitude to my family, who gave me the opportunity to pursue my studies and generously offered their encouragement, and to my partner, Kanna, for her support.

Contents

List of Figures

List of Tables

Chapter 1

Introduction

The Standard Model (SM) is one of the most successful theories in particle physics, providing an extremely precise description of the interactions among fundamental particles such as quarks, leptons, gauge bosons, and the Higgs boson. Its relevance is even more certain with the direct observation of the Higgs boson by the Large Hadron Collider in 2012 [4, 5]. However, the SM also leaves several challenges unresolved. An important issue is that while the SM effectively explains the electromagnetic interaction, the strong interaction, and the weak interaction, it does not contain the gravitational interaction. Since the coupling constant of gravity has a mass dimension, its naive quantization leads to a non-renormalizable field theory.

A quantum theory of gravity is an essential framework for understanding the physics of the early universe. In the modern standard cosmological model, it is believed that the universe underwent an exponential expansion called inflation in its early stages [6–9]. This inflationary theory provides a compelling explanation for the uniformity, isotropy, and flatness of the universe, as suggested by observations of the Cosmic Microwave Background (CMB) [10]. In the inflationary paradigm, quantum fluctuations that existed in the extremely early universe were stretched by the rapid expansion, eventually shaping the universe we observe today. Numerous inflationary models continue to be proposed [11–17], making this a major topic in modern cosmology. Furthermore, modern cosmology has been advancing efforts to understand how the universe emerged before inflation. A leading hypothesis posits that the universe originated from a quantum process out of a state of "nothing" [18, 19]. Therefore, a quantum gravity (QG) beyond the SM is indispensable to comprehend the dynamics of the early universe.

String theory is considered to be the best candidate for the QG. String theory is a quantum theory that takes one-dimensional string-like objects as its most fundamental constituents and describes gravitational interactions through the propagation of closed strings [20, 21]. While this theory is one of the most extensively studied candidates for a Beyond Standard Model capable of explaining gravity, its vacuum structure is known to be extraordinarily complex. In string theory, the background geometry should be ten dimensional spacetime so as to be consistent with quantum theory. To reproduce a cosmological model as a low-energy effective theory, we must compactify the six dimensions. However, no fundamental guiding principle has yet been identified to single out a unique vacuum, resulting in the allowance of an enormous number of vacua[1] [29–31].

[1]This kind of complex structure of vacua also appears at the SM. Recent precision measurements of

The situation where an enormous number of vacua exist is referred to as *landscape*. Under the landscape picture, quantum transitions between metastable vacua are expected to occur universally. Therefore, to advance realistic model building, it is necessary to investigate the inherent instabilities in the models. For example, one of the representative phenomena of vacuum decay in string theory is *brane-flux annihilation* [32, 33]. This dynamics can be understood as a generalized Schwinger effect, where background flux collapses through the formation of a spherical domain wall, known as a Brown-Teitelboim bubble. Moreover, higher-dimensional vacua with compactified dimensions exhibit unique decay phenomena. Such phenomenon is known as the *bubble of nothing* (BoN), a non-perturbative decay channel where, as the name suggests, a bubble devoid of spacetime degrees of freedom expands [34].

In many discussions of vacuum decay, including the examples mentioned above, the formation of true vacuum bubbles in a homogeneous false vacuum is typically considered. On the other hand, in nature, it is well-known that impurities can enhance phase transitions in various systems. Representative examples include enhanced bubbling around sand grains in carbonated water and condensation around dust particles in the air. Similar phenomena have also been confirmed in field and gravitational theories through several specific examples. The idea of catalysis in field theory was first introduced in the context of decay enhancement caused by monopoles in grand unified theories [35, 36]. Subsequently, it has been shown that other topological solitons and compact objects can similarly induce catalytic effects [37–46]. Since solitonic objects naturally emerge after symmetry breaking, it is reasonable to consider inhomogeneous vacuum decay when phase transitions are assumed to occur in high-energy scale. In gravitational theory, black holes have also been suggested to act as catalysts [47, 48], significantly shortening the life-time of the Higgs vacuum [49–51]. Given these effects, we find room to consider the role of impurities and phenomena that enhance decay when constructing models in higher dimensions.

The enhancement of vacuum decay is also intriguing from the perspective of consistency with QGs in effective field theory (EFT). In recent years, significant attention has been drawn to the *Swampland program*, which aims to identify the necessary conditions that EFTs coupled with gravity must satisfy [52–58] (see also [59–64] for reviews). This program originates from the theoretical outlook that the emergence of a vast number of vacua is a consequence of considering EFTs in the absence of gravity, as in the SM. When gravitational effects are taken into account, the set of realizable models is expected to be significantly constrained. The Swampland program seeks to find the mathematical boundary between EFTs consistent with QG at the UV scale and those not. Notably, the QG in question is not limited solely to string theory. In this context, the *swampland* is defined as a set of low-energy effective theories that fail to satisfy the consistency conditions [59]:

> The Swampland can be defined as the set of consistent effective field theories that cannot be completed into quantum gravity in the ultraviolet.

the top quark mass [22, 23] suggest that the electroweak vacuum of the Standard Model is metastable and could decay within a finite life-time. A full calculation of the metastability at one-loop level was done in [24] at first, then the life-time calculation has been updated [25–28]. This situation implies the existence of a true vacuum with even lower energy than the vacuum in which the SM resides.

The complementary set of the swampland, namely the set of EFTs consistent with QG at the UV scale, is referred to as the *landscape* (see Figure 1.1). The boundary between the swampland and the landscape depicted in Figure 1.1 represents the mathematical boundary that this program seeks to identify. In the Swampland program, conjectures are formulated based on empirical insights from previous efforts in unified theories and QG. These conjectures aim to impose constraints on the parameter space of EFTs. The constraints derived from each conjecture are referred to as swampland conditions. While these conditions are just conjectures, it is noteworthy that predictions proposed from different contexts often give similar constraints, leading to a general expectation of their validity. Indeed, for some conjectures or parts thereof, rigorous proofs have been provided [65, 66].

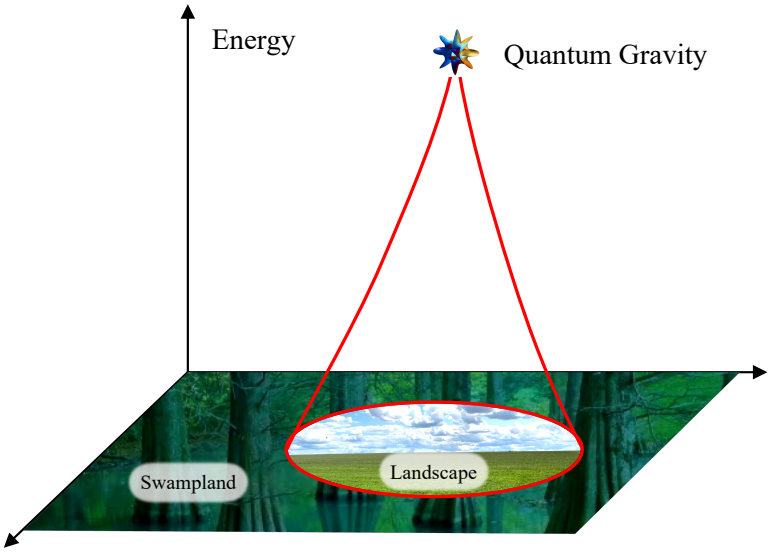

Figure 1.1: The conceptual diagram of the swampland and the landscape. Only parts of EFTs are consistent with QG at the UV scale, and the great majority are considered to belong to the swampland.

The Swampland conjectures provide several insights into the stability of EFTs coupled with gravity. The de Sitter (dS) conjecture is one of the most extensively studied conjectures, asserting that non-supersymmetric dS vacua must either be unstable or decay sufficiently quickly [55–57]. Similarly, the trans-Planckian censorship conjecture (TCC), recently proposed in the context of inflationary theory, imposes strong constraints on the life-time of metastable dS vacua [67–69]. If these conjectures are correct, metastable dS vacua with long life-times would not be UV consistent and could not be realized as EFTs of QG. Therefore, provided the Swampland program, some mechanisms that enhance vacuum transitions deserve consideration as potential avenues for expanding the possibilities of stringy model building.

In light of the above, gaining a deeper understanding of the contributions from objects that enhance vacuum decay is crucial for constructing more realistic models within the framework of string theory. This thesis focuses on mechanisms that enhance decay in higher-dimensional theories and examines two possibilities unique to higher-dimensional

frameworks: Dp-branes and singularities in instanton spacetimes.

Dp-brane

In string theory, higher-dimensional objects, called Dp-branes, exist in addition to strings. Dp-branes are extended objects in (p+1)-dimensional spacetime, defined as a subspace of the ten dimensional space on which the endpoints of open strings reside. [2] At first glance, Dp-branes may appear just static higher-dimensional objects. However, they possess various intriguing physical properties. Dp-branes are not merely extended constructs; they are dynamical objects capable of moving and interacting with each other, much like ordinary particles or solitons.

The gauge fields and scalar fields on the world volume of the brane describe the kinematics of Dp-branes. Therefore, Dp-branes have played a crucial role in many model buildings. Examples include the realization of the Standard Model gauge groups using intersecting Dp-branes [70–74] and brane inflation models [75–80], which represent new paradigms introduced by Dp-branes. For comprehensive reviews, see [81–83] and also refer to standard texts [80, 84–86]. A particularly noteworthy feature of Dp-brane dynamics is the process of pair annihilation and creation of Dp-branes. In field theory, the creation and annihilation processes of particles and antiparticles are universally present. Similarly, it is known that Dp-branes and anti Dp-branes can annihilate through the condensation of tachyon fields [87]. Furthermore, a lower-dimensional D(p-2)-brane is generated when tachyon condensation occurs between original Dp-branes and anti Dp-branes. We can interpret this lower-dimensional brane as a soliton in the effective theory.

Such solitonic branes can significantly affect the stability of vacua in string theory. Specifically, solitonic branes are expected to act as catalysts that enhance vacuum instability, similar to discussions in grand unified theories. Indeed, this idea has been incorporated into several phenomenological models in string theory. The most extensively studied example is D3-brane catalysis [88–90]. These D3-branes dissolve into higher-dimensional branes, forming bubbles in the false vacuum, creating a bound state. Such D3-branes are known to promote the vacuum decay of the original system and induce inhomogeneous decay.

In this thesis, we follow the above ideas to investigate the contributions of Dp-branes in metastable states. In string theory, a metastable state can be constructed by wrapping Dp-branes and anti Dp-branes on a manifold with singularities in its internal space [91–93]. We consider a scenario where D3-branes are also wrapped in the internal space, leading to inhomogeneous vacuum decay. This setup has already been explored in [88]. While the authors of [88] assumed the formation of large bubbles, this thesis provides a more refined analysis that remains valid even when the bubbles are small. We aim to investigate the impact of the D3-branes on the decay rate by the WKB analysis, incorporating the 1-loop fluctuation factor. We show that the WKB analysis breaks down when the catalytic effect is strong and the calculations are reduced to an anharmonic oscillator. Finally, we compare the life-time of the most unstable case, where the potential barrier disappears entirely with the constraints imposed by the TCC.

[2] The "D" in Dp-brane comes from the "D"irichlet boundary conditions imposed on the endpoints of open strings.

Singular Instanton

In gravitational theories, vacuum decay can be mediated by gravitational instantons. While standard discussions typically assume smooth instanton spacetimes, some scenarios consider decay mediated by instantons with singularities. Such *singular instantons* were introduced by Hawking and Turok [94, 95]. In the context of the Hartle-Hawking no-boundary proposal [18], the scenario for the creation of the universe, they employed singular instantons to discuss the emergence of more general open universes. Subsequently, Garriga improved the calculation of contributions from singularities, and further studies on open universes in this context were conducted by numerous authors [96–101].

Typically, the behavior of classical solutions near singularities is non-trivial, and it is generally assumed that the general relativistic description breaks down in such regions. However, what is crucial in discussing singular instantons is that even if an instanton solution possesses singularities, the Euclidean action can remain finite. Since the key physical quantity in the context of decay is the value of the Euclidean action, which determines the decay rate, instanton solutions with singularities may still be admissible if their Euclidean action is finite. Indeed, in the prescription improved by Garriga, the instanton spacetime near the singularity is regularized by cutting off the singular region and introducing a membrane[3], demonstrating that the contribution from the singularity becomes one-third of the Gibbons-Hawking-York (GHY) term. Another regularization method involves replacing the conical singularity with a smooth cap, known as conical deficit regularization [48, 102]. In this approach, the contribution of the deficit angle cancels between the Einstein-Hilbert (EH) term and the GHY term, resulting in a negative contribution to the Euclidean action from the singularity.

Turning to the decay of higher-dimensional vacua, the decay of compactified spacetimes via the BoN is a decay channel mediated by gravitational instantons. The instanton solution governing this decay corresponds to a Euclideanized higher-dimensional black hole solution and, in general, possesses a conical singularity at the location of the horizon in the original Lorentzian spacetime, similar to the instanton solutions discussed by the authors of [48]. In standard discussions, the periodicity of the imaginary time in the instanton solution is chosen appropriately to eliminate such singularities. However, according to the arguments presented in [48], the contribution from the singularity acts to lower the Euclidean action. This implies that decay mediated by singular instantons, where the smoothness condition is relaxed, could represent a dominant decay channel.

Considering the above, we investigate the bubble of nothing decay via singular instanton in this thesis. In our research, we relax the smoothness condition in the case of the decay of the simplest higher-dimensional vacuum, Kaluza-Klein vacuum ($\mathcal{M}_4 \times \mathbb{S}^1$), and derive the contribution of the conical singularity to the Euclidean action based on the conical deficit regularization [48, 102]. As expected, the conical singularity reduces the Euclidean action, implying that the decay via singular instantons is a more dominant decay channel. In addition, we reconstruct the Euclidean action with thermodynamic functions and attempt to give an interpretation for the enhancement of the decay via the singularity. As BoN is an interesting decay phenomenon unique to higher-dimensional theories, the detailed analysis of the decay process forges ahead of model buildings in the context of string theory.

[3] These branes are now referred to as End-of-The-World branes.

Organization of This Thesis

This thesis is organized as follows. In Chap. 2, we provide a review of the formulation of the vacuum decay by Euclidean path integral. In this chapter, we show the standard discussions by Coleman and his collaborators and the 1-loop analysis based on the zeta function regularization. In Chap. 3, we briefly review the TCC at first, then an introduction about the bound state between Dp-branes and D(p-2)-branes. After that, we realize a metastable state geometrically using D5-branes and anti D5-branes and discuss the catalytic effect of D3-branes wrapped in the internal space. This chapter is based on our first study [1] except for the review part. In Chap. 4, we consider the non-perturbative decay of compactified spacetime and show that the singularity in the instanton spacetime can reduce the decay rate. In calculating the Euclidean action, we demonstrate the regularization method of the singularity. This chapter is based on our second study [2]. Chap. 5 is devoted to conclusion. In Appendix A, we add a general relativity-inspired correction to the bound state discussed in Chap. 3 and discuss the stability in the four dimensional spacetime. We also study the overextremality of the bound state from the point of view of the weak gravity conjecture. Appendix B provides supplementary explanations for Chap. 2, Appendix C corresponds to Chap. 3, and Appendix D covers additional details for Chap. 4.

Chapter 2

Basics of Vacuum Decay

In this chapter, we review the framework for describing the dynamics of quantum transitions from a false vacuum to a true vacuum with a lower energy, commonly known as vacuum decay. Tunneling in quantum mechanical systems is described by the WKB approximation, but applying this to systems with many degrees of freedom, such as field theory, requires careful consideration. For calculating the vacuum decay rate in field theory, the Euclidean path integral method proposed by Coleman and the collaborators is highly effective [103, 104]. Their method involves considering a semiclassical approximation in the Euclidean theory, allowing the calculation of the ground-state energy at the 1-loop level. By extracting the imaginary part of the ground-state energy, we can derive the decay rate of the system. This chapter outlines the derivation of this decay rate. In Sec. 2.1, we show a description of tunneling phenomena in one dimensional quantum mechanics by the ordinary WKB approximation at first, then introduce the instanton method proposed by [103, 104]. In Sec. 2.2, we demonstrate the calculation method for the functional determinant representing the contribution from quantum fluctuations around the instanton solution. The calculation of the decay rate in Chap. 3 and Chap. 4 is based on the WKB analysis in this chapter. Since this chapter reviews [103, 104], those already familiar with them can skip. For more comprehensive reviews on vacuum decay or texts on non-perturbative aspects of quantum field theory, see, e.g., [105–108].

2.1 Euclidean formalism of vacuum decay

2.1.1 Tunneling analysis via ordinary WKB

Any particle cannot classically overcome a potential barrier higher than its energy, but it is possible for the particle to go through the barrier quantum mechanically. This phenomenon is referred to as *quantum tunneling* (often simply abbreviated as tunneling) and is a non-perturbative effect unique to quantum mechanics. The rate at which a particle undergoes tunneling is characterized by the transmission coefficient $\mathcal{T}$. Calculating the transmission coefficient exactly is difficult in general potentials, but as shown in Figure 2.1, when the potential is sufficiently high and wide, it is known that the Wentzel-Kramers-Brillouin (WKB) approximation (often called the semiclassical approximation) allows for successful calculation. Using the WKB approximation, the expression for the tunneling probability

at the leading order is known to be given by the following formula.

$$P = |\mathcal{T}|^2 = Ae^{-B/2}, \quad B = \frac{2}{\hbar}\int_a^b |p(q)|dq = \frac{2}{\hbar}\int_a^b \sqrt{2m\,[V(q) - E]}dq \tag{2.1.1}$$

where E is the particle's energy, a and b are the turning points, $V(q)$ is the potential which satisfies $V(a) = V(b) = E$, and A is the overall factor which cannot be determined in the leading semiclassical approximation. See standard texts of quantum mechanics, e.g., [109, 110] for detailed discussions for deriving (2.1.1).

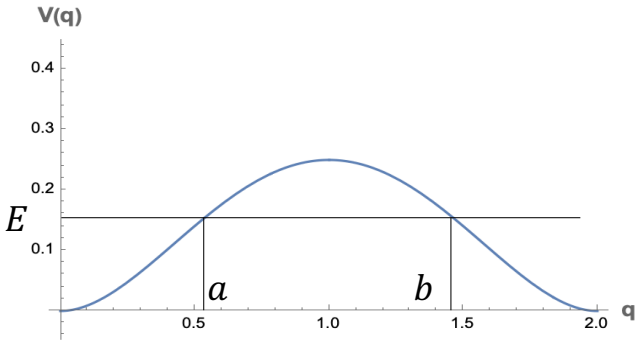

Figure 2.1: Typical potential for a tunneling problem in one dimensional quantum mechanics.

2.1.2 Outline of Euclidean path integral formulation

In the previous section, we showed the ordinary discussion of the tunneling phenomenon in quantum mechanics. The tunneling picture in one dimension is obvious, so it is easy to determine the efficient tunneling path. On the other hand, in the case of many degrees of freedom, such as field theory, it is non-trivial to know through what path tunneling will occur. Moreover, we cannot determine the overall factor A from the ordinary discussion. The method Coleman and his collaborators isadvocated is quite useful in resolving these problems [103, 104]. In this section, we first provide guidelines for deriving the expression for the decay rate by the path integral method. A detailed review will follow in the next section.

Let us consider an unbounded potential with a local minimum at $q = 0$. A typical example is the anharmonic oscillator problem, where the potentials are given by

$$V(q) = \frac{1}{2}q^2 - gq^3 \qquad \text{cubic potential,} \tag{2.1.2}$$

$$V(q) = \frac{1}{2}q^2 - \frac{\lambda}{4}q^4 \qquad \text{quartic potential} \tag{2.1.3}$$

where g and λ are the coupling constants that take positive values. As can be seen from Figure 2.2, these potentials have a barrier at finite $q = q_{\text{barrier}}$ and fall outside the barrier. Thus, the local minima are not perfectly stable vacua and can decay in a finite life-time.

As inferred from the possibility of decay, the wave functions of these systems cannot be bound states. Thus, the energy eigenvalues take complex values such that they have

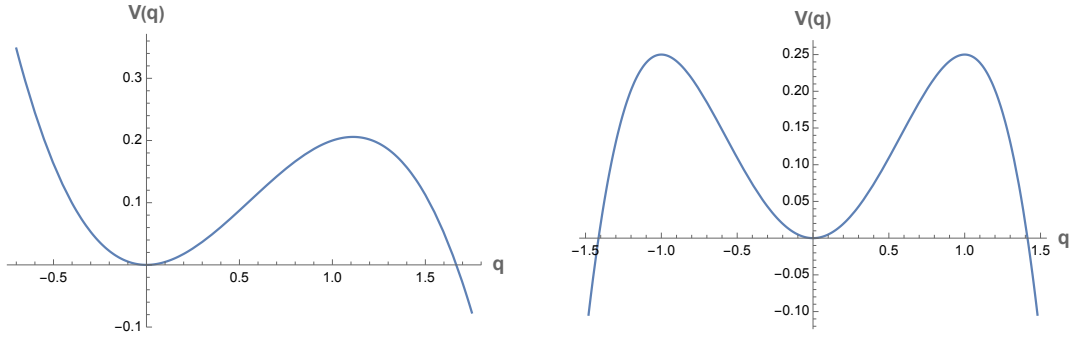

(a) (b)

Figure 2.2: Anharmonic potential with local minimum at $q = 0$. The left panel represents the cubic potential with $g = 0.3$, and the right panel represents the quartic potential with $\lambda = 1$.

imaginary parts as follows

$$E = \mathrm{Re}E - i\frac{\Gamma}{2}, \qquad \Gamma > 0. \tag{2.1.4}$$

Using this complex energy E, the time evolution of the system is given by

$$e^{-iEt/\hbar} = e^{-it\mathrm{Re}E/\hbar}e^{-\Gamma t/2\hbar}. \tag{2.1.5}$$

Then, the imaginary part Γ of (2.1.4) can be interpreted as the decay rate of the metastable state, and its inverse is the life-time: $\tau = \Gamma^{-1}$. Therefore, when deriving the decay rate using the path integral formulation, it is also sufficient to focus on the imaginary part of the energy.

On the other hand, it is hard to completely solve the path integral of metastable systems. Here, the WKB approximation described in the previous section can be used to obtain an analytic representation up to the first order of $\hbar$ expansion. The WKB approximation is the limit where $\hbar$ on exponential weights is considered very small regarding path integrals. Looking at the time evolution operator (2.1.5), we can see that in such a limit, the contribution of the lowest energy level, i.e., the ground-state energy, is dominant. In summary, the essence of the path integral formulation is to obtain the ground-state energy by applying the WKB approximation to the Euclidean path integral and reading its imaginary part. The ground-state energy is related to the transition amplitude calculated by path integral as follows

$$E_0 = -\lim_{\beta\to\infty}\frac{1}{\beta}\log Z(\beta). \tag{2.1.6}$$

2.1.3 Path integral around instanton

In this Section, we show how to calculate the transition amplitudes under the WKB approximation and derive the ground-state energy and its imaginary part. In the derivation, we will see that the contribution of nontrivial solutions of the Euclidean equation of motion (EoM), called instantons, plays an important role. For simplicity, we consider the

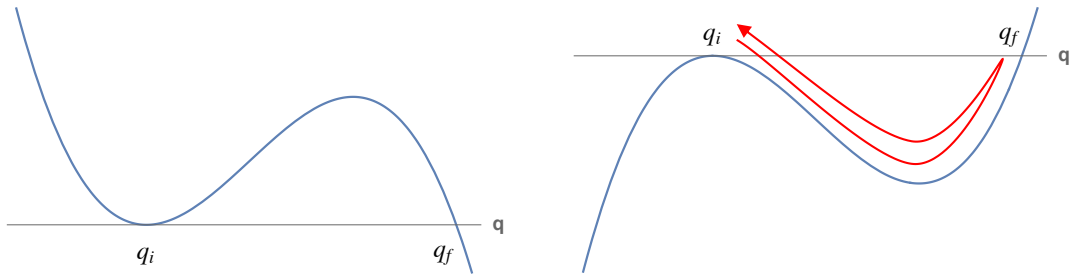

(a) (b)

Figure 2.3: (a) represents a general unbounded potential $V(q)$ with the local minimum, and (b) shows the associated inverted potential $W(q)$.

anharmonic potential as in the previous Section. That is, when the potential is given by

$$V(q) = \frac{1}{2}q^2 + \mathcal{O}(g), \tag{2.1.7}$$

we would like to evaluate the following path integral

$$Z(\beta) = \mathcal{N}\int [dx] e^{-S_E/\hbar}. \tag{2.1.8}$$

The explicit form of the Euclidean action is

$$S_E = \int_{-\beta/2}^{\beta/2} dt_E \left[\frac{1}{2}\left(\frac{dq}{dt_E}\right)^2 + W(q)\right] \tag{2.1.9}$$

where t_E is the Euclidean time and $W(q)$ is the inverted potential given by $W(q) = -V(q)$, see Figure 2.3. We will simply denote t_E as t from here.

As mentioned above, we consider the limit where $\hbar$ is extremely small in the WKB analysis, a classical solution, a saddle point of the Euclidean action S_E gives a dominant contribution in the path integral (2.1.8). The classical solution $\bar{q}$ is the configuration satisfying the following EoM.

$$\frac{\delta S_E}{\delta \bar{q}} = \frac{d^2\bar{q}}{dt^2} + W'(\bar{q}) = 0. \tag{2.1.10}$$

The classical solution corresponds to a configuration that goes from the local minimum q_i to the turning point q_f, which has the same potential value at q_i, then bounce back in the inverted potential as shown in the right panel in the Figure 2.3. Namely, the classical solution satisfies the periodic boundary condition: $\bar{q}(-\beta/2) = \bar{q}(\beta/2)$. From this bouncing picture in Euclidean space, this classical solution is especially called *bounce solution*. Hereafter, such instanton solutions describing vacuum decay are simply called bounce solutions. The bounce solution satisfies the following energy conservation law

$$\frac{1}{2}\bar{q}^2 + W(\bar{q}) = E(\beta), \tag{2.1.11}$$

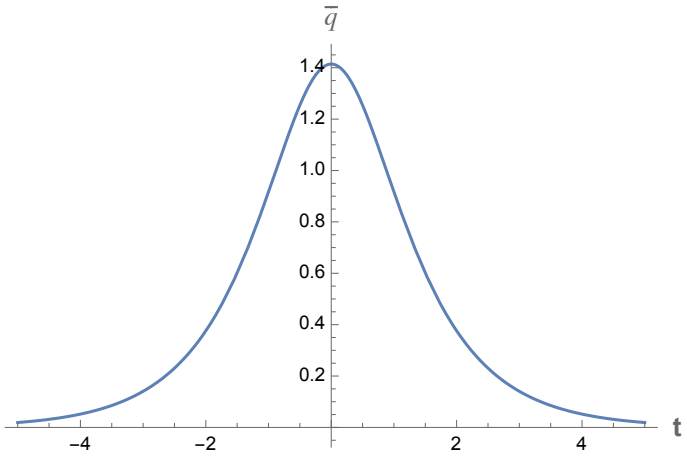

Figure 2.4: A shape of the bounce solution for the quartic potential centered at $t = 0$

For example, if we seek a bounce solution in the case of quartic potential, we obtain $\bar{q} \propto \mathrm{sech}(t - t_0)$ in the limit of $\beta \to \infty$. We can confirm that the shape of the solution is as shown in Figure 2.4. Here, t_0 is an arbitrary constant corresponding to the center of the bounce solution.

For later discussions, we decompose $q(t)$ into the classical solution and the quantum fluctuation as

$$q(t) = \bar{q}(t) + \sum_{n=0} c_n q_n(t), \tag{2.1.12}$$

where $\bar{q}(t)$ is the classical solution that satisfies the periodic boundary condition. At this point, zero mode is not included in the fluctuations, and all of them are assumed to be positive modes: $n > 0$. As described below, this assumption is not strictly true since fluctuations around the bounce solution originally include zero mode and negative mode. However, as a first step, we will limit our discussion to the case where only positive mode exists and then extend it to the case where zero mode and negative mode are included. For q_n, since we are considering periodic configurations, we assume that the fluctuations also satisfy periodic B.C. as

$$q_n\left(-\frac{\beta}{2}\right) = q_n\left(\frac{\beta}{2}\right), \qquad \dot{q}_n\left(-\frac{\beta}{2}\right) = \dot{q}_n\left(\frac{\beta}{2}\right). \tag{2.1.13}$$

Here, $\{q_n\}$ is a complete set of orthogonal functions and satisfies the following relation

$$\int_{-\beta/2}^{\beta/2} dt q_n(t) q_m(t) = \delta_{mn}. \tag{2.1.14}$$

Considering the decomposition (2.1.13), we can rewrite the measure of the path integral as

$$[dq] = \prod_n \frac{dc_n}{\sqrt{2\pi\hbar}}, \tag{2.1.15}$$

where we take the coefficient of dc_n in this way for later simplicity.

Note that the choice of orthonormal basis is arbitrary. To consider the appropriate basis, consider the expansion of the Euclidean action around the bounce solution.

$$S_E \approx S_E[\bar{q}] + \frac{1}{2}\int dt'dt''\delta q(t')\left.\frac{\delta^2 S_E[q(t)]}{\delta q(t')\delta q(t'')}\right|_{q(t)=\bar{q}(t)}\delta q(t''), \tag{2.1.16}$$

where we omit the first variation via EoM. The second variation in the second term is given as the following differential operator

$$M(t',t'') \equiv \left.\frac{\delta^2 S_E[q(t)]}{\delta q(t')\delta q(t'')}\right|_{q(t)=\bar{q}(t)} = \left(-\frac{d^2}{dt'^2} + W''[\bar{q}(t')]\right)\delta(t'-t''). \tag{2.1.17}$$

Adopting the eigenfunctions of this differential operator as the aforementioned orthonormal basis gives us a clear outlook. In other words, let $\{q_n\}$ be an orthogonal function system such that it satisfies the following eigenvalue equation[1]

$$\mathbf{M}q_n = \lambda_n q_n, \tag{2.1.18}$$

where $\mathbf{M}$ is given by

$$\mathbf{M} = \left(-\frac{d^2}{dt^2} + W''[\bar{q}(t)]\right). \tag{2.1.19}$$

Based on the above, performing the path integral, the expression for the transition amplitude approximated around the bounce solution is as follows

$$\begin{aligned} Z_{\text{one}}(\beta) &\approx \mathcal{N}e^{-S_E[\bar{q}]/\hbar}\int\prod_n \frac{dc_n}{\sqrt{2\pi\hbar}}\exp\left[-\frac{1}{2}\int dt'dt''\delta q(t')M(t',t'')\delta q(t'')\right](1+\mathcal{O}(\hbar)) \\ &= \mathcal{N}e^{-S_E[\bar{q}]/\hbar}\int\prod_n \frac{dc_n}{\sqrt{2\pi\hbar}}\exp\left[-\frac{1}{2}\sum_n \lambda_n c_n^2\right](1+\mathcal{O}(\hbar)) \\ &= \mathcal{N}e^{-S_E[\bar{q}]/\hbar}\left[\det\mathbf{M}\right]^{-1/2}(1+\mathcal{O}(\hbar)), \end{aligned} \tag{2.1.20}$$

where the determinant of the differential operator is defined as an infinite product of the eigenvalues:

$$\det\mathbf{M} = \prod_n \lambda_n. \tag{2.1.21}$$

Here, the subscript "one" attached to the transition amplitude indicates the contribution from a *one bounce* solution such that it goes and comes back only once.

Now, in the derivation of (2.1.20), we assumed that the fluctuations are all positive modes. However, there are zero modes ($\lambda_0 = 0$) in the quantum fluctuations around the original bounce solution that originate from the time translation symmetry of the solution. At this time, as can be seen from (2.1.21), the functional determinant becomes zero, and the calculation of the transition amplitude diverges. This is because when zero eigenvalues

[1] Although we are implicitly assuming that the spectrum is discrete, the discussion here can easily be extended to a case where a continuous spectrum exists.

exist, there is no damping factor in the integration with respect to λ_0, and the Gaussian integral diverges. This divergence caused by the zero mode must be handled separately.

Separating the integral of the zero mode, we can write the calculation of transition amplitude as

$$Z_{\text{one}}(\beta) \approx \mathcal{N} e^{-S_E[\bar{q}]/\hbar} \left[\det{}' \mathbf{M}\right]^{-1/2} \int \frac{dc_0}{\sqrt{2\pi\hbar}}, \tag{2.1.22}$$

where the prime symbol given to the determinant indicates that it is determinant minus the contribution of zero eigenvalues. Here, for simplicity of description, we will omit $\mathcal{O}(\hbar)$. As mentioned above, naively performing functional integration on this zero mode will lead to divergence. For this problem, there is a known prescription to rewrite the integral measure using bounce solutions. We first consider the relationship between the zero mode and the bounce solution to understand the procedure. Taking the derivative of EoM (2.1.10) with respect to t, we obtain

$$\left(-\frac{d^2}{dt^2} + W''(\bar{q})\right) \frac{d\bar{q}}{dt} = 0, \tag{2.1.23}$$

This is the same differential equation as the zero mode, and since the bounce solution satisfies the periodic B.C., the boundary conditions are also the same. Therefore, if we denote the proportionality coefficient as N_0, the following relationship equation holds for the time derivative of the bounce solution and zero mode

$$q_0 = \frac{1}{\sqrt{N_0}} \frac{d\bar{q}}{dt}. \tag{2.1.24}$$

The derivation of (2.1.24) here is applicable only to canonical quantum mechanical systems. However, it can be proved from the argument about the second variation that this relation also holds for non-canonical quantum mechanical systems (see Appendix B.1). Using the normalization condition (2.1.14), we can calculate the zero mode normalization constant (2.1.24) as follows

$$N_0 = \int_{-\beta/2}^{\beta/2} dt \left(\frac{d\bar{q}}{dt}\right)^2, \tag{2.1.25}$$

Let us consider the rewriting of the integral measure concerning c_0. Since the bounce solution has time translation symmetry, we generally can choose its center t_1. That is,

$$\bar{q} = \bar{q}(t - t_1). \tag{2.1.26}$$

At this point, since the variation about c_0 and that about t_1 do not change the shape of the solution, they must be proportional. Indeed, noting $d\bar{q}/dt_1 = -d\bar{q}/dt$, we obtain

$$q_0 dc_0 = -\frac{d\bar{q}}{dt_1} dt_1 = \frac{d\bar{q}}{dt} dt_1, \tag{2.1.27}$$

where we choose the overall sign for later convenience because we cannot determine from the discussion here. Using the definition (2.1.24), we get the relation between dc_0 and dt_1 as follow,

$$\frac{dc_0}{\sqrt{2\pi\hbar}} = \sqrt{\frac{N_0}{2\pi\hbar}} dt_1. \tag{2.1.28}$$

We, then, can rewrite the integral about c_0 (2.1.22) as

$$\int \frac{dc_0}{\sqrt{2\pi\hbar}} = \sqrt{\frac{N_0}{2\pi\hbar}} \int_{-\beta/2}^{\beta/2} dt_1 = T\beta\sqrt{\frac{N_0}{2\pi\hbar}}, \tag{2.1.29}$$

and obtain

$$Z_{\text{one}}(\beta) \approx \mathcal{N}\beta\sqrt{\frac{N_0}{2\pi\hbar}} e^{-S_E[\bar{q}]/\hbar} \left[\det{}' \mathbf{M}\right]^{-1/2} \tag{2.1.30}$$

as a result of the path integral. In addition, we used the fact that the moduli space of t_0 is $[-\beta/2, \beta/2]$ in the calculation of (2.1.29).

The above discussion cannot determine the overall coefficient $\mathcal{N}$ in (2.1.29). However, as shown below, we can explicitly rewrite the equation so that $\mathcal{N}$ does not appear. From here, we denote the trivial solution that remains at the local minimum at the inverted potential $W(q)$ by $\bar{q}_{\text{triv}}$. Denoting the contribution to the transition amplitude from the trivial solution as Z_0, the following trivial deformation holds:

$$Z_{\text{one}}(\beta) = Z_0 \times \frac{Z_{\text{one}}(\beta)}{Z_0}, \tag{2.1.31}$$

Since all fluctuations around the trivial solution are positive modes, following the aforementioned discussions, Z_0 is calculated as

$$Z_0 = \mathcal{N} e^{-S_0/\hbar} \left[\det \mathbf{M}_0\right]^{-1/2}. \tag{2.1.32}$$

where $\mathbf{M}_0$ is given by

$$\mathbf{M}_0 = -\frac{d^2}{dt^2} + W''(\bar{q}_{\text{triv}}), \tag{2.1.33}$$

and S_0 is the Euclidean action of the trivial solution. Substituting this Z_0 into (2.1.31), we can derive the following expression for $Z(\beta)$

$$Z_{\text{one}}(\beta) \approx Z_0\beta\sqrt{\frac{N_0}{2\pi\hbar}} e^{-(S_E[\bar{q}]-S_0)/\hbar} \left[\frac{\det{}' \mathbf{M}}{\det \mathbf{M}_0}\right]^{-1/2}. \tag{2.1.34}$$

The difference between the Euclidean action of the bounce solution and the Euclidean action of the trivial solution, which appears on the exponential factor, is called the bounce action, denoted B.

While (2.1.34) represents the transition amplitude approximated around the one bounce solution, classical solutions corresponding to multiple bouncing are also expected to contribute. In other words, the final result is obtained by adding contributions from all solutions, representing the multiple bounces.

$$Z(\beta) = \sum_n Z_n(\beta), \tag{2.1.35}$$

where the subscript n denotes the number of bounces. In the following, bounce (instanton) solutions with two or more bounces are referred to as *multi-bounce* (*multi-instanton*) solutions.

we will consider the multi-bounce (instanton) solution where the number of bounces is n. It is extremely difficult to solve the EoM and obtain the analytical expression. However, if β is much wider than the Euclidean time interval of the bounce and the time centers of each bounce are sufficiently far apart, i.e., the overlap between them is sufficiently small, then the multi-bounce solution can also be regarded as a simple addition of the one-bounce solution. This is the so-called dilute gas approximation. In this case, the Euclidean action of the multi-bounce solution can be simply considered as n times the contribution of the one-bounce solution:

$$S_E[\bar{q}_n] \approx nS_E[\bar{q}], \tag{2.1.36}$$

where $\bar{q}_n$ on the left-hand side represents the exact multi-bounce solution.

We need to estimate fluctuations more carefully around multi-bounce solutions. Also, in the case of multi-bounce solutions, there are zero modes for quantum fluctuations. The prescription for replacing the Gaussian integral for the zero mode with the moduli integral is the same as for the one-bounce solution. However, in the case of the multi-bounce solution, the integrals should be performed keeping in mind that the center of bounce exists for the number of bounces. The i-th bounce center is denoted as t_i, and suppose that there is a magnitude relation between the n centers, $\beta/2 > t_1 > t_2 \cdots > t_n > -\beta/2$. Taking care of the magnitude relation and Performing the moduli integrals with respect to each time center, we obtain the following factors.

$$\int_{-\beta/2}^{\beta/2} dt_1 \int_{-\beta/2}^{t_1} dt_2 \cdots \int_{-\beta/2}^{t_{n-1}} dt_n = \frac{\beta^n}{n!}. \tag{2.1.37}$$

Using (2.1.36) and (2.1.37), we can formally write the expression for the transition amplitude, which adds up the contributions of the multi-bounce solutions, as follows

$$Z(\beta) = \mathcal{N} \sum_n \left(\frac{N_0}{2\pi\hbar}\right)^{n/2} \frac{(e^{-B/\hbar}\beta)^n}{n!} \left[\det{}' \left(-\frac{d^2}{dt^2} + W''[\bar{q}_n]\right)\right]^{-1/2} \tag{2.1.38}$$

$$= Z_0 \sum_n \frac{(Ke^{-B/\hbar}\beta)^n}{n!}, \tag{2.1.39}$$

where K is a factor that includes the functional determinant. The determinant factor K is determined to be consistent with the contribution from the one-bounce solution (2.1.34), that is

$$K = \sqrt{\frac{N_0}{2\pi\hbar}} \left[\frac{\det{}' \mathbf{M}}{\det \mathbf{M}_0}\right]^{-1/2}. \tag{2.1.40}$$

See [107] for a detailed derivation.

So far, we have discussed without much reference to the computation of Z_0. Since the computation of the functional determinant in Z_0 is rather technical, its details will be discussed later in Section 2.2. Here, we shall utilize only the results in the limit of $\beta \to \infty$:

$$Z_0 \propto e^{-W''[\bar{q}_{\rm triv}]\beta/2}. \tag{2.1.41}$$

Substituting this expression to (2.1.39), we find that the transition amplitude under the WKB approximation is

$$Z(\beta) = \mathcal{N} e^{-S_0/\hbar} e^{-W''[\bar{q}_{\rm triv}]\beta/2} \exp\left[K\beta e^{-B/\hbar}\right], \tag{2.1.42}$$

and we obtain the ground-state energy by (2.1.6) as follow

$$E_0 = \frac{\hbar\omega}{2} - \hbar K e^{-B/\hbar}, \tag{2.1.43}$$

where $\omega = W''[\bar{q}_{\rm triv}]$. The first term corresponds to the ground-state energy of the ordinary harmonic oscillator, and the second term is a non-perturbative contribution derived from the bounce solution. In fact, looking at the argument of the exponential factor, we can see that the second term is expanded by the inverse power of $\hbar$, indicating that the contribution is beyond perturbation theory.

2.1.4 Decay of metastable vacua

In Section 2.1.3, we assumed that the quantum fluctuations around the classical solution only include positive modes and the zero mode. However, we need to pay attention to the existence of the negative mode. This negative mode is the cause of the imaginary part in the ground energy and is one of the most important factors in calculating the decay rate.

In the case of quantum mechanical systems, the existence of negative modes can be confirmed from the shape of the zero mode function. As shown in (2.1.24), the zero mode due to time translation symmetry is proportional to the time derivative of the bounce solution. Since the typical bounce solution has the shape shown in Figure 2.4, the zero mode should have the shape shown in Figure 2.5. As you can see, there is one node in zero mode. In the case of differential equations of Schrödinger type such as (2.1.18), there is a correspondence between the number of excitations of eigenstates and the number of nodes of eigenfunctions due to the oscillation theorem. Therefore, there exists a state with lower eigenvalues than the zero mode, i.e., negative modes.

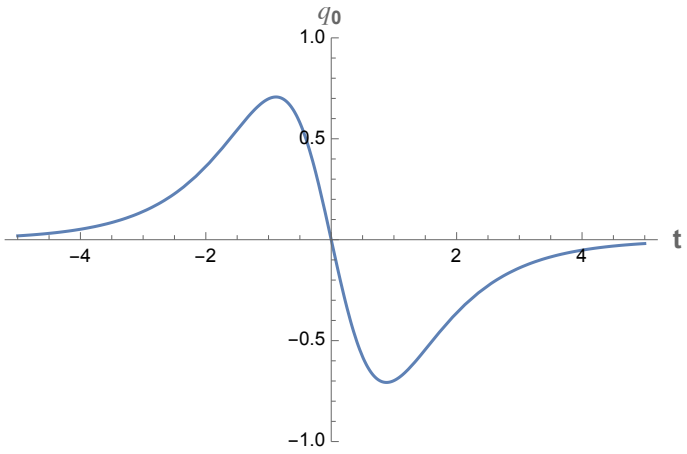

Figure 2.5: Typical shape of zero mode function centered at $t = 0$.

As expected from naive observation of (2.1.40), the existence of the negative mode leads to the imaginary part of the determinant factor K. To perform explicit calculation, we reconsider the path integral around the bounce solution. The Euclidean action can be expanded around the bounce solution as

$$S_E[\bar{q}+\delta q] = S_E[\bar{q}] + \frac{1}{2}(c_{\rm nega})^2\lambda_{\rm nega} + \sum \frac{1}{2}(c_n)^2\lambda_n + \cdots . \tag{2.1.44}$$

Here, the negative mode is explicitly distinguished from the positive modes and the zero mode. To calculate the contribution of the negative mode, we introduce the following variable transformation.

$$\begin{aligned} J &\equiv \int \frac{dc_{\rm nega}}{\sqrt{2\pi\hbar}} e^{-S_E[c_{\rm nega}]/\hbar} \\ &= \int \frac{dc}{\sqrt{2\pi\hbar}} e^{-S_E[c]/\hbar} \end{aligned} \tag{2.1.45}$$

where we changed the variable as $c - b = c_{\rm nega}$ with the maximum value of the bounce solution b. Let us consider the point $c = 0$, i.e. $c_{\rm nega} = b$. Omitting the other modes contributions,

$$q = \bar{q} + c_{\rm nega} q_{\rm nega} \tag{2.1.46}$$

holds, thus $c_{\rm nega} = b$ corresponds to the configuration whose maximum value is 0 i.e. the trivial solution. Therefore, $c = 0$ is the minimum of the Euclidean action S_E. Next, focusing on the other $c = b$, i.e., $c_{\rm nega} = 0$, this point corresponds to the bounce solution because the fluctuation in the negative mode direction does not exist. Since the bounce solution is the only saddle point except for the obvious solution, it must be the local maximum. From the above discussion, a plot of Euclidean action for c is shown in Figure 2.6.

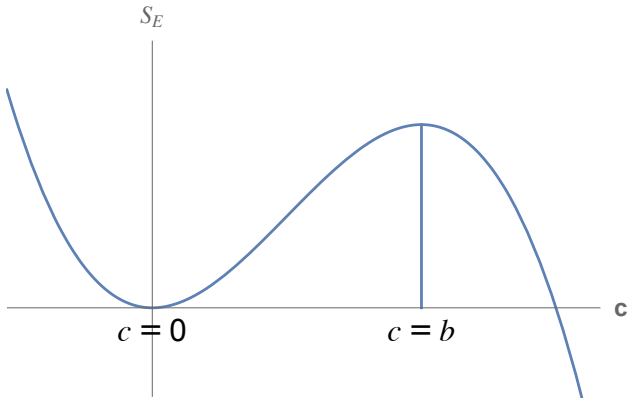

Figure 2.6: c dependence of the Euclidean action.

Seeing the Figure 2.6, we find that the value of the Euclidean action grows as $c \to -\infty$, then the integral with respect to the negative mode in $c < b$ converges. On the other hand, the Euclidean action decreases as $c \to \infty$; thus, the integral diverges in $b < c$. Considering

this situation, we split the integral into two regions as

$$J = \int_{-\infty}^{b} \frac{dc}{\sqrt{2\pi\hbar}} e^{-S_E[c]/\hbar} + \int_{b}^{\infty} \frac{dc}{\sqrt{2\pi\hbar}} e^{-S_E[c]/\hbar}. \tag{2.1.47}$$

The second term is the divergent one. The steepest descent method is highly effective in obtaining the finite result. Doing an analytic continuation to the complex plane, let us change the contour of the integral as

$$J = \int_{-\infty}^{b} \frac{dc}{\sqrt{2\pi\hbar}} e^{-S_E[c]/\hbar} + \int_{b+i0}^{b+i\infty} \frac{dc}{\sqrt{2\pi\hbar}} e^{-S_E[c]/\hbar}. \tag{2.1.48}$$

The contour for $b < c$ is taken down the saddle point. See Figure 2.7 for the deformed contour on the complex plane. Since the radius of the arc takes the limit of infinity in the end, the contribution from the path of C_2 vanishes. Therefore, only the contribution from C_1 should be evaluated. Based on the steepest descent method, we expand $S_E[c]$ around the saddle point as

$$J' \equiv \int_{b+i0}^{b+i\infty} \frac{dc}{\sqrt{2\pi\hbar}} e^{-S_E[c]/\hbar} \approx \int_{b+i0}^{b+i\infty} \frac{dc}{\sqrt{2\pi\hbar}} e^{-S_E[b]/\hbar - S''[b](c-b)^2/2\hbar}. \tag{2.1.49}$$

Transforming the variable as $c - b = ix$, J' will be evaluated as follow

$$J' = \frac{i}{2} \left|S''[b]\right|^{-1/2} e^{-S_E[b]/\hbar}. \tag{2.1.50}$$

The overall coefficient $1/2$ owes to the fact that the interval of integration is $(0, \infty)$. Substituting (2.1.50) into (2.1.34), we obtain the exact contribution of the one bounce solution to the transition amplitude as

$$Z_{\text{one}}(\beta) = Z_0 \beta \sqrt{\frac{N_0}{2\pi\hbar}} \left((\text{real value}) + \frac{i}{2} e^{-S_E[\bar{q}]/\hbar} \left|S''[b]\right|^{-1/2} \right) \left[\frac{\det'' \mathbf{M}}{\det \mathbf{M}_0}\right]^{-1/2}, \tag{2.1.51}$$

where $\det''$ denote the functional determinant where the zero mode and the negative mode are subtracted. Following this expression, the imaginary part of the determinant factor is given by

$$\operatorname{Im} K = \frac{1}{2} \sqrt{\frac{N_0}{2\pi\hbar}} \left| \frac{\det' \mathbf{M}}{\det \mathbf{M}_0} \right|^{-1/2}, \tag{2.1.52}$$

thus, the formula for the decay rate is

$$\Gamma = -2 \operatorname{Im} E_0 = \sqrt{\frac{N_0}{2\pi\hbar}} \left| \frac{\det' \mathbf{M}}{\det \mathbf{M}_0} \right|^{-1/2} e^{-B/\hbar}. \tag{2.1.53}$$

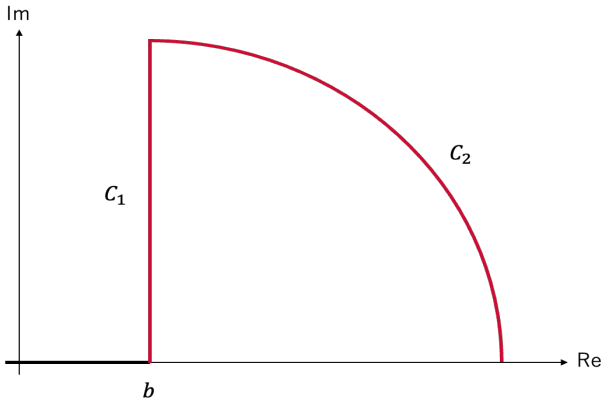

Figure 2.7: The contour of the negative mode integral after the analytic continuation.

2.2 Calculation of functional determinant

As seen in the previous section, the contribution of massive modes in quantum fluctuations around the classical solution can be expressed as the functional determinant. This functional determinant can, naively, be regarded as the infinite product of the eigenvalues of a differential operator. Therefore, in part of models like the Pöschl-Teller potential, where the spectrum can be fully determined, it is straightforward to compute the ratio of determinants. However, even when the spectrum is difficult to determine, the Gel'fand-Yaglom method allows us to compute the functional determinant without detailed knowledge of the spectrum [111]. In this section, we derive the Gel'fand-Yaglom formula and determine the expression for the decay rate in a canonical quantum mechanical system. The description of zeta function regularization and the derivation of the Gel'fand-Yaglom formula in this section are mainly based on [106, 112].

2.2.1 Zeta function regularization

In (2.1.21), the functional determinant was defined as the infinite product of eigenvalues, but this expression is technically ill-defined. Under periodic boundary conditions, the spectrum of $\mathbf{M} = -\frac{d^2}{dt^2} + W''[\bar{q}]$ satisfies the following inequality:

$$\lambda_0 < \lambda_1 < \lambda_2 < \cdots < \lambda_n < \cdots , \tag{2.2.1}$$

Moreover, for large n, the eigenvalues can be approximately expressed as

$$\lambda_n \approx n^2, \quad n \gg 1. \tag{2.2.2}$$

Thus, we must employ some regularization to eliminate the UV divergence.

To handle such divergences, the zeta function regularization method is well-known. In the context of physics, this regularization scheme was introduced as an alternative to avoid ambiguities of dimensional regularization in curved spacetimes [113]. In this method, the spectral zeta function of a differential operator A is defined as:

$$\zeta_A(s) = {\sum_n}' \lambda_n^{-s}, \tag{2.2.3}$$

where the prime indicates that zero modes are excluded from the sum. The derivative of this function is given by

$$-\frac{d}{ds}\zeta_A = \sum_n{}' \lambda_n^{-s} \log \lambda_n. \tag{2.2.4}$$

Taking the limit of $s \to 0$, the functional determinant of the operator A, excluding zero modes, is expressed as

$$\det A = \exp\left[-\zeta_A'(0)\right], \tag{2.2.5}$$

demonstrating how the determinant is defined through zeta function regularization.

Here, in introducing the regularized determinant (2.2.5), we assume that the spectral zeta function is regular at the origin, i.e., it is differentiable. However, when the background spacetime is a d-dimensional Riemannian manifold, it is known that the infinite sum in (2.2.3) converges only for $\mathrm{Re}\, s > d/2$. Since we are considering a quantum mechanical system, we can set $d = 1/2$. Therefore, to define the regularization in (2.2.5), it is necessary to ensure that $\zeta_A(s)$ is regular in the neighborhood of $s = 0$.

The analytic structure of the spectral zeta function has been extensively studied using representations involving the gamma function and the heat kernel (see, e.g., [114]):

$$\zeta_A(s) = \frac{1}{\Gamma(s)} \int_0^\infty \mathrm{Tr} K_A(\tau) \tau^{s-1} d\tau. \tag{2.2.6}$$

Here, $K_A(\tau)$ is the heat kernel of the operator A, defined using the eigenvalues λ_n and eigenfunctions ϕ_n of A as

$$K_A(\tau) = \sum_n e^{-\lambda_n \tau} |\phi_n\rangle\langle\phi_n|. \tag{2.2.7}$$

Thus, the trace of the heat kernel is given by

$$\mathrm{Tr} K_A(\tau) = \sum_n e^{-\lambda_n \tau}. \tag{2.2.8}$$

If zero modes exist, their contributions should be subtracted, leading to

$$\zeta_A(s) = \frac{1}{\Gamma(s)} \int_0^\infty \left(\mathrm{Tr} K_A(\tau) - n_0\right) \tau^{s-1} d\tau, \tag{2.2.9}$$

where n_0 is the number of zero modes. To examine the analytic structure of the spectral zeta function, we split the integral into two regions as follows

$$\zeta_A(s) = \frac{1}{\Gamma(s)} \left[\int_0^1 \left(\mathrm{Tr} K_A(\tau) - n_0\right) \tau^{s-1} d\tau + \int_1^\infty \left(\mathrm{Tr} K_A(\tau) - n_0\right) \tau^{s-1} d\tau \right]. \tag{2.2.10}$$

The second integral converges for all s: in the short-distance region, the lower bound of the integral ensures convergence, while in the large-distance region, $\mathrm{Tr} K_A(\tau) \sim e^{-\lambda_1 \tau}$ leads to exponential suppression, guaranteeing convergence. Here, λ_1 is the smallest non-zero eigenvalue of A. In subsequent discussions, we denote this integral by $F(s)$. On the other hand, the first integral may diverge in the short-distance region and require careful

attention. To confirm this, we rewrite the trace of the heat kernel using the heat kernel expansion (the Seeley-de Witt expansion). On a d-dimensional Riemannian manifold M, the heat kernel expansion is given by

$$\mathrm{Tr}K_A(\tau) = \frac{1}{(4\pi)^{d/2}} \sum_{n=0}^{\infty} \tau^{n-d/2} \int d^d x \sqrt{g} a_n(x). \tag{2.2.11}$$

Here, g is the determinant of the metric $g_{\mu\nu}$ on M. Using (2.2.11), the first integral in (2.2.10) can be computed as

$$\begin{aligned} &\frac{1}{\Gamma(s)} \int_0^1 \left(\mathrm{Tr}K_A(\tau) - n_0\right) \tau^{s-1} d\tau \\ &\qquad = \frac{1}{(4\pi)^{d/2}\Gamma(s)} \sum_{n=0}^{\infty} \frac{1}{s+n-d/2} \int d^d x \sqrt{g} a_n(x) - \frac{n_0}{s\Gamma(s)}. \end{aligned} \tag{2.2.12}$$

Observing this integral, it initially appears that the spectral zeta function has simple poles at

$$s = \frac{d}{2} - n, \quad n \geq 0. \tag{2.2.13}$$

However, the actual number of poles is much smaller. For $n \geq d/2$, i.e., possible poles at $s = -k$ $(k \geq 0)$, the poles are canceled by those of the gamma function. At $s = 0$, the subtraction of zero-mode contributions ensures the following relation:

$$n_0 + \zeta_A(0) = \frac{1}{(4\pi)^{d/2}} \int d^d x \sqrt{g} a_{d/2}(x). \tag{2.2.14}$$

Therefore, poles in (2.2.12) only appear at:

$$s = 1, 2, \cdots, \frac{d}{2}. \tag{2.2.15}$$

This indicates the spectral zeta function is regular at $s = 0$.

2.2.2 Deriving the Gel'fand-Yaglom formula

Let us derive the Gel'fand-Yaglom formula based on the definition of zeta function regularization. First, we must consider how to subtract the zero mode contribution. Assume that the differential operator A has zero mode. Then, consider the operator $A - \lambda$ such that A is shifted by λ. If we write the eigenvalues of A as λ_n, the determinant of this shifted operator can be formally written as follows

$$\det(A - \lambda) = \prod_n (\lambda_n - \lambda) \tag{2.2.16}$$

Taking the derivative with respect to λ yields

$$\begin{aligned} -\frac{\partial}{\partial\lambda} \det(A - \lambda) &= -\frac{\partial}{\partial\lambda} \prod_n (\lambda_n - \lambda) \\ &= \prod_{n\neq -1} (\lambda_n - \lambda) + \prod_{n\neq 0} (\lambda_n - \lambda) + \prod_{n\neq 1} (\lambda_n - \lambda) + \cdots. \end{aligned} \tag{2.2.17}$$

Since all the terms in (2.2.17) except for the second term include the zero mode eigenvalue, only the second term survives in the limit of $\lambda \to 0$ and $\beta \to \infty$. This is nothing more than the determinant with the zero mode subtracted. That is,

$$\det{}'(A) = -\frac{\partial}{\partial\lambda}\det(A-\lambda)\Big|_{\lambda=0} = -\frac{\partial}{\partial\lambda}\exp\left[-\zeta'_{A-\lambda}(s=0)\right]\Big|_{\lambda=0}. \tag{2.2.18}$$

To proceed with the calculation from here, we need to transform $\zeta'_{A-\lambda}(s=0)$. As shown in (2.2.6), the spectral zeta function is given as the Mellin transform of the trace of the heat kernel, so taking its λ derivative and s derivative at $s=0$, we obtain the following equation.

$$\begin{aligned}\frac{d^2}{d\lambda ds}\zeta_{A-\lambda}(s=0) &= \int_0^\infty \mathrm{Tr}e^{-(A-\lambda)\tau}d\tau \\ &= \mathrm{Tr}R_\lambda,\end{aligned} \tag{2.2.19}$$

where R_λ is the resolvent of the differential operator $A-\lambda$ and nothing more than the Green function: $R_\lambda = (A-\lambda)^{-1}$.

For a one-dimensional Schrödinger-type operator, Green's function can be explicitly computed using methods such as variation of parameters. As a preparation, we define the following fundamental matrix

$$M_\lambda(t) = \begin{pmatrix}\psi^1_\lambda(t) & \psi^2_\lambda(t)\\ \dot\psi^1_\lambda(t) & \dot\psi^2_\lambda(t)\end{pmatrix}, \tag{2.2.20}$$

where ψ^1_λ and ψ^2_λ are two independent solutions of the eigenvalue equation $A\psi = \lambda\psi$, satisfying the following boundary conditions,

$$\begin{aligned}\psi^1_\lambda(-\beta/2) = 1, \quad \dot\psi^1_\lambda(-\beta/2) = 0,\\ \psi^2_\lambda(-\beta/2) = 0, \quad \dot\psi^2_\lambda(-\beta/2) = 1.\end{aligned} \tag{2.2.21}$$

At $t=\beta/2$, let us denote M_λ as

$$T(\lambda) = M_\lambda(\beta/2), \tag{2.2.22}$$

which is called the monodromy matrix. Using this monodromy matrix, the Green's function $R_\lambda(t,t')$ can be written as

$$R_\lambda(t,t') = -\left(\psi^1_\lambda(t),\psi^2_\lambda(t)\right)\left(T(\lambda)-\mathbf{1}\right)^{-1}T(\lambda)\begin{pmatrix}\psi^1_\lambda(t')\\ \psi^2_\lambda(t')\end{pmatrix}. \tag{2.2.23}$$

Equivalently, it can be expressed as

$$R_\lambda(t,t') = -\mathrm{Tr}\left\{\left(T(\lambda)-\mathbf{1}\right)^{-1}T(\lambda)Z(t,t';\lambda)\right\}. \tag{2.2.24}$$

Here, $Z(t,t';\lambda)$ is a matrix defined in terms of ψ^1_λ and ψ^2_λ, which satisfy the boundary conditions in (2.2.21), as

$$Z(t,t';\lambda) = \begin{pmatrix}\psi^1_\lambda(t)\psi^2_\lambda(t') & \psi^2_\lambda(t)\psi^2_\lambda(t')\\ -\psi^1_\lambda(t)\psi^1_\lambda(t') & -\psi^2_\lambda(t)\psi^1_\lambda(t')\end{pmatrix}. \tag{2.2.25}$$

Now, let us consider two independent solutions $a_\lambda(t)$ and $b_\lambda(t)$ that satisfy $(A-\lambda)y(t) = 0$. These two solutions satisfy the following relation

$$a_\lambda(t)b_\lambda(t) = \frac{d}{dt}W[\partial_\lambda a_\lambda(t), b_\lambda(t)], \tag{2.2.26}$$

where W is the Wronskian. By integrating both sides of (2.2.26), we obtain

$$\int_{-\beta/2}^{\beta/2} a_\lambda(t)b_\lambda(t)dt = \Big[W[\partial_\lambda a_\lambda(t), b_\lambda(t)]\Big]_{-\beta/2}^{\beta/2}. \tag{2.2.27}$$

Using the relation (2.2.27), the integral of each component of $Z(t,t';\lambda)$ in (2.2.25) can be evaluated as

$$\int_{-\beta/2}^{\beta/2} Z(t,t';\lambda)dt = T(\lambda)^{-1}\frac{dT(\lambda)}{d\lambda}. \tag{2.2.28}$$

Using (2.2.24) and (2.2.28), the trace of R_λ can be rewritten in terms of the monodromy matrix as follows

$$-\mathrm{Tr}R_\lambda = -\int_{-\beta/2}^{\beta/2} R_\lambda(t,t)dt = \frac{d}{d\lambda}\log\det\left(T(\lambda)-\mathbf{1}\right). \tag{2.2.29}$$

Comparing this with the left-hand side of (2.2.19), we obtain the following relation

$$\zeta'_{A-\lambda}(s=0) = -\log\left(C\det\left(T(\lambda)-\mathbf{1}\right)\right), \tag{2.2.30}$$

where C is an arbitrary constant. Substituting this relation to the definition of zeta function regularization, we arrive at

$$\det\left(A-\lambda\right) = C\det\left(T(\lambda)-\mathbf{1}\right). \tag{2.2.31}$$

This arbitrary constant can be determined by examining the asymptotic behavior of the functional determinant as $\mu = -\lambda \to \infty$. The behavior of $\det(A+\mu)$ for large μ can be analyzed using (2.2.10). Since $A+\mu$ contains no zero modes, the spectral zeta function is expressed as:

$$\zeta_{A+\mu}(s) = \frac{1}{\Gamma(s)}\left[\int_0^1 d\tau\,\tau^{s-1}e^{-\mu\tau}\mathrm{Tr}K_A(\tau) + \int_1^\infty d\tau\,\tau^{s-1}e^{-\mu\tau}\mathrm{Tr}K_A(\tau)\right]. \tag{2.2.32}$$

The derivative at $s=0$ for the second term is of order $e^{-\mu}$, which is negligibly small in the region under consideration. Therefore, only the first term needs to be analyzed. Since the coefficient at $n=0$ equals to one, $a_0 = 1$, the leading-order approximation of the heat kernel expansion of $\mathrm{Tr}K_A(\tau)$ yields

$$\mathrm{Tr}K_A(\tau) = \frac{\beta}{\sqrt{4\pi\tau}} + \mathcal{O}(\sqrt{\tau}), \tag{2.2.33}$$

where β originates from the integral over the Euclidean spacetime. Substituting (2.2.33) into the first term of (2.2.32), we obtain

$$\frac{1}{\Gamma(s)}\int_0^1 d\tau\,\tau^{s-1}\mathrm{Tr}K_A(\tau) = \frac{\mu^{1/2-s}}{\Gamma(s)}\left\{\Gamma\left(s-\frac{1}{2}\right) - \int_\mu^\infty du\,u^{s-3/2}e^{-u}\right\}. \tag{2.2.34}$$

For the second term, its contribution is again of order $e^{-\mu}$, and thus, it can be safely ignored in the current region of interest. From this, we estimate the first derivative of the spectral zeta function at $s = 0$ as

$$-2\sqrt{\pi\mu}. \tag{2.2.35}$$

Consequently, the asymptotic form of $\det(A+\mu)$ for large μ is derived as

$$\det(A+\mu) = \exp\left[-\zeta'_{A+\mu}(0)\right] = e^{\sqrt{\mu}\beta}\left(1+\mathcal{O}(\mu^{-1/2})\right). \tag{2.2.36}$$

On the other hand, we can calculate $\det(T(\lambda)-\mathbf{1}) = \det(T(-\mu)-\mathbf{1})$ by definition. For sufficiently large μ, we can approximate the fundamental matrix of $A+\mu$ by the solutions obtained when taking the potential term of A to zero as

$$M_{-\mu}(t) \simeq \begin{pmatrix} \cosh\left(\sqrt{\mu}\left(t+\frac{\beta}{2}\right)\right) & \frac{1}{\sqrt{\mu}}\sinh\left(\sqrt{\mu}\left(t+\frac{\beta}{2}\right)\right) \\ \sqrt{\mu}\sinh\left(\sqrt{\mu}\left(t+\frac{\beta}{2}\right)\right) & \cosh\left(\sqrt{\mu}\left(t+\frac{\beta}{2}\right)\right) \end{pmatrix}. \tag{2.2.37}$$

Substituting this expression to the definition of the monodromy matrix, we can calculate $\det(T(-\mu)-\mathbf{1})$ as follows

$$\begin{aligned} \det\left(T(-\mu)-\mathbf{1}\right) &\simeq \det\begin{pmatrix} \cosh\left(\sqrt{\mu}\beta\right)-1 & \frac{1}{\sqrt{\mu}}\sinh\left(\sqrt{\mu}\beta\right) \\ \sqrt{\mu}\sinh\left(\sqrt{\mu}\beta\right) & \cosh\left(\sqrt{\mu}\beta\right)-1 \end{pmatrix} \\ &\simeq -e^{\sqrt{\mu}\beta}. \end{aligned} \tag{2.2.38}$$

Comparing this calculation to (2.2.36), we can identify the arbitrary constant as $C=-1$. Thus, using the monodromy matrix, the determinant of $A-\lambda$ is expressed as

$$\det\left(A-\lambda\right) = -\det\left(T(\lambda)-\mathbf{1}\right) = \mathrm{Tr}\left(T(\lambda)-\mathbf{1}\right), \tag{2.2.39}$$

where the last equality follows from the definition of the monodromy matrix. Therefore, we obtain the expression of the determinant with zero mode subtracted as follows

$$\det{}'(A) = -\frac{\partial}{\partial\lambda}\mathrm{Tr}\left(T(\lambda)-\mathbf{1}\right)\Big|_{\lambda=0}. \tag{2.2.40}$$

To evaluate the right hand side of (2.2.40), we need to know the small λ expansion of ψ^1_λ and ψ^2_λ:

$$\psi^k_\lambda(t) = \sum_{m=0}^{\infty}\lambda^m\psi^k_{(m)}(t). \tag{2.2.41}$$

The first order expansion of ψ^k_λ is given by

$$\psi^k_\lambda = \psi^k_0 + \lambda\int_{-\beta/2}^{t} g(t,t')\psi^k_\lambda(t')dt', \quad k=1,\ 2, \tag{2.2.42}$$

where $g(t,t')$ is the Volterra-Green function defined as

$$g(t,t') = \psi^1_0(t)\psi^2_0(t') - \psi^2_0(t)\psi^1_0(t'). \tag{2.2.43}$$

Higher-order expansion coefficients can also be obtained by repeatedly solving the integral equations of (2.2.41) and (2.2.42). However, in (2.2.40), after taking λ derivative, we set $\lambda = 0$, so higher-order contributions eventually disappear. Therefore, it is sufficient that we substitute (2.2.42) into the monodromy matrix. Thus, the functional determinant, subtracting the zero-mode contribution, is computed as follows

$$\begin{aligned}\det{}'(A) &= -\frac{\partial}{\partial\lambda}\,\mathrm{Tr}\left(\begin{pmatrix}\psi_\lambda^1(\frac{\beta}{2})-1 & \psi_\lambda^2(\frac{\beta}{2}) \\ \dot\psi_\lambda^1(\frac{\beta}{2}) & \dot\psi_\lambda^2(\frac{\beta}{2})-1\end{pmatrix}\right)\Bigg|_{\lambda=0} \\ &= \psi_0^2\left(\frac{\beta}{2}\right)\int_{-\beta/2}^{\beta/2}\left(\psi_0^1(t)\right)^2 dt - \dot\psi_0^1\left(\frac{\beta}{2}\right)\int_{-\beta/2}^{\beta/2}\left(\psi_0^2(t)\right)^2 dt \\ &\quad + \left(\dot\psi_0^2\left(\frac{\beta}{2}\right) - \psi_0^1\left(\frac{\beta}{2}\right)\right)\int_{-\beta/2}^{\beta/2}\psi_0^1(t)\,\psi_0^2(t)\,dt\ . \end{aligned} \tag{2.2.44}$$

As (2.2.44) is still complicated, we try to transform it to a simpler form focusing on the existence of two zero modes. From the discussion of (2.1.24), although we already know that one of the zero mode is the time derivative of the bounce solution, the other one is non-trivial. Here, note that the bounce solution is a function of energy as well as time:

$$\bar q(t) = \bar q(t;E)\ . \tag{2.2.45}$$

The EoMs themselves can be solved for any energy, which can be interpreted as having *translation* symmetry with respect to energy. Thus, $\chi(t)$ defined as follows is also a zero mode function.

$$\chi(t) = \frac{\partial\bar q(t)}{\partial E}. \tag{2.2.46}$$

Following the energy conservation law, we can examine the boundary condition imposed on $\chi(t)$.

$$\frac{1}{2}\dot{\bar q}^2 + V(\bar q) = E(\beta). \tag{1.4.3}$$

Taking the derivative with respect to E yields

$$\dot{\bar q}\frac{\partial\dot{\bar q}}{\partial E} + \frac{\partial V(\bar q)}{\partial E} = 1. \tag{2.2.47}$$

Using the following equation

$$\frac{1}{\chi(t)}\frac{\partial V(\bar q)}{\partial E} = \left(\frac{\partial\bar q}{\partial E}\right)^{-1}\left(\frac{\partial V}{\partial E}\right) = \frac{\partial V}{\partial\bar q} = -\ddot{\bar q}, \tag{2.2.48}$$

we can rewrite (2.2.47) as follows

$$\dot{\bar q}(t)\dot\chi(t) - \ddot{\bar q}(t)\chi(t) = 1. \tag{2.2.49}$$

This equation can be interpreted as a condition on Wronskian $W[\bar q(t),\xi(t)]$. Since the bounce solution has time translation symmetry, we choose the parameter t_0 as

$$\ddot{\bar q}\left(-\frac{\beta}{2}\right) = 0. \tag{2.2.50}$$

This equation requires that the "particle" is at the potential minimum at $t = -\beta/2$. Substituting this equation into the Wronskian condition (2.2.49), we obtain the following equation

$$\dot{\bar{q}}\left(-\frac{\beta}{2}\right)\dot{\chi}\left(-\frac{\beta}{2}\right) = 1. \tag{2.2.51}$$

With the two zero mode functions, $\dot{\bar{q}}(t)$ and $\chi(t)$, we can construct the two independent solutions $\psi_0^k(t)$ satisfying the boundary condition (2.2.21) as follows

$$\psi_0^1(t) = \frac{\dot{\bar{q}}(t)}{\dot{\bar{q}}(-\beta/2)}, \qquad \psi_0^2(t) = -\chi\left(-\frac{\beta}{2}\right)\dot{\bar{q}}(t) + \dot{\bar{q}}\left(-\frac{\beta}{2}\right)\chi(t). \tag{2.2.52}$$

By the definition (2.2.52), the boundary value of $\psi_0^k(t)$ at $t = \beta/2$ as follow

$$\psi_0^1\left(\frac{\beta}{2}\right) = \dot{\psi}_0^2\left(\frac{\beta}{2}\right) = 1\ , \quad \dot{\psi}_0^1\left(\frac{\beta}{2}\right) = 0\ . \tag{2.2.53}$$

Substituting (2.2.53) to (2.2.44), we obtain

$$\det{}'(A) = \psi_0^2\left(\frac{\beta}{2}\right)\int_{-\beta/2}^{\beta/2}\left(\psi_0^1(t)\right)^2 dt. \tag{2.2.54}$$

This is the desired expression for the determinant.

This formula can be further simplified. Using (2.2.52), (2.2.54) can be rewritten as follows

$$\det{}'(A) = \frac{\chi(\beta/2) - \chi(-\beta/2)}{\dot{\bar{q}}(\beta/2)}\int_{-\beta/2}^{\beta/2}\left(\dot{\bar{q}}(t)\right)^2 dt. \tag{2.2.55}$$

Since $\bar{q}(t)$ is periodic in terms of t, the following equation holds.

$$\bar{q}(t+\beta; E) = \bar{q}(t; E)\ . \tag{2.2.56}$$

Taking the β derivative, we obtain

$$\frac{\chi(t+\beta) - \chi(t)}{\dot{\bar{q}}(t)} = -\left(\frac{\partial E}{\partial \beta}\right)^{-1}\ , \tag{2.2.57}$$

Substituting this equation into (2.2.55), we obtain the final expression for the functional determinant as follows

$$\det{}'(A) = -\left(\frac{\partial E}{\partial \beta}\right)^{-1}\int_{-\beta/2}^{\beta/2}\left(\dot{\bar{q}}(t)\right)^2 dt\ . \tag{2.2.58}$$

2.2.3 One-loop decay rate in metastable vacua

Finally, since we aim to compute the ratio of the determinant to a reference determinant in the $\beta \to \infty$ limit, it is necessary to understand how $\partial E/\partial\beta$ behaves for large β. To

examine the β-dependence of $\partial E/\partial\beta$, let us introduce technical ingredients. Using the bounce solution, β can be expressed as the following integral:

$$\beta = 2\int_{q_-}^{q_+} \frac{1}{\sqrt{(\dot{\bar{q}})^2}} d\bar{q}. \tag{2.2.59}$$

Here, note that q_- and q_+ differ from q_i and q_f in the case of finite β. Following the procedure outlined in [106], let us perform the following trivial transformation:

$$\beta = 2\int_{q_-}^{q_+} \left\{ \frac{1}{\sqrt{(\dot{\bar{q}})^2}} - \frac{1}{\sqrt{G[\bar{q},\bar{E}]}} + \frac{1}{\sqrt{G[\bar{q},\bar{E}]}} \right\} d\bar{q}. \tag{2.2.60}$$

Here, $G[\bar{q},\bar{E}]$ is a Taylor expansion of $(\dot{\bar{q}})^2$ around q_i and $\bar{E} = E(\beta=\infty)$, given by

$$G[\bar{q},\bar{E}] = -W''(q_i)(\bar{q}-q_i)^2 + 2(E-\bar{E}) = V''(q_i)(\bar{q}-q_i)^2 + 2(E-\bar{E}). \tag{2.2.61}$$

The third term in (2.2.60) can be computed explicitly as

$$2\int_{q_-}^{q_+} \frac{1}{\sqrt{G[\bar{q},\bar{E}]}} d\bar{q} = \frac{2}{\sqrt{V''(q_i)}} \log(q_f - q_i) - \frac{1}{\sqrt{V''(q_i)}} \log\left(-\frac{E-\bar{E}}{2V''(q_i)}\right). \tag{2.2.62}$$

Here, we have used the approximation

$$q_- \approx q_i + \sqrt{-\frac{2}{V''(q_i)}(E-\bar{E})}, \tag{2.2.63}$$

valid in the limit of $E \to \bar{E}$. For the first two integrals in (2.2.60), taking the smooth limit $E \to \bar{E}$ ($\beta \to \infty$), we find

$$2\int_{q_-}^{q_+} \left\{ \frac{1}{\sqrt{(\dot{\bar{q}})^2}} - \frac{1}{\sqrt{G[\bar{q},\bar{E}]}} \right\} d\bar{q} \longrightarrow 2\int_{q_i}^{q_f} \left\{ \frac{1}{\sqrt{(\dot{\bar{q}})^2}} - \frac{1}{\sqrt{V''(q_i)}} \frac{1}{\bar{q}-q_i} \right\} d\bar{q}. \tag{2.2.64}$$

Combining (2.2.62) and (2.2.64), we rewrite (2.2.60), yielding the expression for $E(\beta)$ for large β

$$\begin{aligned} E(\beta) \approx -2V''(q_i)(q_f-q_i)^2 \exp\left[2\sqrt{V''(q_i)} \int_{q_i}^{q_f} \left\{ \frac{1}{\sqrt{(\dot{\bar{q}})^2}} - \frac{1}{\sqrt{V''(q_i)}} \frac{1}{\bar{q}-q_i} \right\} d\bar{q} \right] \\ \times \exp\left[-\sqrt{V''(q_i)}\beta \right] + \bar{E}. \end{aligned} \tag{2.2.65}$$

Thus, the derivative of energy concerning β appearing in (2.2.58) is given by the following expression.

$$\begin{aligned} \frac{\partial E}{\partial \beta} \approx 2(V''(q_i))^{3/2}(q_f-q_i)^2 \exp\left[2\sqrt{V''(q_i)} \int_{q_i}^{q_f} \left\{ \frac{1}{\sqrt{\dot{\bar{q}}^2}} - \frac{1}{\sqrt{V''(q_i)}} \frac{1}{\bar{q}-q_i} \right\} d\bar{q} \right] \\ \times \exp\left[-\sqrt{V''(q_i)}\beta \right]. \end{aligned} \tag{2.2.66}$$

Due to the β-dependent factor in (2.2.66), $\det{}'\mathbf{M}$ diverges exponentially in the limit of $\beta \to \infty$. However, this divergence can be eliminated by taking the ratio with the reference determinant $\det \mathbf{M}_0$. The finite expression after this regularization yields

$$\begin{aligned}&\lim_{\beta\to\infty} \frac{\det{}'\mathbf{M}}{\det \mathbf{M}_0} \\ &= -\frac{N_0}{2(V''(q_i))^{3/2}(q_f - q_i)^2} \exp\left[-2\sqrt{V''(q_i)} \int_{q_i}^{q_f} \left\{ \frac{1}{\sqrt{\dot{\bar{q}}^2}} - \frac{1}{\sqrt{V''(q_i)}} \frac{1}{\bar{q} - q_i} \right\} d\bar{q} \right].\end{aligned} \tag{2.2.67}$$

Substituting this result to (2.1.53), we obtain the 1-loop decay rate formula in quantum mechanical systems as follows

$$\Gamma = \frac{(V''(q_i))^{3/4}(q_f - q_i)}{\sqrt{\pi\hbar}} \exp\left[\sqrt{V''(q_i)} \int_{q_i}^{q_f} \left\{ \frac{1}{\sqrt{\dot{\bar{q}}^2}} - \frac{1}{\sqrt{V''(q_i)}} \frac{1}{\bar{q} - q_i} \right\} d\bar{q} \right] e^{-B/\hbar}. \tag{2.2.68}$$

Chapter 3

D3-brane Catalysis in Stringy Vacuum Decay

In this chapter, we will discuss a specific model of the enhancement of vacuum decay constructed purely within the framework of string theory. In string theory, it is known that a metastable state can be geometrically realized by wrapping D5-branes and anti D5-branes on a manifold with singularities [91–93]. In this model, the only dynamical degree of freedom is the radius of the brane bubble that arises in four dimensional spacetime, allowing the problem to be treated as a relatively simple one dimensional quantum mechanical problem. Here, we consider the scenario where D3-branes are wrapped on the internal space and form a bound state with (anti) D5-branes [84–86]. These D3-branes dissolve into the (anti) D5-branes and turn into a magnetic field, playing an important role as catalysts in enhancing the instability of the bubble. We calculate the decay rate of this metastable state using the method reviewed in Chap. 2, and show the magnetic field dependence of the decay rate at the 1-loop level. We also address the limits of applying the WKB approximation in regions with strong catalytic effects and present a result derived by reducing the problem to a cubic anharmonic oscillator system. Finally, we compare the critical life-time where the potential barrier vanishes with the TCC condition.

The organization of this chapter is as follows. In Section 3.1, we review one of the swampland conjectures that motivated our research: the trans-Planckian censorship conjecture. Section 3.2 provides the necessary background on string theory to understand the setup, with a particular focus on the phenomenon where D(p-2)-branes dissolve into Dp-branes and form a bound state [84–86]. This Section is mainly based on [86]. Section 3.3 outlines the geometric realization of a metastable state using branes, based on the work of [91–93]. In Section 3.4, we present the calculation of the bounce action and the exponential prefactor that represents the contribution from quantum fluctuations. Here, we discuss the treatment of zero modes specific to non-canonical theories and the zeta function regularization of the functional determinant for general Sturm-Liouville operators. In Section 3.5, we show that by reducing the Lagrangian to an anharmonic oscillator, the system retains a finite life-time even at the critical value of the magnetic field where the potential barrier disappears. We then compare this life-time with the TCC condition and discuss the resulting constraints on the parameter space. Finally, Section 3.6 is devoted to the discussion and summary of this chapter. Section 3.4 and Section 3.5 are mainly based on our work [1].

3.1 Brief review of trans-Planckian censorship conjecture

The trans-Planckian censorship conjecture (TCC) stems from considerations regarding the growth of fluctuations during inflation. According to observations of the Cosmic Microwave Background (CMB), fluctuations exist in matter and energy [10]. It is well known that inflationary theory explains these large-scale structures effectively. However, since all fluctuations during inflation are stretched out, there was concern that even fluctuations in regions smaller than the Planck length, where quantum gravity dominates, could become enlarged beyond the Hubble radius, eventually becoming observable classically. From the consistency of quantum gravity theory, such fluctuations should remain within the quantum region, and this issue has been a subject of discussion since the early 2000s. This is referred to as the trans-Planckian problem [115].

On the other hand, within the context of string theory, it has been pointed out that constructing a dS vacuum within its framework is extremely difficult. In string theory, to construct a four-dimensional dS vacuum, it is necessary to carefully control, e.g., the geometry of the background spacetime, the fluxes, and the Dp-branes [116]. Given these technical difficulties, it is conceivable that constructing a four-dimensional dS vacuum in string theory, where the internal space is compact and the moduli are perfectly stabilized, may be impossible. In response, the following dS conjecture was proposed [55, 57].

de Sitter conjecture
Scalar potentials of the EFTs coupled to gravity must satisfy one of the conditions.

$$|\nabla V| \geq \frac{c}{M_{\rm pl}} V \quad or \quad \min\left(\nabla_i \nabla_j V\right) \leq -\frac{c'}{M_{\rm pl}^2} V, \quad 0 < c,\ c' = \mathcal{O}(1), \tag{3.1.1}$$

where $|\nabla V| = \sqrt{\sum g^{ij} \partial V_i \partial_j V}$.

If this conjecture is correct, the dS vacuum consistent with QG must be unstable or decay fast enough.

If fluctuations shorter than the Planck length remain within the quantum scale, there must be an upper limit to the duration of inflation. The aforementioned dS conjecture asserts that the vacua of effective theories consistent with quantum gravity must decay sufficiently quickly, at least. If this conjecture is correct, it is expected that theories leading to the trans-Planckian problem would belong to the Swampland. The idea of the authors of [67, 68] is not to address the trans-Planckian problem by deducing it from other swampland conjectures but rather to treat it as one of the independent swampland conjectures. According to their paper, the statement of TCC is as follows.

Trans-Planckian censorship conjecture
In field theories consistent with QG, exponential expansion that fluctuations larger than the Hubble radius are derived from fluctuations smaller than the Planck length cannot occur.
$\Leftrightarrow$ Quantum fluctuations smaller than the Planck length must remain quantum.

The statement in mathematical language is as follows.[1]

$$\frac{a_f}{a_i} < \frac{M_{\rm pl}}{H_f}, \tag{3.1.2}$$

where a_i and a_f are the scale factor of the spacetime at the initial and final state in a time interval. H_f is the Hubble scale at the final state.

This inequality becomes obvious in the limit of decoupling from gravity, i.e., $M_{\rm pl} \to \infty$, which imposes no restrictions.

Applying the condition (3.1.2) to the inflation period, we can obtain the condition on the duration of the inflation as

$$\tau \leq H_I^{-1} \log \frac{M_{\rm pl}}{H_I} \ , \qquad H_I = \sqrt{\frac{8\pi G V_I}{3}}, \tag{3.1.3}$$

where H_I is the Hubble parameter during the inflation. That is, as a consequence of the TCC, a metastable dS vacuum with a life-time exceeding this upper bound would belong to the swampland.

3.2 Dynamics of Dp-brane

3.2.1 Minimal introduction to Dp-brane

Let us denote the string coordinates as $X^n(\tau, \sigma)$. Here, σ parameterizes the coordinates on the worldsheet of the open string, where $\sigma = 0$ corresponds to the starting point and $\sigma = \pi$ corresponds to the endpoint. The variable τ represents the proper time on the string worldsheet. Using these parameters, the relativistic action for a string in D-dimensional spacetime can be written as

$$S_{NG} = -T \int d\tau d\sigma \sqrt{-\det G_{ab}}, \tag{3.2.1}$$

$$G_{ab} = g_{mn} \partial_a X^m \partial_b X^n. \tag{3.2.2}$$

Here, G_{ab} is the induced metric on the worldsheet embedded in D-dimensional spacetime. The expression (3.2.1) is called the Nambu-Goto action. The differential operator in the above equations is defined as $\partial_a \equiv \frac{\partial}{\partial \sigma^a}$, where $\sigma^a = (\tau, \sigma)$. The parameter T represents the string tension and can be expressed in terms of the parameter α', known as the Regge slope, as $T = (2\pi\alpha')^{-1}$. The equations of motion governing the string can be derived by varying the Nambu-Goto action (3.2.1).

[1] More precisely, it is appropriate to write

$$\frac{a_f}{a_i} < \frac{K M_{\rm pl}}{H_f}$$

including a constant K of about $\mathcal{O}(1)$, but since such a difference has little effect on the result, $K = 1$ is chosen here.

A Dp-brane can be introduced as the endpoint of an open string. A Dp-brane is a higher-dimensional object that extends in p-dimensional space, allowing an open string to move freely along directions tangent to its world volume. This implies that the string satisfies the following Neumann boundary conditions:

$$\partial_\sigma X^m(\tau, \sigma = 0) = \partial_\sigma X^m(\tau, \sigma = \pi) = 0, \quad (m = 0, \cdots, p). \tag{3.2.3}$$

On the other hand, the endpoints of the open string cannot move in directions orthogonal to the brane' s world volume. In such directions, the string satisfies Dirichlet boundary conditions:

$$X^a(\tau, \sigma = 0) = X^a(\tau, \sigma = \pi) = \bar{x}^a, \quad (a = p + 1, \cdots, D). \tag{3.2.4}$$

Here, $\bar{x}^a$ are arbitrary constants. When considering the quantum theory of Dp-branes, it is known that Dp-branes cannot be directly quantized. However, as previously mentioned, by treating it as the endpoint of an open string and quantizing the open string attached to the Dp-brane, the allowed modes correspond to the degrees of freedom on the Dp-brane. The mode expansion of an open string ending on a Dp-brane can be written as

$$X^a(\tau, \sigma) = \bar{x}^a + \sqrt{2\alpha'} \sum_{n \neq 0} \frac{\alpha_n^a}{n} e^{-in\tau} \sin n\sigma, \tag{3.2.5}$$

where the commutation relations for the modes are given by

$$\left[\alpha_m^a, \alpha_n^b\right] = m\delta^{ab}\delta_{m+n,0}. \tag{3.2.6}$$

A general state in the open string' s state space is constructed by applying creation operators to the ground state $|p^+, p^2, \cdots, p^p\rangle$. Among these states, there is a massless $U(1)$ gauge field, which corresponds to an electromagnetic field. This implies that an electromagnetic field universally exists on the world volume of a Dp-brane.

On the other hand, provided the fact that electromagnetic fields couple with point particles (0-form) as

$$S_A = -e \int A_\mu(x) dx^\mu \ , \tag{3.2.7}$$

there should exist a 2-form field such that similarly couples to one dimensional string. This kind of field is called a B-field:

$$S_B = -\frac{1}{2} \int d\tau d\sigma \epsilon^{\alpha\beta} \partial_\alpha X^\mu \partial_\beta X^\nu B_{\mu\nu} \left(X(\tau, \sigma)\right) \ . \tag{3.2.8}$$

As we will see in the next section, the existence of this electromagnetic field A_μ and B field $B_{\mu\nu}$ in pairs ensures gauge invariance on the world volume.

Let us now consider the boundary conditions when an electromagnetic field exists on a Dp-brane, as this will be relevant for the subsequent discussion. Since the open string couples to the electromagnetic field at its endpoints, the action is given by

$$S = \int d\tau d\sigma \mathcal{L}_{NG}(\dot{X}, X') + \int d\tau A_m(X) \frac{dX^m}{d\tau}\bigg|_{\sigma=\pi} - \int d\tau A_m(X) \frac{dX^m}{d\tau}\bigg|_{\sigma=0}, \tag{3.2.9}$$

where $\mathcal{L}_{NG}$ is the Nambu-Goto Lagrangian. If F_{mn} is constant, the gauge field can be chosen as

$$A_n(x) = \frac{1}{2} F_{mn} x^m. \tag{3.2.10}$$

Substituting this into (3.2.9), the action can be rewritten as

$$S = \int d\tau d\sigma \mathcal{L}_{NG}(\dot{X}, X') + \frac{1}{2} \int d\tau F_{mn} \left(X^m \, \partial_\tau X^n|_{\sigma=\pi} - X^m \, \partial_\tau X^n|_{\sigma=0} \right). \tag{3.2.11}$$

By considering the variation of this action along the directions parallel to the Dp-brane and selecting an appropriate gauge, the boundary condition becomes:

$$\partial_\sigma X_m - 2\pi\alpha' F_{mn} \partial_\tau X^n = 0, \quad \sigma = 0, \pi. \tag{3.2.12}$$

3.2.2 Effective field theory on Dp-brane

The low-energy effective theory on the world volume of Dp-branes can be derived by requiring the vanishing of the β function in the σ model [117]. The resulting action is known to take the form of the Dirac-Born-Infeld (DBI) action.[2]

$$S_{\text{DBI}} = -T_p \int d^{p+1}\xi \sqrt{-\det\left(G_{ab} + B_{ab} + 2\pi\alpha' F_{ab}\right)}. \tag{3.2.13}$$

Here, G_{ab} is the induced metric, reflecting the geometry of the Dp-brane:

$$G_{ab} = \partial_a X^\alpha \partial_b X_\alpha, \tag{3.2.14}$$

where a and b denote directions along the worldvolume of the Dp-brane in the ten dimensional spacetime. This action is a natural generalization of the Nambu-Goto action to situations where an electromagnetic field exists and is manifestly Lorentz invariant.

The DBI action incorporates the combination $B_{ab} + 2\pi\alpha' F_{ab}$, where the B-field and the gauge field strength appear as a set. The action on the brane must include these quantities to maintain gauge invariance. This can be understood from the action on the world sheet of a string with endpoints on the Dp-brane. The action on the world sheet takes the following form

$$\begin{aligned} S &= S_B + S_A \\ &= -\frac{1}{2} \int_\Sigma d^2\sigma \, \epsilon^{\alpha\beta} \partial_\alpha X^\mu \partial_\beta X^\nu B_{\mu\nu}\left(X(\tau,\sigma)\right) + \int_{\partial\Sigma} d\tau \, A_\mu \partial_\tau X^\mu. \end{aligned} \tag{3.2.15}$$

Here, the gauge transformation for the B-field is defined as

$$\delta B_{\mu\nu} = \partial_\mu \Lambda_\nu - \partial_\nu \Lambda_\mu. \tag{3.2.16}$$

Applying this transformation to the action (3.2.15) leaves the following surface terms due to contributions from the string endpoints

$$\delta S_B = -\int d\tau \left[\Lambda_\nu \partial_\tau X^\nu \big|_{\sigma=\pi} - \Lambda_\nu \partial_\tau X^\nu \big|_{\sigma=0} \right]. \tag{3.2.17}$$

[2] This action was originally proposed in the context of nonlinear electrodynamics to avoid the divergence of the self-energy of a point charge.

This situation indicates that gauge invariance is broken under the transformation of the B-field alone. To resolve this issue, the gauge transformation of the gauge field coupled to the string endpoints must also be considered; that is,

$$\delta A_\nu = \Lambda_\nu. \tag{3.2.18}$$

Under this transformation, the variation of the gauge field term in the action is

$$\delta S_A = \int d\tau \left[\Lambda_\nu \partial_\tau X^\nu\big|_{\sigma=\pi} - \Lambda_\nu \partial_\tau X^\nu\big|_{\sigma=0}\right]. \tag{3.2.19}$$

(3.2.19) precisely cancels the surface terms in (3.2.17), ensuring overall gauge invariance of the action.

3.2.3 T-duality

T-duality is a type of symmetry that connects two theories compactified on $\mathbb{S}^1$ with different radii. T-duality can be applied to any spatial direction, and depending on the chosen direction, it influences the profile of Dp-branes appearing in the dual theory. In this Section, we demonstrate that applying T-duality along a direction in which a Dp-brane is extended results in a D(p-1)-brane while applying it along a direction in which the Dp-brane is not extended results in a D(p+1)-brane. Let us consider the situation where a closed string is wound around a cylinder. If the string wraps once around the cylinder with radius R, the following condition holds:

$$X(\tau, \sigma = 2\pi) - X(\tau, \sigma = 0) = 2\pi R. \tag{3.2.20}$$

By analogy, when the string wraps m times around the cylinder, the following relation is satisfied.

$$X(\tau, \sigma + 2\pi) = X(\tau, \sigma) + 2\pi m R. \tag{3.2.21}$$

Here, we define the winding number ω as

$$\omega \equiv \frac{mR}{\alpha'}, \tag{3.2.22}$$

which allows us to rewrite (3.2.21) in the following form

$$X(\tau, \sigma + 2\pi) = X(\tau, \sigma) + 2\pi\alpha'\omega. \tag{3.2.23}$$

Now, let X^9 be a $\mathbb{S}^1$ compactified direction. If we write X^9 with the right-moving sector and the left-moving sector, each mode expansion is given as follows

$$X^9(\tau, \sigma) = X^9_L(\tau + \sigma) + X^9_R(\tau - \sigma)\ , \tag{3.2.24}$$

$$X^9_L(\tau + \sigma) = \frac{1}{2}(x^9_0 + q^9_0) + \frac{\alpha'}{2}(p^9 + \omega)(\tau + \sigma) + i\sqrt{\frac{\alpha'}{2}} \sum_{n\neq 0} \frac{\bar{\alpha}^9_n}{n} e^{-in(\tau+\sigma)}\ , \tag{3.2.25}$$

$$X^9_R(\tau - \sigma) = \frac{1}{2}(x^9_0 - q^9_0) + \frac{\alpha'}{2}(p^9 - \omega)(\tau - \sigma) + i\sqrt{\frac{\alpha'}{2}} \sum_{n\neq 0} \frac{\alpha^9_n}{n} e^{-in(\tau-\sigma)}\ , \tag{3.2.26}$$

where ω is the winding number defined by (3.2.22). Substituting (3.2.25) and (3.2.26) into (3.2.24), we obtain the mode expansion of X^9 as a following equation.

$$X^9(\tau,\sigma) = x_0^9 + \alpha' p^9 \tau + \alpha' \omega \sigma + i\sqrt{\frac{\alpha'}{2}} \sum_{n\neq 0} \frac{e^{-in\tau}}{n} \left(\bar{\alpha}_n^9 e^{-in\sigma} + \alpha_n^9 e^{in\sigma}\right) \ . \tag{3.2.27}$$

At this point, the mass spectrum is calculated as

$$M^2 = \frac{n^2}{R^2} + \frac{m^2 R^2}{\alpha'^2} + \frac{2}{\alpha'}\left(N^\perp + \bar{N}^\perp - 2\right) \ , \tag{3.2.28}$$

$$N^\perp - \bar{N}^\perp = \alpha' p^9 \omega = nm \ , \tag{3.2.29}$$

where $N^\perp$ and $\bar{N}^\perp$ are the number operators which is defined as

$$N^\perp = \sum_n^\infty \alpha_n^{I\dagger} \alpha_n^I \ , \quad \bar{N}^\perp = \sum_n^\infty \bar{\alpha}_n^{I\dagger} \bar{\alpha}_n^I \ . \tag{3.2.30}$$

The relation between the number operators (3.2.29) is derived from a level-matching condition. Also, n is the quantum number associated with the quantization of the momentum due to the $\mathbb{S}^1$ compactification in the x^9 direction:

$$p^9 = \frac{n}{R} \ . \tag{3.2.31}$$

From the expression in (3.2.28), we can see that the following transformation leaves the spectrum invariant

$$R \to \frac{\alpha'}{R}, \quad n \to m, \quad m \to n. \tag{3.2.32}$$

This transformation is equivalent to introducing the dual coordinates for (3.2.24) as follows

$$\tilde{X}^9 \equiv X_L^9(\tau+\sigma) - X_R^9(\tau-\sigma). \tag{3.2.33}$$

Equation (3.2.33) is equivalent to considering the mapping

$$(X_L^9, X_R^9) \longrightarrow (X_L^9, -X_R^9), \tag{3.2.34}$$

which is called T-duality. In fact, by defining T-duality as in (3.2.34), there is no longer a need to first consider the $\mathbb{S}^1$ compactification.

T-duality can also be confirmed by examining the mass spectrum in the case of open strings. For open strings, T-duality is understood as the following mapping

$$(X_L, X_R) \longrightarrow (X_L, -X_R). \tag{3.2.35}$$

However, in the case of open strings, we must pay attention to the boundary conditions, which becomes apparent when considering derivatives with respect to σ and τ as

$$\partial_\sigma X = X_L'(\tau+\sigma) - X_R'(\tau-\sigma) = \partial_\tau \tilde{X}, \tag{3.2.36}$$

$$\partial_\tau X = X_L'(\tau+\sigma) + X_R'(\tau-\sigma) = \partial_\sigma \tilde{X}. \tag{3.2.37}$$

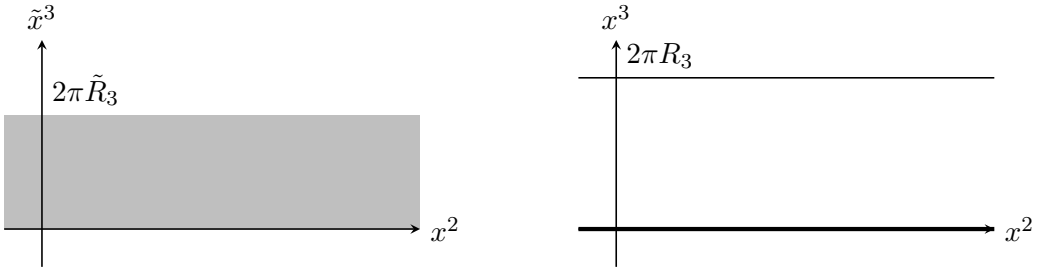

Figure 3.1: T-duality of Dp-branes. The shaded region in the left panel represents the Dp-brane spreading. Taking a T-dual in $\tilde{x}^3$ direction, we obtain a D(p-1)-brane along the dual cylinder as in the right panel.

Comparing (3.2.36) and (3.2.37), we observe that the Dirichlet and Neumann boundary conditions are interchanged before and after T-duality. Recall that a Dp-brane is a higher-dimensional object where open strings have their endpoints. Given this boundary condition exchange, the space in which the Dp-brane exists also changes. When considering T-duality in the direction in which the Dp-brane's world volume expands, Neumann boundary conditions are replaced by Dirichlet boundary conditions, and the Dp-brane transforms into a D(p-1)-branes. Conversely, when T-duality is considered in the direction in which the world volume does not expand, the opposite occurs, forming a D(p+1)-brane.

In the discussion so far, we have ignored the presence of fields on the brane. However, as mentioned in Section 3.2.1, $U(1)$ electromagnetic fields exist on the world volume. Therefore, it is necessary to consider T-duality when electromagnetic fields are present. In particular, it is important to understand the duality in the presence of a magnetic field in order to understand our setup, which we describe in Section 3.3.

Assume that the world volume spans the $(x^2, \tilde{x}^3)$ directions and that the $\tilde{x}^3$ direction is compactified with a radius $\tilde{R}_3$, as shown in Figure 3.1(*a*). Let the coordinates of the open string be expressed as $(X^2, \tilde{X}^3)$. If we apply T-duality along the $\tilde{x}^3$ direction, the dual coordinate X^3 corresponding to $\tilde{X}^3$ resides on a circle with radius $R_3 = \alpha'/\tilde{R}_3$, as depicted in Figure 3.1(*b*). Considering the boundary condition exchange under T-duality, the Dirichlet boundary condition of $\tilde{X}^3$ implies that in the dual space, a D(p-1)-brane exists, extending in the x^2 direction.

When considering the presence of a magnetic field on the world volume, an interesting picture emerges. The boundary conditions for open strings ending on a Dp-brane with a magnetic field are given, from (3.2.12), by the following equations:

$$\begin{cases} \partial_\sigma X^2 - 2\pi\alpha' B \partial_\tau \tilde{X}^3 = 0, \\ \partial_\sigma \tilde{X}^3 + 2\pi\alpha' B \partial_\tau X^2 = 0, \end{cases} \tag{3.2.38}$$

Introducing a dimensionless magnetic field $\mathcal{B} \equiv 2\pi\alpha' B$ and Rewriting the boundary conditions using the light-cone coordinates on the world volume, $\sigma^\pm = \tau \pm \sigma$, we obtain

$$\partial_+ \begin{pmatrix} X^2 \\ \tilde{X}^3 \end{pmatrix} = \begin{pmatrix} \frac{1-\mathcal{B}^2}{1+\mathcal{B}^2} & \frac{2\mathcal{B}}{1+\mathcal{B}^2} \\ -\frac{2\mathcal{B}}{1+\mathcal{B}^2} & \frac{1-\mathcal{B}^2}{1+\mathcal{B}^2} \end{pmatrix} \partial_- \begin{pmatrix} X^2 \\ \tilde{X}^3 \end{pmatrix}. \tag{3.2.39}$$

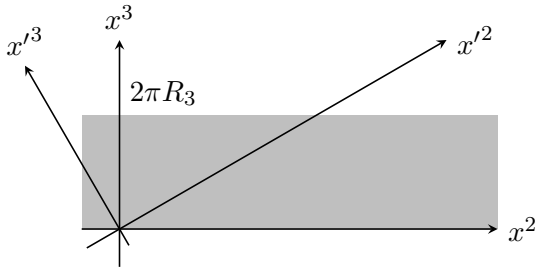

Figure 3.2: D(p-1)-brain rotated by an arbitrary angle α in the dual world, D(p-1)-brain exists along x'^2 axis.

Next, consider a D(p-1)-brane tilted by an angle α counterclockwise from the x^2 direction in the dual world, as shown in Figure 3.2. This D(p-1)-brane is aligned with the x'^2 axis, where the boundary conditions for open strings are of the Neumann type for X'^2 and the Dirichlet type for X'^3:

$$\partial_+ \begin{pmatrix} X'^2 \\ X'^3 \end{pmatrix} = \begin{pmatrix} 1 & 0 \\ 0 & -1 \end{pmatrix} \partial_- \begin{pmatrix} X'^2 \\ X'^3 \end{pmatrix}. \tag{3.2.40}$$

Applying a rotation transformation to rewrite these boundary conditions in terms of (X^2, X^3) and then performing T-duality along the x^3 direction, the final boundary conditions are expressed as

$$\partial_+ \begin{pmatrix} X^2 \\ \tilde{X}^3 \end{pmatrix} = \begin{pmatrix} \cos 2\alpha & -\sin 2\alpha \\ \sin 2\alpha & \cos 2\alpha \end{pmatrix} \partial_- \begin{pmatrix} X^2 \\ \tilde{X}^3 \end{pmatrix}. \tag{3.2.41}$$

By setting $\mathcal{B} = -\tan\alpha$, the boundary conditions in (3.2.39) and (3.2.41) are found to be identical. This correspondence demonstrates that a Dp-brane with a magnetic field on its world volume and a tilted D(p-1)-brane is T-dual to each other. This duality relationship will play a key role in the next Section, where we discuss the bound states of Dp-branes.

3.2.4 D(p-2)-Dp bound states

Let us now consider the situation where a D(p-2)-brane ends on a Dp-brane. The discussion in this section is critically important to the model we are investigating in the next section. We consider a D(p-1)-brane compactified on a torus T^2 with radii R_2 and R_3, where the compactified directions are referred to as x^2 and x^3, respectively (see Figure 3.3). In the left panel of Figure 3.3, the D(p-1)-brane, represented by the black line, wraps once around the x^2 direction while winding n times in the x^3 direction. When we perform a T-duality transformation along the x^3 direction, the system becomes, as discussed in the previous section, a Dp-brane with a magnetic field. Since the T-duality transformation does not change the whole energy, the static energy of the Dp-brane with a magnetic field can be calculated by evaluating the static energy of the D(p-1)-brane wrapped on the torus. This energy is given by

$$E = T_{p-1}(\tilde{g}) V_{p-2} \sqrt{(2\pi R_2)^2 + (2\pi n R_3)^2}, \tag{3.2.42}$$

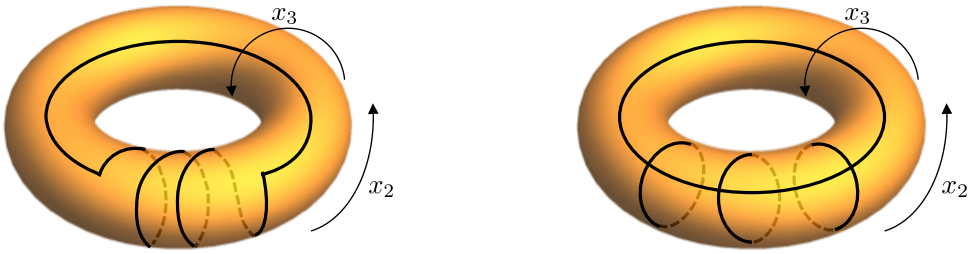

(a) (b)

Figure 3.3: Schematic diagrams for homotopy equivalent configurations ($n = 3$).

where $T_{p-1}(\tilde{g})$ is the D(p-1)-brane tension and V_{p-2} represents the volume along the unwrapped directions. Rewriting this energy in terms of the description of the Dp-brane with a magnetic field, we obtain the following expression

$$E = \sqrt{M_p^2 + (nM_{p-2})^2}, \tag{3.2.43}$$

where M_p is the mass of the Dp-brane, and M_{p-2} is the mass of the D(p-2)-brane.

On the other hand, as shown in the right panel of Figure 3.3, the D(p-1)-brane wrapped on the torus is homotopically equivalent to a configuration having a single D(p-1)-brane in the x^2 direction and n D(p-1)-branes in the x^3 direction. Performing a T-duality transformation along the x^3 direction in the latter configuration results in the D(p-1)-brane compactified in the x^2 direction being transformed into a Dp-brane, while the n D(p-1)-branes compactified in the x^3 direction are transformed into D(p-2)-branes. The total energy of the system, in this case, becomes a simple sum of the energy contributions from the single Dp-brane and the n D(p-2)-branes, namely

$$E = M_p + nM_{p-2}, \tag{3.2.44}$$

Comparing (3.2.43) and (3.2.44), the former is smaller. This indicates the presence of a phenomenon where independently existing Dp-branes and D(p-2)-branes form a bound state, transitioning into a Dp-brane with a magnetic field. In other words, after forming a bound state, the remnants of the lower-dimensional brane appear as electromagnetic fields on the Dp-brane. This process is therefore referred to as *dissolving* of Dp-branes.

3.3 Geometrical realization of metastable state

3.3.1 Geometrically realized vacua with D5 and anti D5

This section reviews a method for realizing metastable states by wrapping D5-branes and anti D5-branes on a singular manifold. Let us consider the following non-compact Calabi-Yau threefold as the internal space [91–93]

$$0 = z_1^2 + z_2^2 + z_3^2 + W'(z_4)^2, \quad W'(z_4) = g(z_4 - a_1)(z_4 - a_2), \tag{3.3.1}$$

where z_i are complex variables, made dimensionless by the finite string length l_s. As is obvious from (3.3.1), this manifold is singular at $z_4 = a_1, a_2$. However, these singularities

can be resolved by replacing their neighborhoods with finite two-spheres and blowing them up. In other words, the points $z_4 = a_1, a_2$ can be treated simply as two-cycles at the endpoints of $\mathbb{S}^3$.

Now, let us wrap N_1 D5-branes on the two-cycle $[C_1]$ at $z_4 = a_1$ and N_2 anti D5-branes on the two-cycle $[C_2]$ at $z_4 = a_2$. The two-cycles $[C_1]$ and $[C_2]$ belong to the same homology class and are not independent: $[C_1] + [C_2] = 0$. This implies that the D5-branes and anti D5-branes annihilate each other, restoring a supersymmetric vacuum. However, to do so, they need to gain the additional energy required to traverse the internal large $\mathbb{S}^3$. This indicates the presence of a potential barrier between the two branes. In other words, this system geometrically realizes a metastable vacuum with supersymmetry broken. For simplicity, we will assume $N_1 = N_2 = 1$ in the following discussion.

Considering a manifold like (3.3.1) as the internal space has the advantage of incorporating stringy corrections while neglecting the effects of four dimensional gravity. In this model, the decay process is dominated by the dynamics of the Dp-branes near the singularities, and the effective theory of these Dp-branes depends on the string length l_s. On the other hand, if we denote the compactification scale as V and the 10-dimensional Newton constant as G_{10}, the 4-dimensional effective Newton constant G_4 is given by $G_4 = V/G_{10}$. By taking the non-compact limit, gravity will be decoupled. In other words, this corresponds to the so-called brane limit, where stringy corrections remain finite while the contributions of four dimensional gravity become negligibly small.

On the other hand, it should be emphasized that this model is just a toy model, given its reliance on the non-compact limit. This chapter implicitly assumes that the non-compact manifold shown in (3.3.1) is embedded within a larger manifold, making the entire space compact. Ideally, one should consider dS vacua on compact manifolds, but their explicit construction remains a topic of ongoing debate [56, 57]. Nonetheless, our current interest lies in the structure near the singularities, and whether the background geometry is compact or not is expected to have little impact on the dynamics near the singularities. Therefore, in the following discussion, we will not explicitly consider the embedding into compact manifolds.

Let us consider the specific geometry of the Dp-branes. As mentioned above, the D5-branes and anti D5-branes are wrapped on $\mathbb{S}^2$, which is a subspace of $\mathbb{S}^3$ at $\psi_I = 0, \pi$, while the remaining three components span the Minkowski space. On the other hand, the domain wall D5-branes that form brane bubbles with a radius R in four-dimensional spacetime are wrapped on the entirety of $\mathbb{S}^3$ in the internal space. For a visual understanding, see Figure 3.4. As discussed later, we will also consider wrapping D3-branes on $\mathbb{S}^3$. Table 3.1 summarizes the full configuration of Dp-branes. Circles indicate that the Dp-brane extends in that direction, while crosses indicate that it does not. Special attention should be paid to triangles ($\triangle$). For example, the configuration of the domain wall D5-brane in the Minkowski space, where all entries are marked as triangles, signifies that it wraps around an $\mathbb{S}^2$ bubble in the Minkowski space. In other words, it does not fully extend throughout the Minkowski space. The same applies to configurations in the internal space.

Based on the above setup, we derive the effective action which describes the decay phenomenon. Main contributions come from the DBI action, so we must calculate this action for (anti) D5-branes and domain wall D5-branes. Let us consider the former case.

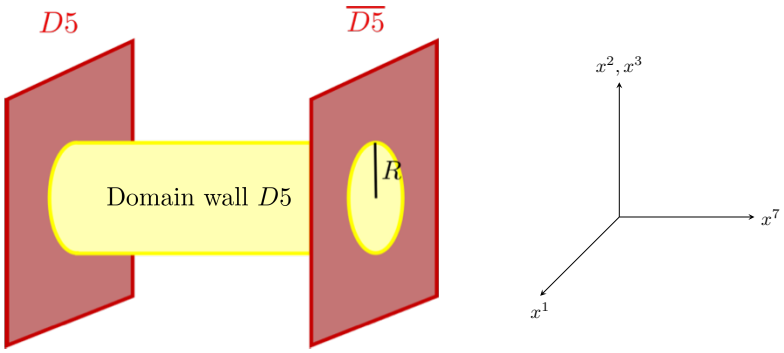

Figure 3.4: A schematic diagram for D5-branes and anti D5-branes wrapped on the tips of the internal $\mathbb{S}^3$. This figure was taken from [1] and slightly modified.

Table 3.1: Branes configurations

	0	1	2	3	4	5	6	7	8	9
D5/antiD5	○	○	○	○	△	△	△	×	×	×
DWD5	○	△	△	△	△	△	△	△	×	×
D3	○	×	×	×	△	△	△	△	×	×

The induced metric on (anti) D5-branes are given by [91–93]

$$\frac{ds^2_{\mathrm{D5}/\overline{\mathrm{D5}}}}{l_s^2} = -dT^2 + d\xi^2 + \xi^2\left(d\theta^2 + \sin^2\theta d\varphi^2\right) + L^2\sin^2\psi_I\left(d\theta_I^2 + \sin^2\theta_I d\varphi_I^2\right), \quad (3.3.2)$$

where T, ξ and L are dimensionless variables in the four dimensional Minkowski spacetime and the subscriptions $_I$ of ψ_I, θ_I and φ_I denote the internal coordinates. Consider the presence of the NS B-field $B^{NS}_{\theta_I\varphi_I}$ in the (θ_I, φ_I) directions of the internal space. In this case, the determinant factor of the DBI action can be computed as follows

$$-\det\left(G_{ab} + B_{ab} + 2\pi\alpha' F_{ab}\right) = \xi^4\sin^2\theta \times \left(L^4\sin^4\psi_I\sin^2\theta_I + (B^{NS}_{\theta_I\varphi_I})^2\right). \quad (3.3.3)$$

Thus, the action of the D5-brane is given by

$$S_{D5} = -T_{D5}\int d^4x\, d\theta_I d\varphi_I \sqrt{L^4\sin^4\psi_I\sin^2\theta_I + (B^{NS}_{\theta_I\varphi_I})^2}. \quad (3.3.4)$$

The action of the anti D5-brane is of the same form. Now, let us define the integrated value of the B-field as

$$r_{NS} = \int_{\mathbb{S}^2} B^{NS}_2. \quad (3.3.5)$$

This implies that the (θ_I, φ_I) components of the B-field can be expressed as:

$$B^{NS}_{\theta_I\varphi_I} = \frac{r_{NS}}{4\pi}\sin\theta_I \equiv b_{NS}\sin\theta_I. \quad (3.3.6)$$

Using (3.3.6), the aforementioned action can be rewritten as

$$S_{D5} = -T_{D5}\int d^4x \int d\theta_I d\varphi_I \sin\theta_I \sqrt{L^4 \sin^4\psi_I + \left(\frac{r_{NS}}{4\pi}\right)^2} = -T_{D5} A(\psi_I)\int d^4x, \quad (3.3.7)$$

where $A(\psi_I) = 4\pi\sqrt{L^4\sin^4\psi_I + (r_{NS}/4\pi)^2}$. The function $A(\psi_I)$ increases as ψ_I varies from 0 to π, indicating the existence of a potential barrier between the D5-brane at $\psi_I = 0$ and the anti D5-brane at $\psi_I = \pi$. Since the branes are located at $\psi_I = 0$ and $\psi_I = \pi$, the correct expression for the DBI action is

$$S_{D5} = -T_{D5} r_{NS}\int d^4x. \quad (3.3.8)$$

Taking into account the formation of a bubble in four-dimensional spacetime and subtracting the contribution of its volume integral, we obtain

$$S_{D5} = -T_{D5} r_{NS}\left(\int d^4x - \int dT \frac{4}{3}\pi R^3\right), \quad (3.3.9)$$

where R is the radius of the brane bubble formed in four dimensional spacetime and is a time-dependent function.

Next, we will derive the DBI action of the domain wall D5-brane. The induced metric on the domain wall D5-brane takes the form as

$$\frac{ds^2_{\text{DWD5}}}{l_s^2} = -dT^2 + R(T)^2\left(d\theta^2 + \sin^2\theta d\varphi^2\right) + L^2\left[d\psi_I^2 + \sin^2\psi_I\left(d\theta_I^2 + \sin^2\theta_I d\varphi_I^2\right)\right]. \quad (3.3.10)$$

Assuming that the configuration of the NS B-field as the background field is the same as that for the D5-brane described earlier, the determinant factor can be computed as follows

$$\begin{aligned} -\det\left(G_{ab} + B_{ab} + 2\pi\alpha' F_{ab}\right) = R(T)^4(1-\dot{R}(T)^2)\sin^2\theta \\ \times L^2\left(L^4\sin^2\theta_I\sin^4\psi_I + (B^{NS}_{\theta_I\varphi_I})^2\right). \end{aligned} \quad (3.3.11)$$

Substituting (3.3.6), the DBI action takes the following form

$$S_{DW} = -4\pi T_{D5}\int dT\sqrt{R^4(1-\dot{R}^2)}\cdot\left[2\pi^2L^3\int_0^\pi d\psi_I\frac{2}{\pi}\sqrt{\sin^4\psi_I + \left(\frac{b_{NS}}{L^2}\right)^2}\right]. \quad (3.3.12)$$

Here, by introducing a new definition for the tension of the domain wall, T_{DW}, as

$$T_{DW} = T_{D5}\left[2\pi^2L^3\int_0^\pi d\psi_I\frac{2}{\pi}\sqrt{\sin^4\psi_I + \left(\frac{b_{NS}}{L^2}\right)^2}\right], \quad (3.3.13)$$

the action of the domain wall D5-brane can be further rewritten as

$$S_{DW} = -4\pi T_{DW}\int dT\sqrt{R^4(1-\dot{R}^2)}. \quad (3.3.14)$$

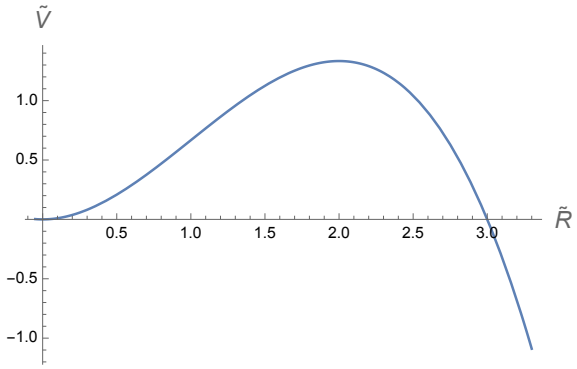

Figure 3.5: The shape of dimensionless potential (3.3.18).

Combining this with the calculation in (3.3.9), the action describing the decay of the system is given by

$$S = 2S_{D5} + S_{DW}. \tag{3.3.15}$$

We can confirm the metastability of the system by observing the shape of the potential. The potential is determined by $V = -L(R, \dot{R} = 0)$, that is,

$$V = T_{DW} 4\pi R^2 - \frac{8}{3} T_{D5} r_{NS} \pi R^3. \tag{3.3.16}$$

Here, we adopted the configuration that the (anti) D5-brane fills up with four dimensional spacetime as the energy reference and subtract $E_{\text{before}} = T_{D5} r_{NS} \int d^3x$. As mentioned above, the theory under consideration now is decoupled from gravity, so we can freely take the reference this way. Introducing a dimensionless parameter as

$$R = c\widetilde{R}, \quad c = \frac{T_{DW}}{2T_{D5} r_{NS}}, \tag{3.3.17}$$

the dimensionless potential can be written as follows

$$\widetilde{V} = \widetilde{R}^2 - \frac{1}{3}\widetilde{R}^3. \tag{3.3.18}$$

See Figure 3.5 for the shape of this potential. Indeed, it can be seen that the system is metastable such that there is a potential barrier at finite $\widetilde{R}$.

In summary, the decay process of this system from the viewpoint of a four dimensional observer can be understood as follows: D5-branes and anti D5-branes annihilate through the decay process, and a spherical bubble, which the true vacuum occupies inside, is generated. We can interpret this bubble as a domain wall D5-brane wrapping on the internal $\mathbb{S}^3$, and also as a throat connecting D5s and anti D5s. While the domain wall bubble has a positive tension, which tends to make the bubble smaller, this system can obtain energy when the bubble expands. If a large enough bubble is generated via the tunneling, the bubble expands, and the metastable vacuum outside the bubble is overwhelmed by the true vacuum. This is all the description of the decay with no catalysis.

3.3.2 Bound state between domain wall D5 and monopole

In this section, we consider the enhancement of the vacuum decay by adding an impurity to the geometrically realized metastable state in the previous section. In particular, we discuss the catalytic effect of D3-branes wrapped in the internal space. As shown in Sec. 3.2.4, these D3-branes dissolve onto D5-branes and behave as a background magnetic flux. Then, the D3-branes can be interpreted as some monopole-like objects from the point of view of a four dimensional observer and can be seen as forming a bound state with bubbles. As a matter of course, the strength of the magnetic field as a remnant of D3-branes is proportional to the number of D3-branes: $b_{D3} \propto \#_{D3}$.

The specific contribution of the magnetic field appears to be the field strength in the DBI action. We can derive the DBI action by assuming that the magnetic field originating from the D3-brane extends vertically from the bubble surface. That is,

$$b_{\theta\varphi} = b_{D3} \sin\theta. \tag{3.3.19}$$

Since the induced metric is given by (3.3.2), the calculation of the determinant factor in the DBI action is changed as follows.

$$-\det\left(G_{ab} + B_{ab} + 2\pi\alpha' F_{ab}\right) = \sin^2\theta \left(\xi^4 + (b_{D3})^2\right) \times \left(L^4 \sin^4\psi_I \sin^2\theta_I + (B^{NS}_{\theta_I\varphi_I})^2\right). \tag{3.3.20}$$

Here, as in (3.3.16), considering the configuration that (anti) D5-branes fill in four dimensional spacetime as the energy reference and subtracting the contribution, the DBI action of the D5-brane in the presence of a magnetic field is given by the following expression.

$$\begin{aligned} S_{D5} &= -T_{D5} r_{NS} \int dT \left(\int_R^\infty - \int_0^\infty\right) d\xi \left(4\pi\sqrt{\xi^4 + (b_{D3})^2}\right) \\ &= T_{D5} r_{NS} \int dT \int_0^R d\xi \left(4\pi\sqrt{\xi^4 + (b_{D3})^2}\right) \\ &= T_{D5} r_{NS} \int dT \left[4\pi b_{D3} R_2 F_1\left(-\frac{1}{2}, \frac{1}{4}, \frac{5}{4}, -\frac{R^4}{(b_{D3})^2}\right)\right]. \end{aligned} \tag{3.3.21}$$

As for the domain wall D5-brane, the induced metric is given by (3.3.10), then the calculation of the determinant factor is altered as

$$\begin{aligned} -\det\left(G_{ab} + B_{ab} + 2\pi\alpha' F_{ab}\right) = \left(R(T)^4 + (b_{D3})^2\right)\left(1 - \dot{R}(T)^2\right)\sin^2\theta \\ \times L^2 \left(L^4 \sin^2\theta_I \sin^4\psi_I + (B^{NS}_{\theta_I\varphi_I})^2\right). \end{aligned} \tag{3.3.22}$$

Integrating this factor on the world volume, we obtain the following action.

$$S_{DW} = -4\pi T_{DW} \int dT \sqrt{\left(R(T)^4 + (b_{D3})^2\right)\left(1 - \dot{R}^2\right)}, \tag{3.3.23}$$

where the expression of the domain wall tension is the same as (3.3.13). Combining this with (3.3.21), we find the final form of the DBI action for the bound state as

$$\begin{aligned} S_{\rm DBI} &= S_{DW} + 2S_{D5} \\ &= \int dT \left[-4\pi T_{DW}\sqrt{\left(R^4 + (b_{D3})^2\right)\left(1 - \dot{R}^2\right)}\right. \\ &\qquad \left. + 2T_{D5} r_{NS}\left[4\pi b_{D3} R_2 F_1\left(-\frac{1}{2}, \frac{1}{4}, \frac{5}{4}, -\frac{R^4}{(b_{D3})^2}\right)\right]\right] + \cdots, \end{aligned} \tag{3.3.24}$$

where the ellipsis denotes unimportant terms, which are independent of R and do not contribute to the dynamics.

Following the previous section, let us confirm the metastability of the bound state by seeing the shape of the potential. The DBI potential is given by

$$V_{\rm DBI} = 4\pi T_{DW}\sqrt{(R^4+(b_{D3})^2)} - 2T_{D5}r_{NS}\left[4\pi b_{D3}R_2F_1\left(-\frac{1}{2},\frac{1}{4},\frac{5}{4},-\frac{R^4}{(b_{D3})^2}\right)\right]. \tag{3.3.25}$$

If we introduce the dimensionless magnetic field as $b_{D3} = c^2\widetilde{b}_{D3}$, where c is the dimensionless factor defined in (3.3.17), we can write the dimensionless Lagrangian and potential as follow.

$$L_{DBI} = 4\pi T_{DW}c^2\widetilde{L}_{DBI}, \tag{3.3.26}$$

$$\widetilde{L}_{DBI} = -\sqrt{\left(\widetilde{R}^4+(\widetilde{b}_{D3})^2\right)\left(1-\dot{\widetilde{R}}^2\right)} + \widetilde{b}_{D3}\widetilde{R}_2F_1\left(-\frac{1}{2},\frac{1}{4},\frac{5}{4},-\frac{\widetilde{R}^4}{(\widetilde{b}_{D3})^2}\right), \tag{3.3.27}$$

$$\widetilde{V}_{DBI} = \sqrt{\widetilde{R}^4+(\widetilde{b}_{D3})^2} - \widetilde{b}_{D3}\widetilde{R}_2F_1\left(-\frac{1}{2},\frac{1}{4},\frac{5}{4},-\frac{\widetilde{R}^4}{(\widetilde{b}_{D3})^2}\right). \tag{3.3.28}$$

Figure 3.6 shows potentials for different magnetic field values. As in Figure 3.5, we can see the existence of potential barriers at finite $\widetilde{R}$. On the other hand, unlike in Figure 3.5, the positions of the minima are slightly shifted from the origin. This reflects the nonlinearity of the DBI action.[3]

As seen from the shape of the potential for each magnetic strength, we can confirm a tendency for the potential barrier to become lower as the magnetic field becomes strong, which implies that the instability of the bubble is reinforced. This means that D3-branes wrapped in the internal space indeed play a role as catalysts. We can identify the critical value of the magnetic field where the potential barrier completely vanishes by studying the condition for the existence of the potential minimum. The minimum can be derived by solving the following algebraic equation.

$$\begin{aligned}\frac{\partial\widetilde{V}_{DBI}}{\partial\widetilde{R}} &= \frac{2\widetilde{R}^3}{\sqrt{\widetilde{R}^4+(\widetilde{b}_{D3})^2}} - \sqrt{\widetilde{R}^4+(\widetilde{b}_{D3})^2} \\ &\Leftrightarrow \quad \widetilde{R}^4 - 2\widetilde{R}^3 + (\widetilde{b}_{D3})^2 = 0.\end{aligned} \tag{3.3.29}$$

By numerical computations, the range of magnetic fields such that $\widetilde{R}$ has a real solution is given by

$$0 \le \widetilde{b}_{D3} \le \frac{3\sqrt{3}}{4} \equiv \widetilde{b}_{\rm crit}, \tag{3.3.30}$$

[3]This means the bubble has a finite radius even before tunneling. In other words, from the viewpoint of an observer in four dimensional spacetime, there appears to be a monopole-like compact object. Although it is not the purpose of the research in this thesis, in the context of the Swampland program, the construction of such charged compact objects and their stabilization have been widely investigated, and the bound states of bubbles and D3-branes treated in this chapter may provide one concrete way to realize such a compact object. See Appendix A for a detailed discussion.

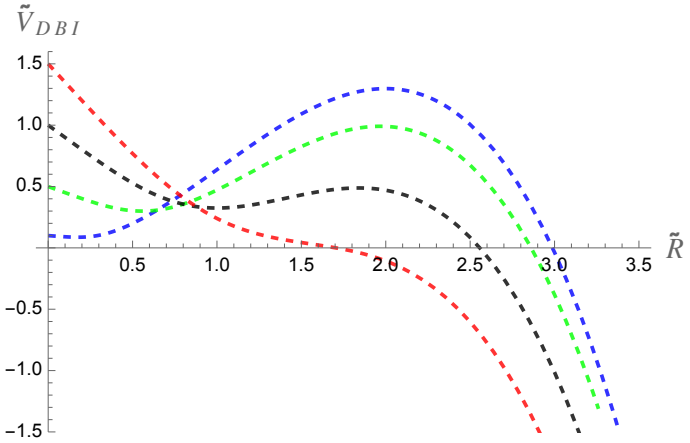

Figure 3.6: The schematic picture of dimensionless DBI potential (3.3.28) for $\widetilde{b}_{D3} = 0.1$(blue), 0.5(green), 1(black), 1.5(red). This Figure is taken from [1].

When a magnetic field stronger than the critical value b_{crit} is applied, the potential shape becomes like the red line in Figure 3.6, and the potential barrier no longer exists. At this time, the vacuum is always unstable and decays immediately without tunneling.

3.4 Complete 1-loop analysis of vacuum decay

3.4.1 Bounce solution and bounce action

For simplicity, we shall utilize the dimensionless DBI Lagrangian (3.3.27) for the 1-loop analysis in this section. As stated in section 2.1, we have to find the bounce configuration to obtain the decay rate of the brane bubble. From the DBI Lagrangian (3.3.27), the Euclidean EoM is

$$\partial_s \left(\sqrt{\frac{\widetilde{R}^4 + (\widetilde{b}_{D3})^2}{1+\dot{\widetilde{R}}^2}} - \widetilde{b}_{D3}\widetilde{R}\,{}_2F_1\left(-\frac{1}{2},\frac{1}{4},\frac{5}{4},-\frac{\widetilde{R}^4}{(\widetilde{b}_{D3})^2}\right)\right) = 0, \tag{3.4.1}$$

where s is the dimensionless Euclidean time, defined by $t_E = cs$. Solving this EoM with respect to $d\widetilde{R}/ds$ yields

$$\begin{aligned}\frac{d\widetilde{R}}{ds} = \pm & \frac{1}{\left[-E + \widetilde{b}_{D3}\widetilde{R}\,{}_2F_1\left(-\frac{1}{2},\frac{1}{4},\frac{5}{4},-\frac{\widetilde{R}^4}{(\widetilde{b}_{D3})^2}\right)\right]} \\ & \times \sqrt{\widetilde{R}^4 + \widetilde{b}^2 - \left[-E + \widetilde{b}_{D3}\widetilde{R}\,{}_2F_1\left(-\frac{1}{2},\frac{1}{4},\frac{5}{4},-\frac{\widetilde{R}^4}{(\widetilde{b}_{D3})^2}\right)\right]^2},\end{aligned} \tag{3.4.2}$$

where $-E$ is a constant of integration, corresponding to the static energy. We put the negative sign here for later convenience. Since the time derivative of the bounce solution must be zero at the minimum, $\widetilde{R}_{\text{min}}$, in the limit of $\beta \to \infty$, an explicit form of $\bar{E} =$

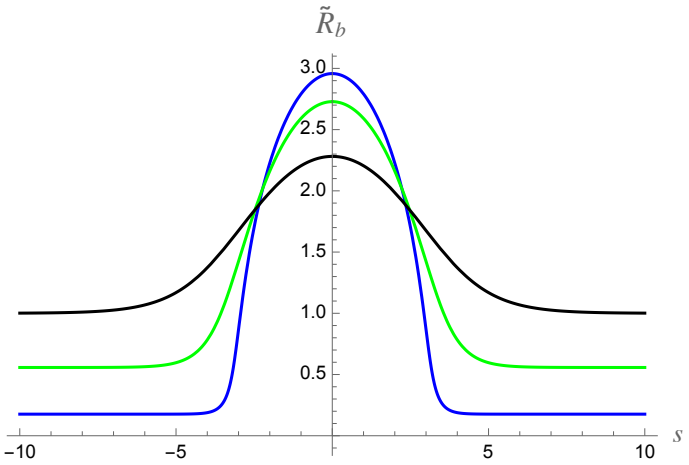

Figure 3.7: Bounce solutions for different magnetic field strengths. The blue line denote the configuration for $\tilde{b}_{D3} = 0.1$, the green line for $\tilde{b}_{D3} = 0.5$, and the black line for $\tilde{b}_{D3} = 1$. This Figure is taken from [1].

$E(\beta \to \infty)$ is given by

$$-\bar{E} = \sqrt{\widetilde{R}_{\rm min}^4 + (\widetilde{b}_{D3})^2} - \widetilde{b}_{D3}\widetilde{R}_{\rm min}{}_2F_1\left(-\frac{1}{2}, \frac{1}{4}, \frac{5}{4}, -\frac{\widetilde{R}_{\rm min}^4}{(\widetilde{b}_{D3})^2}\right). \tag{3.4.3}$$

Although it is impossible to find an analytical solution for the nonlinear equation (3.4.1) (or (3.4.2)), we can see the behavior of the bounce solution and the magnetic field dependence by numerical calculations (see Figure 3.7). From Figure 3.7, we can read off the magnetic field dependence of the local minimum and the turning point of the solution: $\widetilde{R}_{\rm min} = \widetilde{R}_b(s \to \pm\infty)$ becomes larger and $\widetilde{R}_{\rm max} = \widetilde{R}_b(s = 0)$ becomes smaller as the magnetic field increases. As can be seen from Figure 3.7 and Figure 3.8, when b_{D3} is small, the bounce solution rises sharply near the origin (turning point) and shows a non-standard shape compared to an anharmonic oscillator. This feature arises from the extremely small coefficients of the kinetic terms, which strongly suggest the influence of nonlinearity.

Taking the difference between the Euclidian action of the bounce solution and the contribution of the trivial solution, we obtain

$$\widetilde{B} = 2\int_{\widetilde{R}_{\rm min}}^{\widetilde{R}_{\rm max}} d\widetilde{R}_b \sqrt{\widetilde{R}_b^4 + (\widetilde{b}_{D3})^2 - \left[-\bar{E} + \widetilde{b}_{D3}\widetilde{R}_{b}{}_2F_1\left(-\frac{1}{2}, \frac{1}{4}, \frac{5}{4}, -\frac{\widetilde{R}_b^4}{(\widetilde{b}_{D3})^2}\right)\right]^2}. \tag{3.4.4}$$

The overall coefficient of 2 comes from the fact that the contributions from the outward route and the return of the bounce solution are equal. This bounce action apparently depends on the magnetic field, and Figure 3.9 shows the numerical calculation of the bounce action for each magnetic field. As can be seen from Figure 3.9, the bounce action decreases monotonically as the magnetic field increases and takes zero at $\widetilde{b}_{D3} = \widetilde{b}_{\rm crit}$. This phenomenon implies that the catalyst promotes vacuum decay in the parameter region where the exponential factor becomes dominant in calculating the life-time.

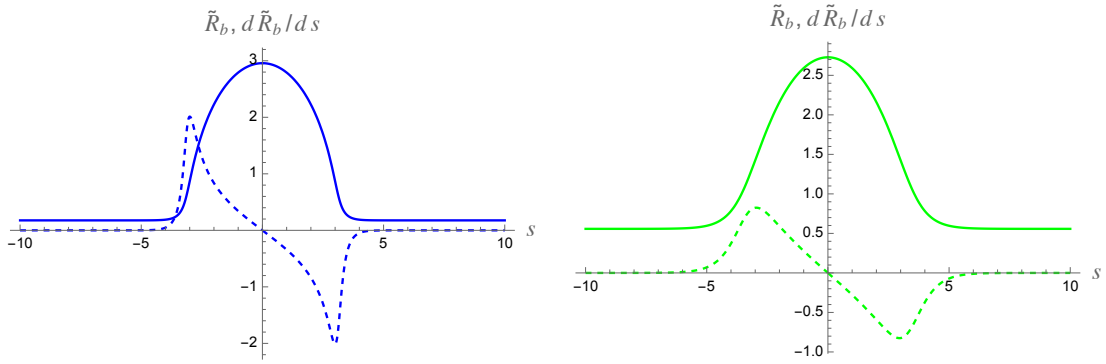

(a) (b)

Figure 3.8: Bounce solutions and their time derivatives for different magnetic field strength. The left panel represents $\tilde{b}_{D3} = 0.1$, and the right panel represents $\tilde{b}_{D3} = 0.5$. These Figure is cited from [1].

3.4.2 Zero mode normalization factor

The next step is to calculate the zero mode normalization factor. As we proved in appendix B.1, the zero mode is proportional to the time derivative of bounce action as

$$\widetilde{R}_0 = \frac{1}{\sqrt{\widetilde{N}_0}} \frac{d\widetilde{R}_b}{ds}, \tag{3.4.5}$$

for any Lagrangian. We can compute the normalization factor via the normalization condition of the zero mode

$$\widetilde{N}_0 = \int_{-\beta/2}^{\beta/2} \left(\frac{d\widetilde{R}_b}{ds}\right)^2 ds = 2\int_{\widetilde{R}_{\rm min}}^{\widetilde{R}_{\rm max}} d\widetilde{R}_b \frac{d\widetilde{R}_b}{ds} \ . \tag{3.4.6}$$

Note that this normalization factor does not coincide with the bounce action, contrary to the standard argument. In the canonical theories, we can explicitly confirm that the zero mode normalization factor and the bounce action are the same value from the Liouville theorem (see, e.g., [103, 104]). In contrast, the calculation of the normalization factor in the present model yields

$$\begin{aligned}\widetilde{N}_0 &= 2\int_{\widetilde{R}_{\rm min}}^{\widetilde{R}_{\rm max}} d\widetilde{R}_b \frac{d\widetilde{R}_b}{ds} \\ &= 2\int_{\widetilde{R}_{\rm min}}^{\widetilde{R}_{\rm max}} d\widetilde{R}_b \frac{\sqrt{\widetilde{R}_b^4 + (\tilde{b}_{D3})^2 - \left[-\bar{E} + \tilde{b}_{D3}\widetilde{R}_{b2}F_1\left(-\frac{1}{2}, \frac{1}{4}, \frac{5}{4}, -\frac{\widetilde{R}_b^4}{(\tilde{b}_{D3})^2}\right)\right]^2}}{-\bar{E} + \tilde{b}_{D3}\widetilde{R}_{b2}F_1\left(-\frac{1}{2}, \frac{1}{4}, \frac{5}{4}, -\frac{\widetilde{R}_b^4}{(\tilde{b}_{D3})^2}\right)},\end{aligned} \tag{3.4.7}$$

which is not the same as the bounce action: $-\bar{E} + \tilde{b}_{D3}\widetilde{R}_{b2}F_1\big(-1/2, 1/4, 5/4, -\widetilde{R}_b^4/(\tilde{b}_{D3})^2\big)$ in the denominator did not appeared in (3.4.4). This discrepancy essentially comes from the non-linearity of the DBI action. We can confirm the difference in magnetic field

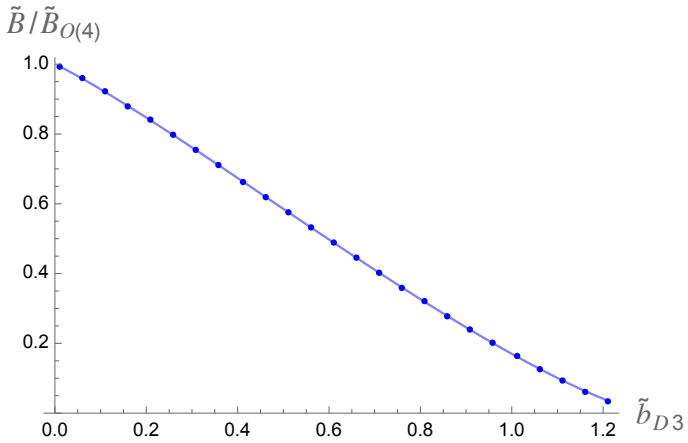

Figure 3.9: The numerical calculation of the bounce action normalized by the bounce action without catalyst. Solid dots denote the values of the bounce action for each magnetic field, and the solid line interpolates them. The ratio is less than one in all regions, which shows the catalytic effect of the magnetic field. This Figure is taken from [1].

dependence between the normalization factor and the bounce action by the numerical calculation (see Figure 3.10 and Figure 3.9). Comparing these two figures, both factors are monotonically decreasing with respect to the magnetic field but show a different behavior in the intermediate region. Given the above, when considering non-canonical theories, we need to replace $\widetilde{B}$ in the prefactor with $\widetilde{N}_0$

In the end, let us comment on the singular behavior of $\widetilde{N}_0$ at the point where the magnetic field strength is zero. In contrast to the bounce action, the numerical calculation shows that $\widetilde{N}_0$ diverges at the origin. This peculiar behavior suggests that the description by the low-energy EFT breaks down at this point. The absence of a magnetic field suggests that the monopole has disappeared, leading to the restoration of $O(4)$ symmetry. This situation signals the emergence of new zero modes, thereby indicating that the EFT, which does not incorporate these factors, is no longer valid at this point.

3.4.3 Zeta regularized functional determinant

To accomplish the complete 1-loop analysis, we must evaluate the determinant factor in the decay rate formula:

$$\Gamma \equiv 2\mathrm{Im}E_0 = \sqrt{\frac{N_0}{2\pi}} \left| \frac{\det' T[\widetilde{R}_b]}{\det T[\widetilde{R}_{\min}]} \right|^{-1/2} e^{-B} \ . \tag{3.4.8}$$

A general formula for the second variation of the Euclidean action is given by (B.1.2), then we define the Strum-Liouville operator here over the interval $(-\beta/2, \beta/2)$ as

$$T_{-\beta/2,\beta/2} \equiv -\frac{d}{ds}\left(\frac{\partial^2 \tilde{L}}{\partial \dot{\tilde{R}}^2}\frac{d}{ds}\right) + \frac{\partial^2 \widetilde{L}}{\partial \widetilde{R}^2} - \frac{d}{ds}\frac{\partial^2 \widetilde{L}}{\partial \widetilde{R}\partial \dot{\widetilde{R}}} = -\frac{d}{ds}\left(P[\widetilde{R}]\frac{d}{ds}\right) + Q[\widetilde{R}] \ , \tag{3.4.9}$$

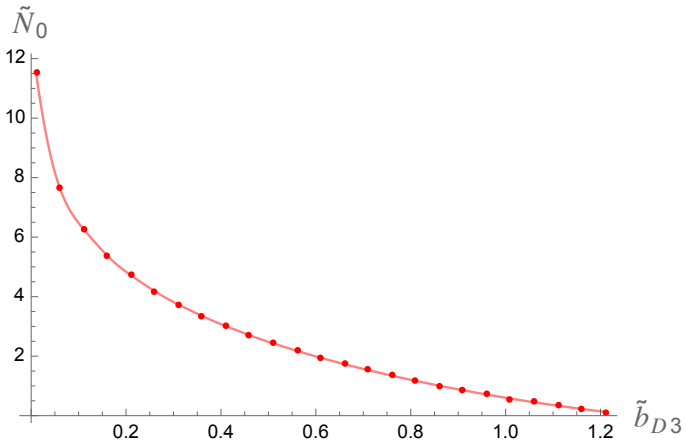

Figure 3.10: Magnetic field dependence of the zero mode normalization factor. This Figure is a slightly modified and quoted version of the one published in [1].

and certainly, the ratio of functional determinants is given by

$$\frac{\det' T[\widetilde{R}_b]}{\det T[\widetilde{R}_{\min}]} = \frac{\det' \left[-\frac{d}{ds}\left(P[\widetilde{R}_b]\frac{d}{ds}\right) + Q[\widetilde{R}_b]\right]}{\det \left[-\frac{d}{ds}\left(P[\widetilde{R}_{\min}]\frac{d}{ds}\right) + Q[\widetilde{R}_{\min}]\right]} \ . \tag{3.4.10}$$

Based on the zeta function regularization described in section 2.2.1, this ratio is expressed by

$$\frac{\det' T[\widetilde{R}_b]}{\det T[\widetilde{R}_{\min}]} = \exp\left[-\left(\zeta'(0;T[\widetilde{R}_b]) - \zeta'(0;T[\widetilde{R}_{\min}])\right)\right] \ , \tag{3.4.11}$$

where $\zeta(s;T)$ is the spectral zeta function defined as

$$\zeta(s;T_{-\beta/2,\beta/2}) \equiv \sum_j \lambda_j^{-s} \ . \tag{3.4.12}$$

When we see (3.4.11), we know that we need to take s derivative of the spectral zeta function at $s = 0$. However, significant difficulties arise. Due to the complicated kinetic term in the DBI Lagrangian, the coefficient $P[\widetilde{R}_b]$ becomes a time-dependent continuous function. Consequently, we must evaluate (3.4.11) for general Sturm-Liouville operators. At this point, the so-called *contour deformation method*, introduced by Kirsten and McKane, proves highly effective, enabling explicit computations [118, 119]. Based on their approach, the derivative of the zeta function at $s = 0$ is expressed as [120]

$$\zeta'(0;T_{A,B}) = i\pi n - \ln\left(2c\left|\frac{F_{m_0}}{\Gamma_{k_0}}\right|\right) \ . \tag{3.4.13}$$

See Appendix C.1 for detailed discussions about its derivation. n is the number of negative modes in the eigenvalues, which is fixed to one in our case. While the constant c is evaluated by $P[\widetilde{R}_b]$ and the weight function in the Strum-Liouville operator, we do not have to calculate it because Γ_{k_0}, which is one of the expansion coefficients of the large λ

expansion for the characteristic function, is calculated as $\Gamma_{k_0} = \Gamma_{-1} = -2ic$. See [120] for details. In contrast, F_{m_0} is the lowest order coefficient of the small λ expansion for the characteristic function, that is,

$$F_{A,B}(\lambda) = F_{m_0}\lambda^{m_0} + \sum_{m=2}^{\infty} F_m \lambda^m \ , \tag{3.4.14}$$

where m_0 is the multiplicity of the zero mode. Refer to appendix C for the definition of the characteristic function. Thus, the functional determinant with zero mode extracted is

$$\det{}' \left[-\frac{d}{ds}\left(P[\widetilde{R}_b]\frac{d}{ds} \right) + Q[\widetilde{R}_b] \right] = -|F_{m_0}| \ . \tag{3.4.15}$$

In the case of vacuum decay, the zero mode multiplicity equals one, so F_{m_0} is just the first-order coefficient of the small λ expansion.

Before considering the expansion, we must know its original expression. We need the characteristic function for the Sturm-Liouville problem with periodic boundary condition, following the definition (C.1.10), we obtain

$$\begin{aligned} F_{\varphi,R}(\lambda) = &\left\{ \psi_\lambda^1\left(\frac{\beta}{2}\right) - \psi_\lambda^1\left(-\frac{\beta}{2}\right) \right\} \left\{ \psi_\lambda^{2[1]}\left(\frac{\beta}{2}\right) - \psi_\lambda^{2[1]}\left(-\frac{\beta}{2}\right) \right\} \\ &- \left\{ \psi_\lambda^2\left(\frac{\beta}{2}\right) - \psi_\lambda^2\left(-\frac{\beta}{2}\right) \right\} \left\{ \psi_\lambda^{1[1]}\left(\frac{\beta}{2}\right) - \psi_\lambda^{1[1]}\left(-\frac{\beta}{2}\right) \right\}, \end{aligned} \tag{3.4.16}$$

where $\psi_\lambda^1(s)$ and $\psi_\lambda^2(s)$ are the independent solutions of the Strum-Liouville operator, which satisfy the following boundary conditions.

$$\psi_\lambda^1\left(-\frac{\beta}{2}\right) = \psi_\lambda^{2[1]}\left(-\frac{\beta}{2}\right) = 1, \quad \psi_\lambda^{1[1]}\left(-\frac{\beta}{2}\right) = \psi_\lambda^2\left(-\frac{\beta}{2}\right) = 0. \tag{3.4.17}$$

Using these boundary conditions, we can transform the characteristic function to a simpler form as

$$\begin{aligned} F_{\varphi,R}(\lambda) &= \left\{ \psi_\lambda^1\left(\frac{\beta}{2}\right) - 1 \right\} \left\{ \psi_\lambda^{2[1]}\left(\frac{\beta}{2}\right) - 1 \right\} - \psi_\lambda^2\left(\frac{\beta}{2}\right) \psi_\lambda^{1[1]}\left(\frac{\beta}{2}\right) \\ &= 2 - \psi_\lambda^1\left(\frac{\beta}{2}\right) - \psi_\lambda^{2[1]}\left(\frac{\beta}{2}\right). \end{aligned} \tag{3.4.18}$$

The first-order coefficients of $\psi_\lambda^1(s)$ and $\psi_\lambda^{2[1]}(s)$ is given by the Volterra integral equation as follows

$$\begin{aligned} \psi_{\lambda,1}^1(s) &= \int_{-\beta/2}^{s} r(x)dx g(0,s,x)\,\psi_0^1(x) \\ &= \int_{-\beta/2}^{s} dx \left\{ \psi_0^1(s)\,\psi_0^2(x) - \psi_0^1(x)\,\psi_0^2(s) \right\} \psi_0^1(x) \ , \end{aligned} \tag{3.4.19}$$

$$\begin{aligned} \psi_{\lambda,1}^{2[1]}(s) &= \int_{-\beta/2}^{s} r(x)dx g^{[1]}(0,s,x)\,\psi_0^2(x) \\ &= \int_{-\beta/2}^{s} dx \left\{ \psi_0^{1[1]}(s)\,\psi_0^2(x) - \psi_0^1(x)\,\psi_0^{2[1]}(s) \right\} \psi_0^2(x), \end{aligned} \tag{3.4.20}$$

where $g(\lambda, s, x)$ is Volterra Green's function. Note that the weight function equals one by definition. Substituting the coefficients to (3.4.18), we obtain

$$F_{\varphi,R,1} = -\int_{-\beta/2}^{\beta/2} dx \left[\left\{ \psi_0^1\left(\frac{\beta}{2}\right)\psi_0^2(x) - \psi_0^1(x)\psi_0^2\left(\frac{\beta}{2}\right) \right\} \psi_0^1(x) + \left\{ \psi_0^{1[1]}\left(\frac{\beta}{2}\right)\psi_0^2(x) - \psi_0^1(x)\psi_0^{2[1]}\left(\frac{\beta}{2}\right) \right\} \psi_0^2(x) \right] . \tag{3.4.21}$$

To go further, it is convenient to rewrite $\psi_0^1(s)$ and $\psi_0^2(s)$ as a linear combination of $\dot{\widetilde{R}}_b(s)$ and $\chi(s)$ as in (2.2.52). Let us introduce a transformation matrix as follows

$$\begin{pmatrix} \psi_0^1(s) \\ \psi_0^2(s) \end{pmatrix} = \begin{pmatrix} a_{11} & a_{12} \\ a_{21} & a_{22} \end{pmatrix} \begin{pmatrix} \dot{\widetilde{R}}_b(s) \\ \chi(s) \end{pmatrix} , \tag{3.4.22}$$

where $\chi(s)$ is another zero mode solution introduced in (2.2.52). Using the boundary conditions at $s = -\beta/2$, we find the following relations

$$\psi_0^1\left(-\frac{\beta}{2}\right) = a_{11}\dot{\widetilde{R}}_b\left(-\frac{\beta}{2}\right) + a_{12}\chi\left(-\frac{\beta}{2}\right) = 1 , \tag{3.4.23}$$

$$\psi_0^2\left(-\frac{\beta}{2}\right) = a_{21}\dot{\widetilde{R}}_b\left(-\frac{\beta}{2}\right) + a_{22}\chi\left(-\frac{\beta}{2}\right) = 0 , \tag{3.4.24}$$

$$\psi_0^{1[1]}\left(-\frac{\beta}{2}\right) = P[\widetilde{R}_b\left(-\frac{\beta}{2}\right)]\left\{ a_{11}\ddot{\widetilde{R}}_b\left(-\frac{\beta}{2}\right) + a_{12}\dot{\chi}\left(-\frac{\beta}{2}\right) \right\} = 0 , \tag{3.4.25}$$

$$\psi_0^{2[1]}\left(-\frac{\beta}{2}\right) = P[\widetilde{R}_b\left(-\frac{\beta}{2}\right)]\left\{ a_{21}\ddot{\widetilde{R}}_b\left(-\frac{\beta}{2}\right) + a_{22}\dot{\chi}\left(-\frac{\beta}{2}\right) \right\} = 1 . \tag{3.4.26}$$

Solving these equations, we obtain

$$(a_{11}, a_{12}, a_{21}, a_{22}) = \left(\frac{1}{\dot{\widetilde{R}}_b(-\beta/2)}, 0, -\frac{\chi(-\beta/2)}{P[\widetilde{R}_b(-\beta/2)]\dot{\widetilde{R}}_b(-\beta/2)\dot{\chi}(-\beta/2)}, \frac{1}{P[\widetilde{R}_b(-\beta/2)]\dot{\chi}(-\beta/2)} \right) . \tag{3.4.27}$$

Hence, we can determine the boundary value at $s = \beta/2$ as

$$\psi_0^1\left(\frac{\beta}{2}\right) = \frac{\dot{\widetilde{R}}_b(\beta/2)}{\dot{\widetilde{R}}_b(-\beta/2)} = 1 , \qquad \psi_0^{1[1]}\left(\frac{\beta}{2}\right) = 0 , \tag{3.4.28}$$

$$\psi_0^2\left(\frac{\beta}{2}\right) = \frac{\chi(\beta/2) - \chi(-\beta/2)}{P[\widetilde{R}_b(-\beta/2)]\dot{\chi}(-\beta/2)} , \qquad \psi_0^{2[1]}\left(\frac{\beta}{2}\right) = 1 , \tag{3.4.29}$$

where we utilized the periodicity of the bounce solution and the boundary condition $\ddot{\widetilde{R}}_b(\pm\beta/2) = 0$. Substituting these into (3.4.21), we can transform $F_{\varphi,R,1}$ into a form

using the bounce solution and χ as follow

$$\begin{aligned} F_{\varphi,R,1} &= \psi_0^2\left(\frac{\beta}{2}\right)\int_{-\beta/2}^{\beta/2} ds\,\left|\psi_0^1(s)\right|^2 \\ &= \frac{\chi(\beta/2)-\chi(-\beta/2)}{P[\widetilde{R}_b(-\beta/2)]\dot{\chi}(-\beta/2)}\cdot\frac{1}{(\dot{\widetilde{R}}_b(-\beta/2))^2}\int_{-\beta/2}^{\beta/2} ds(\dot{\widetilde{R}}_b(s))^2 \\ &= \frac{N_0}{P[\widetilde{R}_b(-\beta/2)]\dot{\widetilde{R}}_b(-\beta/2)\dot{\chi}(-\beta/2)}\cdot\frac{\chi(\beta/2)-\chi(-\beta/2)}{\dot{\widetilde{R}}_b(-\beta/2)}\,. \end{aligned} \tag{3.4.30}$$

As we showed in (2.2.57), the following relation holds also in this case

$$\frac{\chi(s+\beta)-\chi(s)}{\dot{\widetilde{R}}_b(s)} = -\left(\frac{\partial E}{\partial\beta}\right)^{-1}\,. \tag{3.4.31}$$

For the factor $P[\widetilde{R}_b(-\beta/2)]\dot{\widetilde{R}}_b(-\beta/2)\dot{\chi}(-\beta/2)$ in (3.4.30), it can be calculated by the energy conservation law, which is given by

$$\left(\frac{d\widetilde{R}_b}{ds}\right)^2 = \frac{\widetilde{R}_b^4+b^2}{\left[-E+b\widetilde{R}_{b2}F_1\left(-\frac{1}{2},\frac{1}{4},\frac{5}{4},-\frac{\widetilde{R}_b^4}{b^2}\right)\right]^2}-1\,. \tag{3.4.32}$$

If we differentiate the both side by E at $s=-\beta/2$, we obtain

$$\begin{aligned} 2\dot{\widetilde{R}}_b\left(-\frac{\beta}{2}\right)\dot{\chi}\left(-\frac{\beta}{2}\right) &= \chi\left(-\frac{\beta}{2}\right)\frac{\partial}{\partial\widetilde{R}}\left(\frac{\widetilde{R}_b^4+b^2}{\left[-E+b\widetilde{R}_{b2}F_1\left(-\frac{1}{2},\frac{1}{4},\frac{5}{4},-\frac{\widetilde{R}_b^4}{b^2}\right)\right]^2}\right)\Bigg|_{s=-\beta/2} \\ &\quad+\frac{\partial}{\partial E}\left(\frac{\widetilde{R}_b^4+b^2}{\left[-E+b\widetilde{R}_{b2}F_1\left(-\frac{1}{2},\frac{1}{4},\frac{5}{4},-\frac{\widetilde{R}_b^4}{b^2}\right)\right]^2}\right)\Bigg|_{s=-\beta/2} \\ &= \frac{2}{\sqrt{\widetilde{R}_{\rm min}^4+b^2}} = \sqrt{\frac{2}{\widetilde{R}_{\rm min}^3}}. \end{aligned} \tag{3.4.33}$$

We can relate the final expression with $P_{\rm min}=P[\widetilde{R}_{\rm min}]$ as

$$P_{\rm min} = \left.\frac{\partial^2 L_E}{\partial\dot{\widetilde{R}}_b^2}\right|_{s=-\beta/2} = \sqrt{2\widetilde{R}_{\rm min}^3}. \tag{3.4.34}$$

Then, we get

$$\dot{\widetilde{R}}_b\left(-\frac{\beta}{2}\right)\dot{\chi}\left(-\frac{\beta}{2}\right) = \frac{1}{P_{\rm min}} \quad\Leftrightarrow\quad P_{\rm min}\dot{\widetilde{R}}_b\left(-\frac{\beta}{2}\right)\dot{\chi}\left(-\frac{\beta}{2}\right) = 1. \tag{3.4.35}$$

Thus, (3.4.30) becomes

$$F_{\varphi,R,1} = \frac{N_0}{P[\widetilde{R}_b(-\beta/2)]\dot{\widetilde{R}}_b(-\beta/2)\dot{\chi}(-\beta/2)} \cdot \frac{\chi(\beta/2)-\chi(-\beta/2)}{\dot{\widetilde{R}}_b(-\beta/2)} = -N_0 \left(\frac{\partial E}{\partial \beta}\right)^{-1}. \tag{3.4.36}$$

Therefore, we find that the expression for the functional determinant is formally identical in both canonical and non-canonical cases.

The technical ingredient introduced in the section 2.2.3 is valid for the calculation of $\partial E/\partial\beta$. In this case, $G[\widetilde{R}_b]$, which is the Taylor expansion of $(d\widetilde{R}_b/ds)^2$ around $\widetilde{R} = \widetilde{R}_{\rm min}$ and $-E = \bar{E} = \sqrt{\widetilde{R}_{\rm min}^4 + b^2} - b\widetilde{R}_{\rm min}{}_2F_1\left(-\frac{1}{2}, \frac{1}{4}, \frac{5}{4}, -\frac{\widetilde{R}_{\rm min}^4}{b^2}\right)$ is given by

$$G(\widetilde{R}_b, E) \simeq \omega^2 \left(\widetilde{R} - \widetilde{R}_{\rm min}\right)^2 + \frac{2}{P_{\rm min}}(E + \bar{E}), \tag{3.4.37}$$

where $\omega = \sqrt{Q_{\rm min}/P_{\rm min}}$. Then, we can perform the third integral in (2.2.60) as follow

$$2\int_{\widetilde{R}_-}^{\widetilde{R}_+} \frac{1}{\sqrt{G(\widetilde{R}_b, C)}} d\widetilde{R}_b = \omega^{-1}\log\left(\left(\widetilde{R}_+ - \widetilde{R}_{\rm min}\right)^2\right) - \omega^{-1}\log\left(\frac{-(C+E)}{2Q_{\rm min}}\right). \tag{3.4.38}$$

Following the procedure from (2.2.64) to (2.2.66), we finally obtain the β derivative of the energy as

$$\frac{\partial E}{\partial \beta} = 2\left(\widetilde{R}_{\rm max} - \widetilde{R}_{\rm min}\right)^2 \frac{Q_{\rm min}^{3/2}}{P_{\rm min}^{1/2}} \exp\left[2\omega \int_{\widetilde{R}_{\rm min}}^{\widetilde{R}_{\rm max}} \left\{\frac{1}{\sqrt{(\dot{\widetilde{R}}_b)^2}} - \omega^{-1}\frac{1}{\widetilde{R} - \widetilde{R}_{\rm min}}\right\} d\widetilde{R}_b\right] \times \exp\left[-\omega\beta\right]. \tag{3.4.39}$$

As is clear from this expression, (3.4.36) suffers from exponential divergence in the limit of $\beta \to \infty$. However, taking the ratio with the reference determinant, we obtain a finite expression given by

$$\frac{\det'\left[-\frac{d}{ds}\left(P[\widetilde{R}_b]\frac{d}{ds}\right) + Q[\widetilde{R}_b]\right]}{\det\left[-\frac{d}{ds}\left(P[\widetilde{R}_{\rm min}]\frac{d}{ds}\right) + Q[\widetilde{R}_{\rm min}]\right]} = -\frac{N_b}{2\left(\widetilde{R}_{\rm max} - \widetilde{R}_{\rm min}\right)^2}\frac{P_{\rm min}^{1/2}}{Q_{\rm min}^{3/2}} \exp\left[-2\omega \int_{\widetilde{R}_{\rm min}}^{\widetilde{R}_{\rm max}} \left\{\frac{1}{\sqrt{(\dot{\widetilde{R}}_b)^2}} - \omega^{-1}\frac{1}{\widetilde{R} - \widetilde{R}_{\rm min}}\right\} d\widetilde{R}_b\right]. \tag{3.4.40}$$

By doing a numerical calculation of the square root of the absolute value of this ratio, as shown in Figure 3.11, we find that this value is a monotonically increasing function with respect to the magnetic field strength.

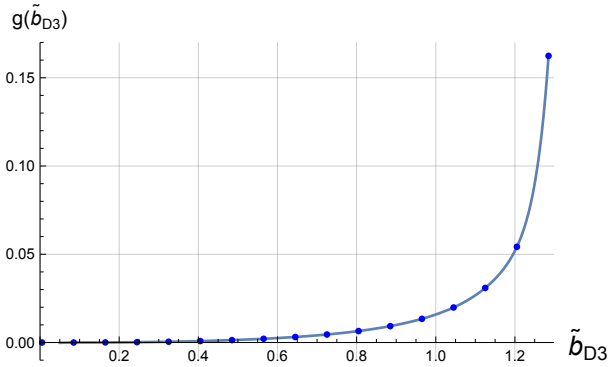

Figure 3.11: Magnetic field dependence of the absolute value of square root for the determinant ratio, denoted as $g(\tilde{b}_{D3})$. A smooth line connects numerical calculations for each strength. This Figure is taken from [1].

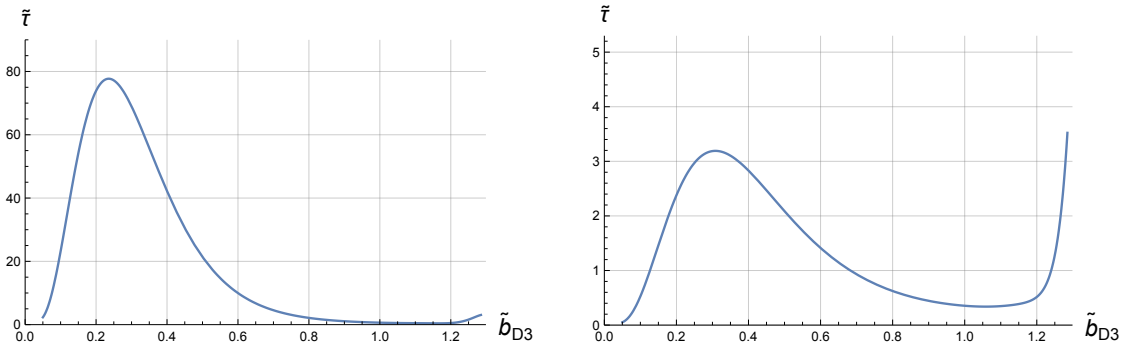

Figure 3.12: The life-time calculations for $A_B = 1.5(\text{left}), 1.1(\text{right})$. $\tilde{\tau}$ represents the dimensionless τ. When the magnetic field is small, the life-time calculation shows an unintuitive behavior against naive expectations, which implies that the WKB breaks down. Taking into account this, the numerical evaluation in the region $\tilde{b}_{D3} \leq 0.3$ should be considered unreliable. These figure is cited from [1]

Since the inverse of the decay rate gives the life-time, substituting the calculation of the functional determinant into (3.4.8), we finally obtain

$$\tau = \frac{\sqrt{\pi}}{\left(\widetilde{R}_{\rm max} - \widetilde{R}_{\rm min}\right)} \frac{P_{\rm min}^{1/4}}{Q_{\rm min}^{3/4}} \exp\left[-\omega \int_{\widetilde{R}_{\rm min}}^{\widetilde{R}_{\rm max}} \left\{ \frac{1}{\sqrt{(\dot{\widetilde{R}}_b)^2}} - \omega^{-1} \frac{1}{\widetilde{R} - \widetilde{R}_{\rm min}} \right\} d\widetilde{R}_b \right] e^B \ . \tag{3.4.41}$$

Numerical calculation of the life-time with respect to the magnetic field strength is shown in Figure 3.12.

3.5 Implication from TCC

3.5.1 Reduction to cubic oscillator

The approximations employed in our life-time calculation consist of two key elements: the steepest descent approximation and the dilute gas approximation. For the steepest descent approximation to hold, the contribution of the classical solution must dominate, and the exponential function must decrease rapidly around the saddle point. Therefore, the validity of this approximation requires the following conditions:

$$A_B \widetilde{B} \gg 1 \ , \quad A_B \det{}'\big(P[\widetilde{R}_b]\frac{d^2}{ds^2} + Q[\widetilde{R}_b]\big) \gg 1 \ . \tag{3.5.1}$$

These conditions are satisfied when A_B is sufficiently large, even if the functional determinant is somewhat smaller. However, the condition is violated if A_B is not very large and the determinant is relatively small. This behavior is a distinctive feature of our noncanonical theory. In this context, the DBI action serves as a low-energy effective theory, where the coefficients of the kinetic term exhibit unusual behavior as $b \to 0$. Such tendencies are characteristic of situations where new particles emerge at low energies, and in this case, new zero modes might arise due to the restoration of $O(4)$ symmetry. Notably, we have not encountered a comparable phenomenon in the analysis of cubic oscillators like those discussed in [121], as the kinetic terms in those cases did not display this specific behavior.

The dilute gas approximation is another approximation imposed when performing the instanton method. Let us assume that the overall factor A_B is sufficiently large and the steepest descent approximation is correct. Observing the bounce solution reveals that as b_{D3} decreases, the shape of the solution becomes more abrupt, and the overlap between bounce solutions diminishes, as can be understood from Figure 3.7. Consequently, the dilute gas approximation holds valid when b_{D3} is small.

In summary, if $A_B \gg 1$, both approximations remain valid for small values of b_{D3} up to a certain range. However, as the magnetic field increases sufficiently, the bounce solution broadens, rendering the dilute gas approximation invalid and causing the calculation to break down, as signaled by the divergence of τ near $b_{\rm crit}$. In the region where b_{D3} is extremely small, the functional determinant becomes excessively small, leading to the failure of the saddle point approximation. This is corroborated by the numerical results in Figure 3.12, which show that the life-time drops to zero in the small magnetic field region, contrary to intuitive expectations. A similar trend is observed for $A_B \geq 1$. However, as discussed earlier, when A_B is not sufficiently large, the second condition of the saddle point approximation is violated more readily. In other words, the reliable range of the calculation is narrower compared to the case where $A_B \gg 1$.

As b_{D3} increases, the life-time initially decreases monotonically but diverges at the critical strength of the magnetic field. This behavior is physically implausible, as the life-time should not increase while the potential becomes less stable. This anomaly indicates the breakdown of the leading-order contribution derived from the WKB approximation. To achieve an accurate calculation, it becomes necessary to include contributions that account for interactions between bounce solutions, which are omitted in the dilute gas approximation. In principle, this approach should yield the correct results. However, a longstanding issue arises in this context: even when higher-order terms are calculated through perturbative expansion, the resulting series is known to be an asymptotic series

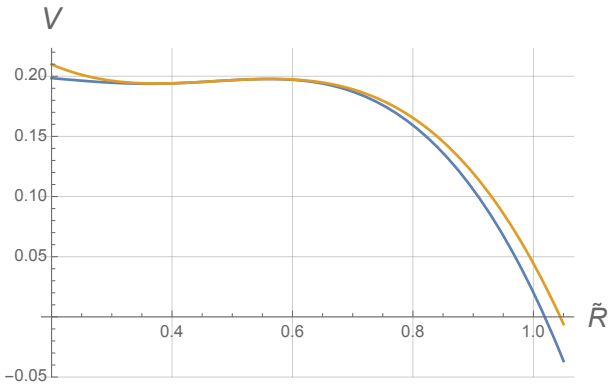

Figure 3.13: Comparison between our DBI potential, represented by the blue line, and the fitting curve with cubic potential, represented by the orange line. This Figure is taken from [1].

with zero radius of convergence [122]. A quartic oscillator is a well-known example of this behavior [123,124]. Consequently, obtaining precise higher-order corrections in this model poses significant challenges, making rigorous analysis difficult.

Nevertheless, since our purpose is to calculate the life-time with a strong catalytic effect, it is unnecessary to conduct a detailed analysis for all values of b_{D3}. When b_{D3} is near the critical strength, the potential can be well approximated by a cubic potential, see Figure 3.13. Thus, we focus on applying an analysis of cubic oscillators based on variational perturbation expansion (VPE) [125, 126]. The Lagrangian considered by Kleinert and Mustapic is expressed as [121]

$$L_{KM} = \frac{m}{2}\dot{x}^2 + \left[\frac{m\omega^2}{2}x^2 - \lambda x^3\right], \tag{3.5.2}$$

where the overall sign of the potential is positive, reflecting the Euclidean framework. We then shift the variable to move the potential minima away from the origin, eliminating the quadratic term,

$$x = y + \frac{m\omega^2}{6\lambda}. \tag{3.5.3}$$

Substituting this transformation, the original Lagrangian becomes

$$L_{KM} = \frac{m}{2}\dot{y}^2 + \left[\frac{m^2\omega^4}{12\lambda}y - \lambda y^3 + \frac{m^3\omega^6}{108\lambda^2}\right] + \cdots. \tag{3.5.4}$$

To compare to the sifted Lagrangian (3.5.4), let us perform the expansion of our DBI action around the inflection point. When the DBI potential is almost flat, since the change of the bounce solution is extremely moderate, we can expand the kinetic term as $\sqrt{1+\dot{R}^2} \simeq 1 + \dot{R}^2/2$. If we expand R around the inflection point denoted by R_v with $R = R_v + y$, we obtain

$$S = \int dt_E c^{-1} A_B \left[\sqrt{\widetilde{R}_v^4 + \tilde{b}_{D3}^4}\frac{\dot{y}^2}{2} + V(\widetilde{R}_v, \tilde{b}_{D3}) - f(\widetilde{R}_v, \tilde{b}_{D3})c^{-1}y - h(\widetilde{R}_v, \tilde{b}_{D3})c^{-3}y^3\right]. \tag{3.5.5}$$

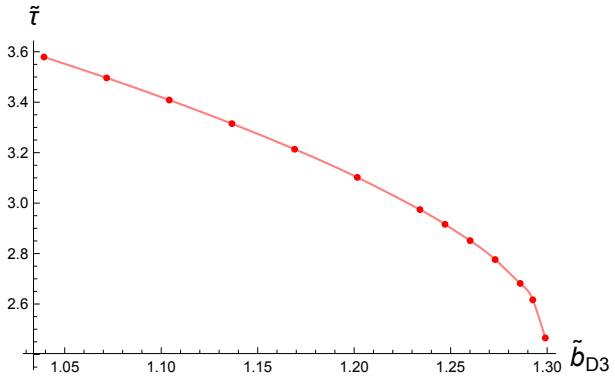

Figure 3.14: A dimensionless life-time with $A_B = 1$. This Figure is taken from [1].

Trivially, the Lagrangian is given by

$$L \simeq A_B\Big[\sqrt{\widetilde{R}_v^4 + \tilde{b}_{D3}^4}\,\frac{\dot{y}^2}{2} + V(\widetilde{R}_v, \tilde{b}_{D3}) - f(\widetilde{R}_v, \tilde{b}_{D3})y - h(\widetilde{R}_v, \tilde{b}_{D3})y^3\Big], \tag{3.5.6}$$

where y and t_E are dimensionful values. Comparing this approximated Lagrangian with L_{KM}, we find the following relations.

$$m = c^{-1}A_B\sqrt{\widetilde{R}_v^4 + \tilde{b}_{D3}^2}\ , \quad \frac{m^2\omega^4}{12\lambda} = c^{-2}A_B f(\widetilde{R}_v, \tilde{b}_{D3})\ , \quad \lambda = c^{-4}A_B h(\widetilde{R}_v, \tilde{b}_{D3})\ . \tag{3.5.7}$$

Given the comparison above, we can apply the result for the complex energy of a cubic potential, presented in [121]. Let us now consider the limit where the potential barrier vanishes. The authors of [121] derived the decay rate up to the leading order using the VPE, which is expressed as

$$\Gamma = -2\mathrm{Im}E_0 \simeq 2 \times (0.448)\left(\frac{\lambda^2}{\mathrm{m}^3}\right)^{1/5}\left(1 - 0.186\Big(\frac{\mathrm{m}^3\omega^5}{\lambda^2}\Big)^{\frac{2}{5}}\right)\ . \tag{3.5.8}$$

The specific value -0.186 was extracted from the graph in [121], which may involve a discrepancy of about factor 2, though this does not significantly affect the overall result. Figure 3.14 presents the life-time calculation for b_{D3} near the critical magnetic field strength, demonstrating that the life-time decreases as the instability is enhanced.

Using the approximated calculation above, we can roughly estimate the magnetic field dependence of the life-time by linking the results from the WKB calculation when b_{D3} is small with those near b_{cr}. This approach assumes that the life-time decreases monotonically as the potential becomes less stable. Interestingly, the decay rate does not approach zero, even in the limit where the potential barrier vanishes.

Beyond the dilute gas approximation, the imaginary part of the complex energy tends to be smaller due to the interaction between bounce solutions. Therefore, the life-time, defined as the inverse of the decay rate, becomes longer. This statement is consistent with the behavior of the numerical calculation in Figure 3.15 showing that the life-time is evaluated to be shorter because of the ignoring the interaction.

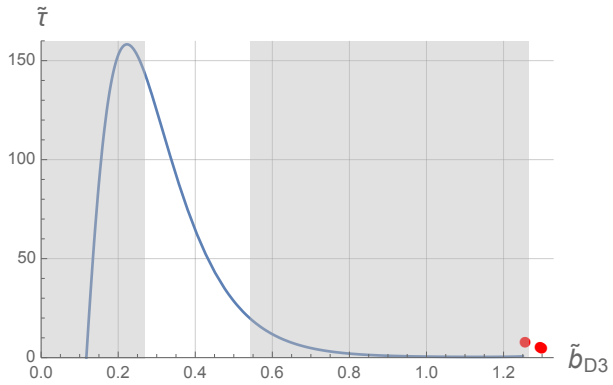

Figure 3.15: The numerical result of the WKB approximation, represented by the blue line, and the VPE, represented by the red dots, with $A_B = 1.5$. Although neither result is reliable in the shaded region, we anticipate a monotonically decreasing function that smoothly connects the two results based on the physical assumptions. This Figure is taken from [1].

3.5.2 Comparison to TCC condition

Let us compare the critical life-time obtained in the previous section, $\tau_{\rm cr}$, with the TCC condition. We can denote the critical life-time as follows

$$\tau_{\rm cr} \simeq \frac{1}{2\times 0.448}\frac{T_{DW}}{\Delta V}A_B^{\frac{1}{5}}\left(\frac{h^2}{(\widetilde{R}_v^4+\tilde{b}_{D3}^2)^{3/2}}\right)^{-1/5}\Big|_{\rm cr} \simeq 2.46 A_B^{\frac{1}{5}}\frac{T_{DW}}{\Delta V}, \tag{3.5.9}$$

where we used (3.5.8). $T_{DW}/\Delta V$ is the factor c introduced in (3.3.17). Substituting the above expression in the TCC condition, we obtain

$$2.46 A_B^{\frac{1}{5}}\frac{T_{DW}}{\Delta V} \leq H_I^{-1}\log\frac{M_{\rm pl}}{H_I}, \tag{3.5.10}$$

where H_I is the Hubble constant and $M_{\rm pl} = \sqrt{3/8\pi G}$ is the reduced Planck mass. Denoting radii of 2-cycles at $z_4 = a_1$ and a_2 as ℓ and the size of the internal $\mathbb{S}^3$ as L, since our setup is based on the string theory, we have

$$\Delta V = 2nV_* \sim \frac{nM_{\rm st}^6\ell^2}{g_s}, \quad T_{DW} \sim \frac{L^3M_{\rm st}^6}{g_s}, \tag{3.5.11}$$

where n is the number of the (anti) D5-branes. Note that these estimation always include $\mathcal{O}(1)$ ambiguity due to the lack of perfect determination of the whole geometry, see section 3.3. Also we can estimate the Hubble constant as $H_I = \sqrt{V/3M_{\rm pl}^2} \sim \sqrt{\Delta V/M_{\rm pl}^2}$, then the inequality (3.5.10) becomes

$$2.46\left(\frac{4\pi}{n^8}\right)^{1/5}\frac{L^{27/5}}{\ell^{16/5}}M_{\rm st}^{6/5}g_s^{-1/5} \lesssim \frac{M_{\rm st}L^3}{\ell\sqrt{g_sn}}\log\left(\frac{M_{\rm st}^5L^6}{\ell g_s^{3/2}n^{1/2}}\right), \tag{3.5.12}$$

where we used $A_B = 4\pi T_{DW}^4/\Delta V^3 \sim 4\pi L^{12} M_{\rm st}^6/g_s l^6 n^3$ and $M_{\rm pl}^2 = M_{\rm st}^8 L^6/g_s^2$. Here, it is convenient to introduce new parameters α and β as $L = \alpha l_s$, $\ell = \beta l_s$, where l_s represents the string length. Substituting these expression into (3.5.12), we find

$$2.46 \frac{(4\pi)^{1/5}}{n^{11/10}} \frac{\alpha^{12/5}}{\beta^{11/5}} \lesssim g_s^{-3/10} \log\left(\frac{\alpha^6}{\beta g_s^{3/2} n^{1/2}}\right) . \tag{3.5.13}$$

as a final result. To avoid D5-branes and anti D5-brane condensing very quickly, it would be plausible to consider that L is larger than ℓ, namely $\alpha > \beta$. Additionally, it is important to note that ℓ must satisfy $\ell \gtrsim l_s$; otherwise, the α' perturbation would cause EFT to break down.

Figure 3.16 shows the g_s-dependence of the LHS and the RHS of (3.5.13). As seen from this Figure, the TCC condition seems to be satisfied for $g_s \lesssim \mathcal{O}(1)$. As stated above, we should note that our evaluations inevitably contain the ambiguity of $\mathcal{O}(1)$. Here, we describe some features of the parameter dependence of the constraint.

- The allowable region of g_s where the TCC condition is satisfied is extended if we adopt a large value as n, see (a) and (b). In this thesis, we assumed that n is up to $\mathcal{O}(10)$.
- If we fix α to a smaller value, the allowable region of g_s is extended, see (a) and (c), or (b) and (f).
- Seen from (d) and (e), the smaller β, the smaller the allowable region of g_s is. Moreover, if α and β take comparable value, the TCC condition (3.5.13) implies $g_s \lesssim \mathcal{O}(1)$, see (c), (e), and (f).

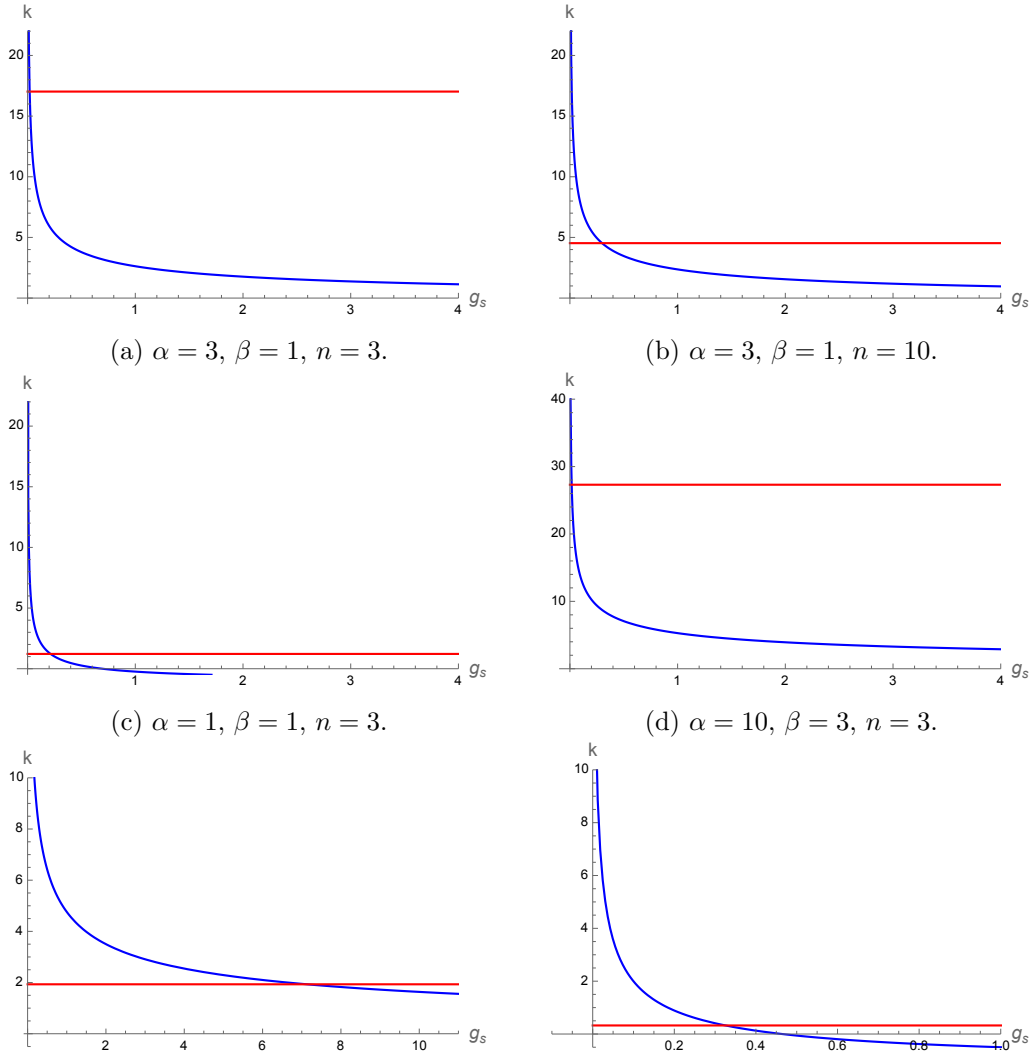

(a) $\alpha = 3$, $\beta = 1$, $n = 3$.

(b) $\alpha = 3$, $\beta = 1$, $n = 10$.

(c) $\alpha = 1$, $\beta = 1$, $n = 3$.

(d) $\alpha = 10$, $\beta = 3$, $n = 3$.

(e) $\alpha = 10$, $\beta = 10$, $n = 3$.

(f) $\alpha = 1$, $\beta = 1$, $n = 10$.

Figure 3.16: Red lines represent the LHS of (3.5.13), and blue lines represent the RHS for various parametrizations. The label k on the vertical axis is the value of the LHS and the RHS. The TCC is satisfied where the blue lines are above the red lines. These Figures are taken from [1].

3.6 Discussion and summary

In this chapter, we first reviewed one of the swampland conjectures, the trans-Planckian censorship conjecture. This conjecture has attracted much attention in the context of the swampland program. We have applied the TCC condition to the geometrically realized metastable vacuum in string theory under the assumption of the positive energy vacuum. A monopole like D3-brane plays an important role as a catalyst that induces the decay of the dS vacua, and the life-time of the vacua becomes much shorter. Given the enhanced decay, we have investigated the allowed parameter spaces where the life-time of vacua

satisfies the condition.

Regarding calculation techniques, this chapter also addresses considerations for WKB analysis in non-canonical quantum mechanical systems. In Sec. 3.4.2, we demonstrated that, unlike conventional canonical theories, the normalization constant for zero modes does not generally coincide with the bounce action in non-canonical systems. In Sec. 3.4.3, we showed that the fluctuation operator takes the form of the Sturm-Liouville type and successfully generalized the traditional methods for computing functional determinants by applying the contour deformation method.

It would be of significant interest to extend this study by employing established solutions in various dimensions to examine the permitted regions within the framework of the swampland program. In this chapter, we adopted the same assumptions as those presented in [67, 68], including the existence of de Sitter vacua. However, the strictest form of the de Sitter conjecture [56, 57] excludes such vacua. Thus, we consider it worthwhile to investigate the potential existence of de Sitter vacua under the influence of catalysts within the context of string theory. Nevertheless, as this line of inquiry falls outside the scope of the present work, we defer it to future research.

The generalized Gel'fand-Yaglom formula presented in this study is generic and can be applied to various problems. The DBI action addressed in this work can be regarded as a natural generalization of the Nambu-Goto action, representing the effective action for relativistic defects. Therefore, an application to the WKB analysis of metastable defects is expected to be immediately feasible. Additionally, exploring quantum fluctuations in vacuum decay with gravitational corrections is an intriguing avenue. In vacuum decay within a gravitational background, gravitational corrections to the bubble are introduced, and the differential operator governing fluctuations does not generally take the form of a Schrödinger-type operator. Calculating quantum fluctuations in such cases remains an important challenge and is a promising direction for our future work.

Chapter 4

Decay of Compactified Spacetime via Singular Instanton

This chapter discusses a decay phenomenon distinct from the previous chapter, specific to compactified spacetimes. Higher-dimensional vacua with compactified dimensions can exhibit decay channels where *bubbles of nothing* (BoN), regions without spacetime degrees of freedom, overwhelms the entire spacetime [34]. The instanton mediating this decay is a Euclidean black hole solution, and typically, a prescription is applied to fix the period of the Euclidean time such that no conical singularities appear at the horizon. However, we can also argue that the Euclidean action, rather than the metric, plays a crucial role in the computation of decay rates. In this case, if the contribution of the conical singularity to the Euclidean action is finite, the presence of the singularity may be permissible. Based on this perspective, we examine the contribution of the conical singularity to the bounce action in the simplest higher-dimensional vacuum, the five dimensional Kaluza-Klein vacuum, which decays through the expansion of a bubble of nothing. The contribution from the singularity reduces the bounce action, suggesting that the decay mediated by the singular instanton might be more dominant. We reproduce the bounce action calculation using thermodynamic functions and attempt to provide a thermodynamic interpretation of how the singularity enhances the decay.

The organization of this chapter is as follows. Section 4.1 reviews the decay of the Kaluza-Klein vacuum via the BoN, based on [34]. In Section 4.2, we discuss the decay mediated by singular instantons, demonstrating that the decay is enhanced compared to smooth instantons. Here, we demonstrate how to deal with the singularity via the conical deficit regularization. Moreover, we reconstruct the bounce action using thermodynamic functions and attempt to provide a thermodynamic interpretation of the contributions from singularities. Finally, Section 4.3 is devoted to the discussion and summary of this chapter. This chapter is based on collaboration with Prof. Yutaka Ookouchi and Mr. Ryota Sato [2].

4.1 Review of bubble of nothing

4.1.1 Non-perturbative instability of Kaluza-Klein vacuum

In this section, we review the decay of the Kaluza-Klein vacuum following the original paper by Witten [34]. Kaluza-Klein vacuum is the vacuum solution of the Einstein equation in five dimensional spacetime: $R_{\mu\nu} = 0$. This solution consists of ordinary four dimensional flat spacetime, namely Minkowski vacuum, and $\mathbb{S}^1$ compactified space. Thus, the topology of this spacetime is given by

$$X_5 = \mathcal{M}_4 \times \mathbb{S}^1. \tag{4.1.1}$$

Here, $\mathbb{S}^1$ is a circle with radius R. A metric corresponding to this spacetime is

$$ds^2 = -dt^2 + dx^2 + dy^2 + dz^2 + d\varphi^2, \tag{4.1.2}$$

where φ is the coordinate for the compactified dimension.

While it is confirmed that the Kaluza-Klein vacuum (4.1.2) is stable against perturbative fluctuations, this vacuum possesses a semiclassical instability. An instanton solution that mediates this non-perturbative decay is the one that approaches the Euclidean Kaluza-Klein vacuum asymptotically [34],

$$ds^2 = \left(1 - \frac{\alpha}{r^2}\right)^{-1} dr^2 + r^2 d\Omega_3^2 + \left(1 - \frac{\alpha}{r^2}\right) d\phi^2, \tag{4.1.3}$$

where $d\Omega_3$ is the standard round metric, and ϕ represents a imaginary time defined as $\phi = it$. This is the Euclidean five dimensional Schwarzschild black hole [127]. It is well known that Euclidean black holes have conical singularities at the position of the horizon for the original Lorentzian spacetime, and (4.1.3) is no exception. To see the singularity, we need to see the behavior of the instanton spacetime near the singularity. Let us introduce a new coordinate as follows

$$\rho \equiv \sqrt{\alpha}\left(1 - \frac{\alpha}{r^2}\right)^{1/2}, \tag{4.1.4}$$

With this coordinate, we obtain the approximated expression of (4.1.3) near the singularity as

$$ds^2 \simeq d\rho^2 + \alpha^2 d\Omega_3^2 + \rho^2 d\left(\frac{\phi}{\sqrt{\alpha}}\right)^2. \tag{4.1.5}$$

In this coordinate system, the singularity is at $\rho = 0$. Generally, the period of $\phi/\sqrt{\alpha}$ is not equal to 2π, resulting in a conical singularity at $\rho = 0$, as depicted in Figure 4.1. However, if the smoothness condition $\alpha = R^2$ is satisfied, the period of the variable ϕ becomes $2\pi R$, eliminating the deficit angle. This nonsingular instanton solution was introduced by Witten and is referred to as the bubble of nothing because spacetime terminates smoothly at $r = R$, leaving no spacetime inside. In the section 4.2, we will investigate singular solutions that do not fulfill the smoothness condition.

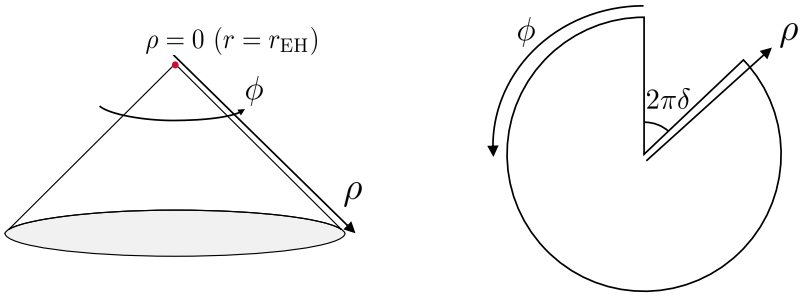

Figure 4.1: Schematic picture near the conical singularity of the instanton solution. The left panel shows a conceptual diagram of the vicinity of the singularity, and the right panel shows a geometry net.

4.1.2 Bounce action for bubble of nothing instanton

Now, we will review the calculation of the bounce action of the BoN instanton. In the following sections, we will compute curvatures for various spaces and hypersurfaces, so pay attention to the notation. For details on the notation, refer to Appendix D.1. The gravitational action in five dimensional spacetime is given by

$$I = -\frac{1}{16\pi G_5}\int_{\mathscr{V}} \mathcal{R}\sqrt{g}d^5x - \frac{1}{8\pi G_5}\oint_{\partial\mathscr{V}} (\mathcal{K}-\mathcal{K}_0)\sqrt{\tilde{g}}d^4\tilde{x}, \tag{4.1.6}$$

where the first volume integral is the Einstein-Hilbert (EH) term, and the second is a boundary term called Gibbons-Hawking-York (GHY) term [128,129]. $\mathcal{R}$ is the Ricci scalar, and $\mathcal{K}$ is the trace of extrinsic curvature, which is defined with *outward* unit normal vector $\tilde{n}_\alpha$ perpendicular to the hypersurface as

$$\mathcal{K} \equiv \tilde{n}^{\alpha}_{;\alpha}, \tag{4.1.7}$$

where the subscription $_{;\alpha}$ denotes the covariant derivative. Let us define the "positive" ward unit normal vector n_α of the hypersurface for which scalar function Φ also takes a constant value here.

$$n_\alpha \equiv \frac{\partial_\alpha \Phi}{\sqrt{|g^{\mu\nu}\Phi_{,\mu}\Phi_{,\nu}|}}. \tag{4.1.8}$$

For instance, r constant hypersurface is characterized by $\Phi = r - r_0 = 0$, where r_0 is an arbitrary constant. It should be noted that the outward unit normal does not necessarily coincide with the unit normal vector n_α, which points in the positive direction of the coordinates. See Figure 4.2 for intuitive understanding. While the nondynamical term $\mathcal{K}_0$ does not contribute to the variation, its inclusion is essential to ensure the finiteness of the Euclidean action. The five dimensional Newton constant, G_5, can be expressed in terms of the compactification radius R and the four dimensional Newton constant G_4 as $G_5 = 2\pi R G_4$. Here, $\tilde{x}$ represents the coordinates on the boundary surface $\partial\mathscr{V}$, and the induced metric on this surface is denoted as $\tilde{g}_{ab}$.

Since the BoN instanton solution is the Euclidean Schwarzshild solution, which is Ricci flat, then the EH term has no contribution to calculating the Euclidean action, that is

$$-\frac{1}{16\pi G_5}\int_{\mathscr{V}} \mathcal{R}\sqrt{g}d^5x = 0. \tag{4.1.9}$$

With regard to the GHY term, we need to be a bit more careful. Since the instanton spacetime is non-compact in a spatial sense, there is seemingly no contribution to the boundary integral. However, as seen from the conformal diagram, there exists an asymptotic boundary at $r \to \infty$. Therefore, we should consider the boundary integral on Σ_r, that is

$$-\oint_{\partial\mathscr{V}} (\mathcal{K} - \mathcal{K}_0)\sqrt{\tilde{g}}d^4\tilde{x} = \lim_{r_\infty \to \infty}\Big(-\int_{\Sigma_{r_\infty}} (\mathscr{K} - \mathscr{K}_0)\sqrt{\gamma}d^4z\Big), \tag{4.1.10}$$

where $\int_{\Sigma_{r_\infty}}$ denotes the boundary integral on the asymptotic boundary Σ_{r_∞}, and γ is the determinant of the induced metric. $\mathscr{K}$ is calculated by a positiveward unit normal vector as

$$\mathscr{K} \equiv r^{\alpha}_{;\alpha}. \tag{4.1.11}$$

In this case, $\tilde{n}^\alpha$ and r^α are identical, so the sign before the boundary integral is the same. The three dimensional round metric can be written by

$$r^2 d\Omega_3^2 = r^2\left\{d\theta_1^2 + \sin^2\theta_1(d\theta_2^2 + \sin^2\theta_2 d\theta_3^2)\right\}, \tag{4.1.12}$$

where $0 \le \theta_{1,2} \le \pi$ and $0 \le \theta_3 \le 2\pi$. Then, the induced metric on a r constant hypersurface, Σ_r, is given by

$$\gamma_{ij}dz^i dz^j = r^2 d\theta_1^2 + r^2\sin^2\theta_1 d\theta_2^2 + r^2\sin^2\theta_1\sin^2\theta_2 d\theta_3^2 + \left(1 - \frac{R^2}{r^2}\right)d\phi^2. \tag{4.1.13}$$

Now, the scalar quantity characterizing the hypersurface Σ_{r_∞} is $\Phi = r - r_\infty = 0$, then the positiveward unit normal vector is expressed as

$$r_\alpha = \frac{\partial_\alpha(r - r_\infty)}{\sqrt{|g^{rr}\Phi_{,r}\Phi_{,r}|}} = \frac{\partial_\alpha r}{\sqrt{f(r)}}. \tag{4.1.14}$$

As a consequence, using (4.1.13), we can calculate the trace of the extrinsic curvature on Σ_r as follows

$$\mathscr{K} = r^{\alpha}{}_{;\alpha} = \frac{3}{r}\left(1 - \frac{R^2}{r^2}\right)^{\frac{1}{2}} + \frac{R^2}{r^3}\left(1 - \frac{R^2}{r^2}\right)^{-\frac{1}{2}}. \tag{4.1.15}$$

Next, we need to calculate the nondynamical term. Since $\mathscr{K}_0$ is defined as the extrinsic curvature of hypersurfaces embedded into the flat spacetime, we must identify the concrete embedding into the flat spacetime given by

$$ds^2 = d\tilde{r}^2 + \tilde{r}^2 d\tilde{\Omega}_3^2 + d\tilde{\phi}^2. \tag{4.1.16}$$

To realize appropriate embedding, it is plausible to impose the following relations to the coordinates

$$\tilde{r} \equiv r, \quad \tilde{\Omega}_3 \equiv \Omega_3, \quad d\tilde{\phi} \equiv \sqrt{1 - \frac{R^2}{r^2}}d\phi, \tag{4.1.17}$$

It is evident that the flat spacetime (4.1.16) corresponds to the original instanton spacetime with $R = 0$. Consequently, $\mathscr{K}_0$ can be determined by substituting $R = 0$ into (4.1.15), yielding

$$\mathscr{K}_0 = \frac{3}{\tilde{r}} = \frac{3}{r}. \tag{4.1.18}$$

Then, substituting (4.1.15) and (4.1.18) into the boundary integral in the GHY term, we can perform the calculation as

$$\begin{aligned}
&-\int_{\Sigma_{r_\infty}} (\mathscr{K} - \mathscr{K}_0)\sqrt{\gamma} d^4z \\
&= -\int_{\Sigma_{r_\infty}} \left\{ \frac{3}{r}\left(1 - \frac{R^2}{r^2}\right)^{\frac{1}{2}} + \frac{R^2}{r^3}\left(1 - \frac{R^2}{r^2}\right)^{-\frac{1}{2}} - \frac{3}{r} \right\} r^3 \sin^2\theta_1 \sin\theta_2 \sqrt{1 - \frac{R^2}{r^2}} d^4z \\
&\simeq -\int_{\Sigma_{r_\infty}} \left\{ 3r^2 - 2R^2 - 3r^2\left(1 - \frac{R^2}{2r^2}\right) \right\} \sin^2\theta_1 \sin\theta_2 d^4z \\
&= R^2\pi^2 \cdot 2\pi R,
\end{aligned} \tag{4.1.19}$$

where we took an approximation in the third line by taking $r_\infty \to \infty$ into account. Therefore, the on-shell value of the GHY term is given by

$$-\frac{1}{8\pi G_5}\oint_{\partial\mathscr{V}} (\mathcal{K} - \mathcal{K}_0)\sqrt{\tilde{g}} d^4\tilde{x} = \frac{\pi R^2}{8G_4}. \tag{4.1.20}$$

Provided the calculations (4.1.9) and (4.1.20), we find that the Euclidean action of the BoN instanton is

$$I \simeq \frac{\pi R^2}{8G_4}. \tag{4.1.21}$$

Originally, the bounce action B is defined as the difference between the Euclidean action of the instanton solution and that of the trivial solution. However, since the latter corresponds to the flat vacuum solution in the present case, its Euclidean action is clearly zero. Thus, we arrive at the final result[1]

$$B \simeq I - I_0 = \frac{\pi R^2}{8G_4}. \tag{4.1.22}$$

The decay rate per unit volume is of order of $\exp(-\pi R^2/8G_4)$

It should be emphasized that the above semiclassical analysis is applicable only when the Kaluza-Klein radius is significantly larger than the Planck length. If this condition is not met, the accuracy of the approximation becomes worse, rendering the quantitative discussion unreliable. Nevertheless, it is highly plausible that the non-perturbative decay of the Kaluza-Klein vacuum would still occur.

In this context, it is important to note that the compactification radius cannot be determined at the classical level. Typically, quantum corrections will fix the radius, but the details of effective potential depend on the specific matter fields present. In other words, the quantitative reliability of this analysis relies on how the radius is stabilized once quantum effects are taken into account.

[1]This result is different from the original calculation made in [34] by factor 2, but this discrepancy has been verified by several studies [130, 131].

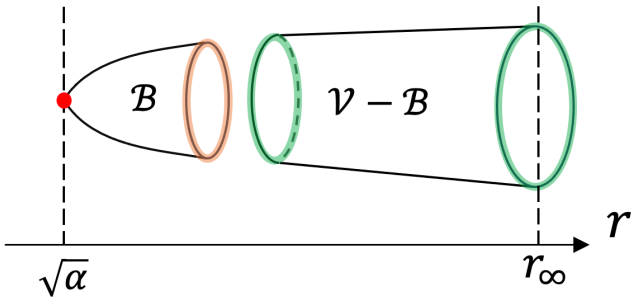

Figure 4.2: Schematic diagram for the geometry of the BoN instanton spacetime split into two near the singularity denoted by a red dot. The orange border is the boundary of singular part, $\partial\mathscr{B}$, the green border is that of nonsingular part, $\partial\left(\mathscr{V}-\mathscr{B}\right)$. This figure is taken from [2].

4.2 Singular bubble of nothing

4.2.1 Conical deficit regularization

The concept of regularizing conical singularities with smooth caps was initially introduced in the study of cosmic strings [132, 133]. Following this idea, Fursaev and Solodukhin pioneered a systematic method to regularize Riemannian manifolds with conical singularities [102]. Their approach involved substituting spacetimes containing singularities with regular manifolds while imposing boundary conditions that ensured smoothness at the boundaries. They demonstrated that the Ricci scalar exhibits δ function-like behavior, consistent with the Gauss-Bonnet theorem, in the limit where the regularization parameter vanishes.

Gregory, Moss, and Withers extended the ideas of [102] by including a discussion of the GHY term [48]. They found that the contribution from the smooth cap to the action is negative and independent of the deficit angle. Importantly, The cap they employed is off-shell as it is. However, the final calculation is independent of the details of the spacetime of the cap since we take the limit that brings the slicing surface to the horizon position. This work has been influential, particularly in studying black hole-induced decay of the Higgs vacuum [49–51].

While [48] focused on the Schwarzschild-de Sitter metric, their method is broadly applicable for regularizing conical singularities in Euclidean black hole solutions. In the following section, we apply this regularization technique to the singular BoN instanton and compute its contribution to the Euclidean action.

In the previous section, we examined the case where the BoN instanton satisfies the smoothness condition, $\alpha = R^2$. In this section, we relax this condition and focus on metrics that exhibit a conical singularity at $r = \sqrt{\alpha}$, based on the procedure given in [48]. To compute the bounce action for the BoN instanton solution with singularities, we divide the instanton spacetime into two distinct regions: the singular spacetime, $\mathscr{B}$, and the nonsingular spacetime, $\mathscr{V}-\mathscr{B}$.

As a consequence of splitting, the gravitational action (4.1.6) is also divided into the Euclidean action near the singularity, $I_{\mathscr{B}}$, and the Euclidean action without the singularity,

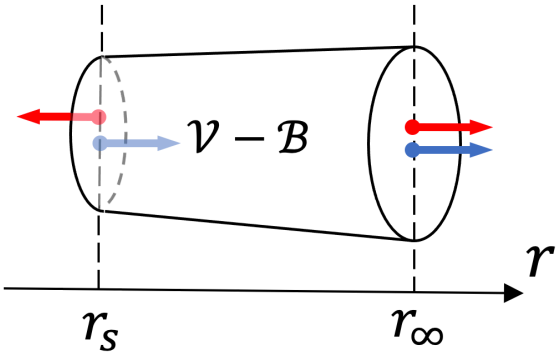

Figure 4.3: Comparison between outward unit normal vectors $\tilde{n}^\alpha$ represented by red allows and positiveward unit normal vectors r^α represented by blue allows. These unit normal vectors do not necessarily coincide. This figure is cited from [2].

$I_{\mathscr{V}-\mathscr{B}}$. That is,

$$I = I_{\mathscr{V}-\mathscr{B}} + I_{\mathscr{B}}, \tag{4.2.1}$$

$$I_{\mathscr{V}-\mathscr{B}} = -\frac{1}{16\pi G_5}\int_{\mathscr{V}-\mathscr{B}} \mathcal{R}\sqrt{g}d^5x - \frac{1}{8\pi G_5}\oint_{\partial(\mathscr{V}-\mathscr{B})} (\mathcal{K}-\mathcal{K}_0)\sqrt{\tilde{g}}d^4\tilde{x}, \tag{4.2.2}$$

$$I_{\mathscr{B}} = -\frac{1}{16\pi G_5}\int_{\mathscr{B}} \mathcal{R}\sqrt{g}d^5x - \frac{1}{8\pi G_5}\oint_{\partial\mathscr{B}} (\mathcal{K}-\mathcal{K}_0)\sqrt{\tilde{g}}d^4\tilde{x}. \tag{4.2.3}$$

Here, the second terms in $I_{\mathscr{V}-\mathscr{B}}$ and $I_{\mathscr{B}}$ account for contributions from not only the asymptotic boundary at infinity but spatial boundaries introduced by slicing the spacetime. In the following sections, we will evaluate $I_{\mathscr{V}-\mathscr{B}}$ and $I_{\mathscr{B}}$ separately, taking the limit where the splitting surface approaches the singularity. Finally, we will sum up the two contributions to obtain the total Euclidean action.[2]

4.2.2 Euclidean action for non-singular part

We proceed to compute the on-shell action for the manifold without the singularity. Since the BoN instanton solution is Ricci-flat everywhere except at the singularity, the contribution from the EH term will vanish. However, the boundary integral has a non-zero contribution at the spatial boundary Σ_{r_s} and the asymptotic boundary Σ_{r_∞}, as illustrated in Figure 4.3. Thus, evaluating the on-shell action reduces to focusing on two boundary integrals

$$\begin{aligned} &-\oint_{\partial(\mathscr{V}-\mathscr{B})} (\mathcal{K}-\mathcal{K}_0)\sqrt{\tilde{g}}d^4\tilde{x} \\ &\qquad = \lim_{r_s\to\sqrt{\alpha}}\int_{\Sigma_{r_s}} (\mathscr{K}-\mathscr{K}_0)\sqrt{\gamma}d^4z - \lim_{r_\infty\to\infty}\int_{\Sigma_{r_\infty}} (\mathscr{K}-\mathscr{K}_0)\sqrt{\gamma}d^4z. \end{aligned} \tag{4.2.4}$$

[2]For spacetimes without conical singularities, the integrals over the spatial boundaries of $\mathscr{V}-\mathscr{B}$ and $\mathscr{B}$ cancel each other, as they have the same magnitude but opposite signs. However, this cancellation is nontrivial in the presence of singularities because special contributions from the singularities may arise. As shown in later calculations, these terms indeed coincide even when singularities are present.

Here, $\mathscr{K}$ represents the trace of the extrinsic curvature, defined using the positiveward unit normal vector r^α to the r constant surfaces. It is important to note the relative signs of $\tilde{n}^\alpha$ and r^α on Σ_{r_s} and Σ_{r_∞} are respectively as follows

$$\tilde{n}^\alpha = -r^\alpha \quad \text{on } \Sigma_{r_s}, \tag{4.2.5}$$
$$\tilde{n}^\alpha = r^\alpha \quad \text{on } \Sigma_{r_\infty}. \tag{4.2.6}$$

As a result, we should pay attention to the fact that the signs of the boundary integrals differ. The induced metric on Σ_r is expressed as

$$\gamma_{ij}dz^i dz^j = r^2 d\theta_1^2 + r^2 \sin^2\theta_1 d\theta_2^2 + r^2 \sin^2\theta_1 \sin^2\theta_2 d\theta_3^2 + \left(1 - \frac{\alpha}{r^2}\right) d\phi^2. \tag{4.2.7}$$

This metric determines the traces of the extrinsic curvatures in the boundary integrals. Scalar functions characterizing Σ_{r_s} and Σ_{r_∞} are given by $\Phi = r - r_s = 0$ and $\Phi = r - r_\infty = 0$, respectively. Thus, the positiveward unit normal vectors, derived from the definition (4.1.8), are given by

$$r_\alpha^{(s)} = \frac{\partial_\alpha (r - r_s)}{\sqrt{|g^{rr}\Phi_{,r}\Phi_{,r}|}} = \frac{\partial_\alpha r}{\sqrt{f(r)}}\ , \qquad r_\alpha^{(\infty)} = \frac{\partial_\alpha (r - r_\infty)}{\sqrt{|g^{rr}\Phi_{,r}\Phi_{,r}|}} = \frac{\partial_\alpha r}{\sqrt{f(r)}}. \tag{4.2.8}$$

It is evident that the expression for r_α is identical for both boundaries. Consequently, the extrinsic curvature for each hypersurface is computed as

$$\mathscr{K} = r^\alpha{}_{;\alpha} = g^{\alpha\mu} r_{\mu;\alpha} = \frac{3}{r}\left(1 - \frac{\alpha}{r^2}\right)^{\frac{1}{2}} + \frac{\alpha}{r^3}\left(1 - \frac{\alpha}{r^2}\right)^{-\frac{1}{2}}. \tag{4.2.9}$$

We need to consider the nondynamical term. As the embedding method into the flat spacetime is the same as explained in the section 4.1.2, we obtain

$$\mathscr{K}_0 = \frac{3}{r}. \tag{4.2.10}$$

This expression is just what we fix α to zero in (4.2.9). Substituting (4.2.9) and (4.2.10) into (4.2.4), we find the boundary integral as follows

$$\int_{\Sigma_{r_s, r_\infty}} (\mathscr{K} - \mathscr{K}_0)\sqrt{\gamma} d^4 z = \int_{\Sigma_{r_s, r_\infty}} \left\{ 3r^2 - 2\alpha - 3r^2\left(1 - \frac{\alpha}{r^2}\right)^{\frac{1}{2}} \right\} \sin^2\theta_1 \sin\theta_2 d^4 z. \tag{4.2.11}$$

This expression is identical to the one obtained by replacing R^2 with α in the third line of (4.1.19). Finally, we take the limits $r_s \to \sqrt{\alpha}$ and $r_\infty \to \infty$, respectively. For the integral over Σ_{r_s}, the limit $r_s \to \sqrt{\alpha}$ can be directly applied in (4.2.11), leading to the following calculation

$$\lim_{r_s \to \sqrt{\alpha}} \int_{\Sigma_{r_s}} (\mathscr{K} - \mathscr{K}_0)\sqrt{\gamma} d^4 z = \int_{\Sigma_{\sqrt{\alpha}}} \alpha \sin^2\theta_1 \sin\theta_2 d^4 z = 2\pi^2 \alpha \cdot 2\pi R. \tag{4.2.12}$$

In contrast, the integral over Σ_{r_∞} is evaluated as follows

$$-\lim_{r_\infty \to \infty} \int_{\Sigma_{r_\infty}} (\mathscr{K} - \mathscr{K}_0)\sqrt{\gamma} d^4 z \simeq \lim_{r_\infty \to \infty} \int_{\Sigma_{r_\infty}} \frac{\alpha}{2} \cdot \sin^2\theta_1 \sin\theta_2 d^4 z = \frac{2\pi^2\alpha}{2} \cdot 2\pi R. \tag{4.2.13}$$

Here, we used an approximation valid for large r, as in (4.1.19). Substituting (4.2.12) and (4.2.13) into (4.2.4), the contribution from the GHY term is found to be

$$-\frac{1}{8\pi G_5}\oint_{\partial(\mathscr{V}-\mathscr{B})}(\mathcal{K}-\mathcal{K}_0)\sqrt{\tilde{g}}d^4\tilde{x} \simeq \frac{1}{8\pi G_5}\cdot 2\pi^2\alpha\cdot 2\pi R+\frac{1}{8\pi G_5}\cdot\frac{2\pi^2\alpha}{2}\cdot 2\pi R=\frac{3\pi\alpha}{8G_4}. \tag{4.2.14}$$

In the middle expression, the first term arises from the spatial boundary that divides spacetime. Although the boundary integral yields a finite value, this might appear to conflict with the argument presented by the authors of [48]. However, this discrepancy can be attributed to the presence of the asymptotic boundary in the BoN instanton solution. Thus, our result remains consistent with their conclusion. For further details, see Appendix D.2.

Given the above discussion, the on-shell action of the spacetime with the singularity removed is as follows

$$I_{\mathscr{V}-\mathscr{B}} \simeq \frac{3\pi\alpha}{8G_4}. \tag{4.2.15}$$

4.2.3 Euclidean action for cap

In this section, we compute the Euclidean action of the spacetime with the conical singularity, denoted as $I_{\mathscr{B}}$, using the method of conical deficit regularization [48, 102]. Before applying the regularization, we introduce new coordinates and analyze their behavior near the singularity. These coordinates are defined as follows

$$\rho \equiv r\sqrt{f}, \quad f=1-\frac{\alpha}{r^2}. \tag{4.2.16}$$

Using these coordinates, the instanton solution can be expressed as

$$ds^2 = f(r(\rho))d\phi^2+d\rho^2+r(\rho)^2d\Omega_3^2. \tag{4.2.17}$$

Here, the conical singularity originally located at $r=\sqrt{\alpha}$ is mapped to $\rho=0$ in this coordinate system. Moreover, by replacing ϕ with a 2π-periodic variable χ, the metric of the instanton spacetime can be rewritten as

$$ds^2 = F(\rho)^2d\chi^2+d\rho^2+r(\rho)^2d\Omega_3^2, \quad F(\rho)^2\equiv f(r(\rho))R^2, \tag{4.2.18}$$

where the following relation has been used

$$\frac{d\phi}{2\pi R}=\frac{d\chi}{2\pi}. \tag{4.2.19}$$

To understand the behavior of the coordinates near the singularity, we perform a Taylor expansion around $\rho=0$. From the definition in (4.2.18), we find that $F(0)=0$ at the singularity. Therefore, the Taylor expansion of $F(\rho)$ near $\rho=0$ is given by

$$F(\rho)\simeq\rho F'(0), \tag{4.2.20}$$

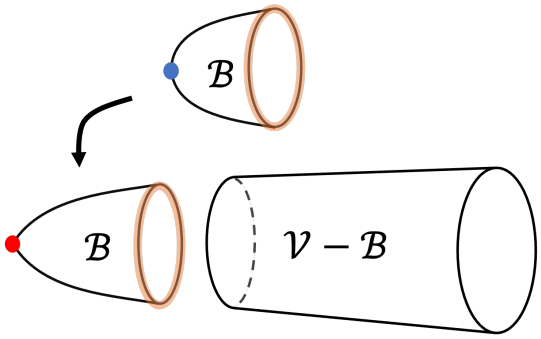

Figure 4.4: Schematic image of the regularization by replacing the conical singularity with smooth cap. This figure is taken from [2].

where the prime symbol ($\prime$) denotes differentiation with respect to ρ. Substituting (4.2.20) into (4.2.18), the instanton solution near the singularity becomes approximately

$$ds^2 \simeq d\rho^2 + \rho^2 d(F'(0)\chi)^2 + r(0)^2 d\Omega_3^2. \tag{4.2.21}$$

This expression implies that there is no singularity at $\rho = 0$ if $F'(0)\chi$ is 2π-periodic quantity, i.e., if $F'(0) = 1$. However, since $F'(0) \neq 1$ in general, the deficit angle $2\pi\delta$ appears, defined as

$$\delta = 1 - \frac{F(\rho)}{\rho}\bigg|_{\rho\to 0} = 1 - F'(0), \tag{4.2.22}$$

where the last step follows from (4.2.20). Given the explicit expression for $F(\rho)$, its derivative can be directly calculated. Using (4.2.16) and (4.2.18), the deficit angle is explicitly found to be

$$\delta = 1 - \frac{R}{\sqrt{\alpha}}, \tag{4.2.23}$$

Keeping the above analysis in mind, let us proceed with regularization. Specifically, we regularize the spacetime by cutting out the region near the singularity and replacing it with a smooth manifold, as illustrated in Figure 4.4. While this paper adopts such a regularization without providing explicit proof, this smoothing process is expected to occur naturally within the framework of string theory. For instance, in [134], the authors demonstrated that conical singularities can be resolved through closed string tachyon condensation. If we interpret the singularity as an indication of missing degrees of freedom, its inclusion in the theory would naturally lead to a regularization. However, it is crucial to emphasize that the calculations presented here are independent of the specific details of the regularization method. Therefore, our conclusions remain unchanged regardless of the approach used to regularize the singularity.

Following the procedure proposed in [48], we introduce a regularized metric as follows

$$ds^2 = \tilde{F}(\rho)^2 d\chi^2 + d\rho^2 + r(\rho)^2 d\Omega_3^2, \tag{4.2.24}$$

where the tilde-added function reflects the profile specific to regularized spacetime. In other words, $\tilde{F}'(0) = 1$ holds now because there is no conical singularity in the regularized spacetime. We represent the splitting position as $\rho = \epsilon$, where ϵ is an extremely small quantity. We will take $\epsilon \to 0$ in the last of our calculation. Additionally, since the regularized metric should coincide with the original metric at $\rho = \epsilon$, the deficit angle needs to satisfy $\delta = 1 - \tilde{F}(\epsilon)/\epsilon$. Since ϵ is the tiny quantity, we can rewrite this relation as

$$\delta \simeq 1 - \tilde{F}'(\epsilon). \tag{4.2.25}$$

Using the expression (4.2.25), we can derive the specific form of the gravitational action written with the deficit angle. Let us evaluate the EH action at first. The Ricci scalar for (4.2.24) is given by

$$\mathcal{R} = -\frac{2\tilde{F}''}{\tilde{F}} - \frac{6r''(\rho)}{r(\rho)} - \frac{6\tilde{F}'r'(\rho)}{\tilde{F}r(\rho)} - \frac{6(1-r'(\rho)^2)}{r(\rho)^2}. \tag{4.2.26}$$

Among these terms, the divergent terms as $\epsilon \to 0$ will dominate the calculation. By definition, order estimates for $\tilde{F}(\rho)$ and its second derivative are

$$\tilde{F} \simeq \epsilon\tilde{F}'(0) = \mathcal{O}(\epsilon), \tag{4.2.27}$$

$$\tilde{F}'' = \mathcal{O}\left(\frac{\tilde{F}'(\epsilon) - \tilde{F}'(0)}{\epsilon - 0}\right) = \mathcal{O}\left(\frac{(1-\delta)-1}{\epsilon}\right) = \mathcal{O}\left(-\frac{\delta}{\epsilon}\right), \tag{4.2.28}$$

then we find

$$-\frac{2\tilde{F}''}{\tilde{F}} = \frac{\mathcal{O}\left(\frac{\delta}{\epsilon}\right)}{\mathcal{O}(\epsilon)} = \mathcal{O}\left(\frac{\delta}{\epsilon^2}\right), \tag{4.2.29}$$

$$-\frac{\tilde{F}'r'}{\tilde{F}r} = \frac{\mathcal{O}(\epsilon)}{\mathcal{O}(\epsilon)} = \mathcal{O}\left(\epsilon^0\right). \tag{4.2.30}$$

These estimates show that in the limit $\epsilon \to 0$, only the first term in the Ricci scalar diverges and contributes to the action integral. Thus, the EH term in this limit is computed as

$$\begin{aligned}
-\frac{1}{16\pi G_5}\int_{\mathscr{B}} \mathcal{R}\sqrt{g}d^5x &= \lim_{\epsilon\to 0}\left(-\frac{1}{16\pi G_5}\int_0^\epsilon d\rho \int_{\Sigma_\rho} d^4z\tilde{F}(\rho)r(\rho)^3\sin^2\theta_1\sin\theta_2\mathcal{R}\right) \\
&\simeq \lim_{\epsilon\to 0}\left\{-\frac{\pi^2}{4G_5}\int_0^\epsilon d\rho\tilde{F}(\rho)r(\rho)^3\left(-\frac{2\tilde{F}''}{\tilde{F}}\right)\right\} \\
&\simeq \lim_{\epsilon\to 0}\left(\frac{\pi^2 r(\epsilon)^3}{2G_5}\int_0^\epsilon d\rho\tilde{F}''\right).
\end{aligned} \tag{4.2.31}$$

Substituting the expansion $r(\epsilon) \simeq \sqrt{\alpha} + \epsilon r'(0)$ into the above, we get

$$\begin{aligned}
-\frac{1}{16\pi G_5}\int_{\mathscr{B}} \mathcal{R}\sqrt{g}d^5x &\simeq \lim_{\epsilon\to 0}\left\{\frac{\pi^2}{2G_5}\left(\sqrt{\alpha}+\epsilon r'(0)\right)^3\int_0^\epsilon d\rho\tilde{F}''\right\} \\
&= \lim_{\epsilon\to 0}\left(\frac{\pi^2\alpha^{\frac{3}{2}}}{2G_5}\left[\tilde{F}'(\epsilon) - \tilde{F}'(0)\right]\right) \\
&= -\frac{\pi^2\alpha^{\frac{3}{2}}}{2G_5}\delta.
\end{aligned} \tag{4.2.32}$$

Thus, we have obtained the on-shell contribution from the Einstein-Hilbert term.

The next task is to calculate the GHY term. Since the nondynamical term can be calculated as

$$\begin{aligned}\oint_{\partial\mathscr{B}} \mathcal{K}_0\sqrt{\tilde{g}}d^4\tilde{x} &= \lim_{r_s\to\sqrt{\alpha}}\int_{\Sigma_{r_s}} \mathscr{K}_0\sqrt{\gamma}d^4z \\ &= \lim_{r_s\to\sqrt{\alpha}}\int_{\Sigma_{r_s}} \frac{3}{r}\cdot r^3\left(1-\frac{\alpha}{r^2}\right)^{\frac{1}{2}}\sin^2\theta_1\sin\theta_2 d^4z \\ &= 0, \end{aligned} \tag{4.2.33}$$

from (4.2.10), all we have to do here is to evaluate the boundary term due to $\mathscr{K}$. Using the metric (4.2.24), we find[3]

$$\mathscr{K} = \frac{\tilde{F}'}{\tilde{F}} + \frac{3r'}{r}. \tag{4.2.34}$$

Only the first term affects the final result in the limit $\epsilon \to 0$, so the boundary integral is given by

$$\begin{aligned}\frac{1}{8\pi G_5}\int_{\partial\mathscr{B}} \mathcal{K}\sqrt{\tilde{g}}d^4\tilde{x} &= \frac{1}{8\pi G_5}\int_{\Sigma_\epsilon} \mathscr{K}\sqrt{\gamma}d^4z \\ &= \lim_{\epsilon\to 0}\left(\frac{4\pi^3}{8\pi G_5}\tilde{F}(\epsilon)r(\epsilon)^3\mathscr{K}\right) \\ &= \lim_{\epsilon\to 0}\left\{\frac{\pi^2}{2G_5}\tilde{F}(\epsilon)r(\epsilon)^3\left(\frac{\tilde{F}'(\epsilon)}{\tilde{F}(\epsilon)}\right)\right\} \\ &= \lim_{\epsilon\to 0}\left(\frac{\pi^2 r(\epsilon)^3}{2G_5}\tilde{F}'(\epsilon)\right). \end{aligned} \tag{4.2.35}$$

It is important to note that the orientation of the positiveward unit normal vector and the outward normal vector are the same, so the sign of the integral does not change in the first line. Using (4.2.25) and the expansion $r(\rho) \simeq \sqrt{\alpha} + \epsilon r'(0)$, the boundary integral becomes

$$\frac{1}{8\pi G_5}\oint_{\partial\mathscr{B}} \mathcal{K}\sqrt{\tilde{g}}d^4\tilde{x} \simeq \lim_{\epsilon\to 0}\left\{\frac{\pi^2}{2G_5}\left(\sqrt{\alpha}+\epsilon r'(0)\right)^3\tilde{F}'(\epsilon)\right\} = \frac{\pi^2\alpha^{\frac{3}{2}}}{2G_5}(1-\delta). \tag{4.2.36}$$

Therefore, the calculation of the on-shell value of the GHY term in the limit of $\epsilon \to 0$ is performed as

$$-\frac{1}{8\pi G_5}\oint_{\partial\mathscr{B}} (\mathcal{K}-\mathcal{K}_0)\sqrt{\tilde{g}}d^4\tilde{x} \simeq -\frac{\pi^2\alpha^{\frac{3}{2}}}{2G_5}(1-\delta). \tag{4.2.37}$$

With the calculation so far, we have all the factors we need. substituting (4.2.32) and (4.2.37) into (4.2.3), we obtain

$$\begin{aligned} I_{\mathscr{B}} &\simeq -\frac{\pi^2\alpha^{\frac{3}{2}}}{2G_5}\delta - \frac{\pi^2\alpha^{\frac{3}{2}}}{2G_5}(1-\delta) \\ &= -\frac{\pi\alpha^{\frac{3}{2}}}{4G_4 R}. \end{aligned} \tag{4.2.38}$$

[3]The coefficient in the second term is different from the derivation in [48] by factor 2, but this discrepancy is not crucial for the final results.

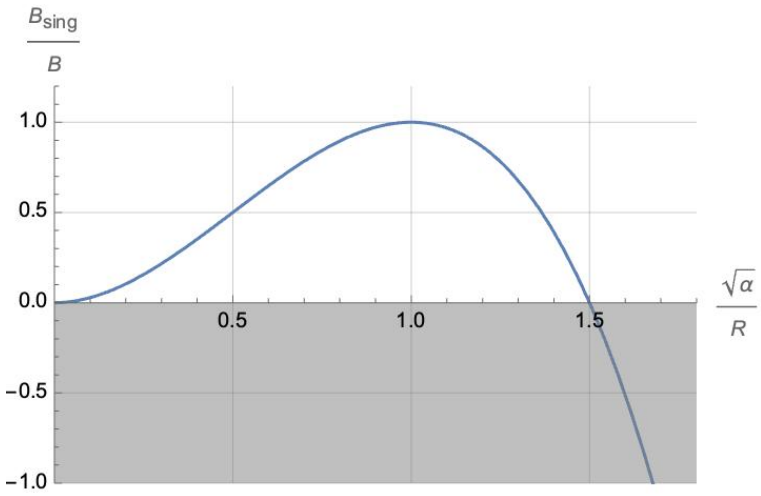

Figure 4.5: The ratio between the bounce actions for the singular BoN instanton solution and that for the nonsingular solution is shown as a function of $\sqrt{\alpha}/R$. In the graph, the ratio is nondimensionalized by $\sqrt{\alpha}/R$.

This is precisely the contribution to the on-shell action from the conical singularity. (4.2.38) is independent of the value of the deficit angle, as shown in [48].

4.2.4 Total bounce action

Together with the calculation displayed so far, we now derive the total bounce action B_{singular}. Substituting (4.2.15) and (4.2.38) into the Euclidean action (4.2.1), we obtain

$$B_{\text{singular}} \simeq \frac{\pi R^2}{8G_4}\left(\frac{3\alpha}{R^2} - \frac{2\alpha^{3/2}}{R^3}\right) = B\left(\frac{3\alpha}{R^2} - \frac{2\alpha^{3/2}}{R^3}\right), \tag{4.2.39}$$

where B is the Witten's original bounce action. Figure 4.5 shows the variation of the ratio between B_{singular} and B with respect to $\sqrt{\alpha}/R$. This result demonstrates that $B_{\text{singular}} = B$ when $\sqrt{\alpha} = R$, which reproduces the result for the original smooth instanton. Therefore, our analysis is consistent with Witten's result [34]. Additionally, since the decay rate $\gamma \propto e^{-B/\hbar}$ increases as the bounce action becomes small, (4.2.39) implies that the singularity enhances the decay of the Kaluza-Klein vacuum. The parameter δ, which corresponds to the deficit angle and is given by (4.2.23), suggests that the larger the deficit angle is, the more the vacuum decay is enhanced. Here, $0 < \alpha < R^2$ corresponds to the region where the deficit angle is negative, which is physically interpreted as the region where the cone of singularity is inverted.

Here, we would like to discuss the validity of our analysis for the singular instanton. In the region where the bounce action is negative, corresponding to the shaded region in Figure 4.5, the decay rate grows exponentially, causing the semiclassical approximation to break down. Furthermore, since the accuracy of the semiclassical approximation improves with a larger Euclidean action, it is expected to become less accurate as B_{singular} approaches 0. The asymmetry observed around $\sqrt{\alpha} = R$, even in the part of the graph

where the bounce action is positive, is likely a consequence of the diminished accuracy of the approximation.

Finally, it should be highlighted that the mechanism by which the singularity's contribution enhances the decay rate can be analyzed from a thermodynamic standpoint, as we will describe in Section 4.2.5. The discussion in Section 4.2.5 suggests that this enhancement of decay may primarily stem from the increase in entropy in Euclidean space. The notion of decay enhancement driven by entropy growth has also been noted in several previous works [135, 136], and it is particularly fascinating that a comparable interpretation may be relevant to the scenario under consideration. For more details, refer to the subsequent Section.

4.2.5 Thermodynamical interpretation

We have seen the enhancement of the decay via singularity in the instanton spacetime. Now, let us attempt an interpretation from a thermodynamic point of view. It is widely known that Euclidean gravitational theories can be related to thermodynamics [129, 137, 138]. Regarding the semiclassical analysis, we can also evaluate the Euclidean action via thermodynamic functions calculated in the Euclidean spacetime [130, 139]. Since the Euclidean action coincides with the Helmholtz free energy divided by the Hawking temperature, it is plausible to concentrate on the calculation of the free energy [140]. At this point, we can express the free energy by the ADM energy E and the black hole entropy S as follows

$$W = E - TS, \tag{4.2.40}$$

where the temperature is given as an inverse of the periodicity in the ϕ direction, that is, $T = (2\pi R)^{-1}$. This periodicity is constant with or without singularity. For an asymptotically flat and geometrically complete manifold, the ADM energy is well-defined through a boundary integral over the codimension-two surface [141]. Similarly, entropy can be computed using the Bekenstein-Hawking formula [142–144]. Indeed, if the instanton spacetime is smooth and has no singularities, we can calculate these two quantities as follows

$$E = \frac{3\pi R^2}{8G_5}, \tag{4.2.41}$$

$$S = \frac{A}{4G_5} = \frac{2\pi^2 R^3}{4G_5}. \tag{4.2.42}$$

Thus, substituting these into (4.2.40), we obtain

$$W = \frac{\pi R^2}{8G_5} = \frac{\pi R^2}{8G_4 \cdot 2\pi R}, \tag{4.2.43}$$

where we used $G_5 = 2\pi R G_4$ in the last deformation. By dividing this free energy by the Hawking temperature, we can reproduce Witten's result as

$$B = \frac{W}{T} = \frac{\pi R^2}{8G_4}. \tag{4.2.44}$$

If conical singularities exist, we should perform calculations of energy and entropy with the appropriate regularization in mind. First, we will focus on the derivation of the ADM

energy. For asymptotically flat and smooth spacetimes, the ADM energy is defined by choosing the lapse function as $N = 1$ and the shift function as $N^a = 0$. Moreover, the following Hamiltonian constraint,

$$K^{ab}K_{ab} - K^2 - {}^4R = 0, \tag{4.2.45}$$

is imposed to a given Hamiltonian[4]:

$$\begin{aligned}(16\pi G_5)H = \int_{\Sigma_t} \left[N\left(K^{ab}K_{ab} - K^2 - {}^4R\right) - 2N_a\left(K^{ab} - Kh^{ab}\right)_{|b}\right]\sqrt{h}\ \mathrm{d}^4y \\ - 2\oint_{S_t}\left[N\left(k - k_0\right) - N_a\left(K^{ab} - Kh^{ab}\right)r_b\right]\sqrt{\sigma}\mathrm{d}^3\theta.\end{aligned} \tag{4.2.46}$$

Here, in the case of manifolds with conical singularities, it is not immediately clear whether the curvatures in the constraint condition converge. However, we can demonstrate that (4.2.45) holds universally, regardless of whether regularization is applied. The positiveward unit vector normal to ϕ constant surface is given by

$$n_\alpha = \frac{\partial_\alpha\phi}{|g^{\phi\phi}\Phi_{,\phi}\Phi_{,\phi}|^{\frac{1}{2}}} = \frac{\partial_\alpha\phi}{|f(r)^{-1}|^{\frac{1}{2}}} = \sqrt{f}\partial_\alpha\phi. \tag{4.2.47}$$

Since the instanton spacetime has no dependence on ϕ, each component of the extrinsic curvature is zero. We can also calculate the four dimensional Ricci scaler on the hypersurface as

$${}^4R = -\frac{6r''(\rho)}{r(\rho)} + \frac{6(1 - r'(\rho)^2)}{r(\rho)^2}, \tag{4.2.48}$$

where ρ is the radial coordinate introduced in (4.2.16). We can give the explicit form of the derivative of r with respect to ρ as

$$r' = \left(1 - \frac{\alpha}{r^2}\right)^{\frac{1}{2}}, \quad r'' = \frac{\alpha}{r^3}. \tag{4.2.49}$$

Using this expression, we soon confirm that the Ricci scalar vanishes. Therefore, the constraint condition above still holds for our singular manifold. Then, the ADM energy can be calculated by the definition

$$E = -\frac{1}{8\pi G_5}\oint_{S_{\phi r}}(k - k_0)\sqrt{\sigma}d^3\theta, \tag{4.2.50}$$

where $S_{\phi r}$ denote the (ϕ, r)-constant three surface.

To obtain the ADM energy based on (4.2.50), all we have to do is calculate the trace of the extrinsic curvature. From the definition, we obtain

$$k = \frac{3\sqrt{f(r)}}{r}. \tag{4.2.51}$$

[4]In order to derive the Hamiltonian, we must compute the Ricci scalar of the EH term on the hypersurface, which results in the emergence of a new boundary term. While the Gauss theorem is generally applicable in this context, it cannot be directly used for singular manifolds. However, if a smooth cap is introduced to replace the region near the singularity using conical deficit regularization, the Gauss theorem can be applied as usual.

We can calculate k_0 simply by taking α to zero in (4.2.51) as

$$k_0 = \frac{3}{r}. \tag{4.2.52}$$

For the BoN instanton solution, even this simplified calculation gives the correct result. Since the difference between (4.2.51) and (4.2.52) has no divergence near the singularity, the boundary integral clearly converges. When we use the conical deficit regularization described in section 4.2, contributions from the two spatial boundaries appear but ultimately cancel each other out. As a result, just like in the case of smooth manifolds, we only need to consider the contribution from the asymptotic boundary, yielding

$$E = \frac{3\pi\alpha}{8G_5}. \tag{4.2.53}$$

This expression coincides with (4.2.41) when $\sqrt{\alpha} = R$ and indicates that no special correction comes from the singularity to the energy, at least at the classical level.

Let us now consider the entropy. The microscopic degrees of freedom of black holes remain an open question, and due to their ambiguity, various approaches to entropy calculation have been proposed. For a comprehensive review, see [145]. Here, we employ a traditional method that defines entropy as the semiclassical approximation of the thermodynamic potential in the microcanonical ensemble [146]. The Euclidean action for the microcanonical ensemble is expressed as a Legendre transformation of the standard gravitational action as follows

$$I_{mc,\mathrm{E}} \equiv I_{grav,\mathrm{E}} - \beta \int_{\mathcal{B}_\tau} d^{n-2}z \left(N\tilde{\varepsilon} - N^a \tilde{j}_a\right), \tag{4.2.54}$$

where ε and j_a are the quasi-local energy and the angular momentum density defined by the Brown-York tensor [147]. Here, the tilde means that those quantities contain the volume element. β is the inverse temperature, which is given by $\beta = 2\pi R$ in the present case. Based on this Euclidean action, the entropy of a black hole is given by [146]

$$S = -\Gamma_{mc} = -I_{mc,\mathrm{E}}\big|_{\mathrm{cl}}. \tag{4.2.55}$$

We have already computed the gravitational action in (4.2.39). The subtracted term in the Legendre transformation corresponds to the ADM energy and is given by

$$\beta \int_{\partial(\mathscr{V}-\mathscr{B})} d^{n-2}z \left(N\tilde{\varepsilon} - N^a \tilde{j}_a\right) = \frac{3\pi\alpha\beta}{8G_5}, \tag{4.2.56}$$

where we choose $N \to 1$, $N^a \to 0$. Therefore, the entropy calculated via the microcanonical ensemble becomes

$$S = \frac{2\pi^2\alpha^{3/2}}{4G_5}, \tag{4.2.57}$$

which perfectly matches the result obtained from the Bekenstein-Hawking formula.

Using the calculation of the ADM energy and the entropy, we can obtain the bounce action as

$$B_{\text{singular}} = \frac{E - TS}{T} = \frac{3\pi\alpha}{8G_4} - \frac{\pi\alpha^{3/2}}{4RG_4} = \frac{\pi R^2}{8G_4}\left(\frac{3\alpha}{R^2} - \frac{2\alpha^{3/2}}{R^3}\right), \tag{4.2.58}$$

which corresponds to the result (4.2.39) obtained in the previous section. We can regard this consistency as one of the evidence for the correctness of the prescription used in [48].

How can we understand the enhancement of instability caused by conical singularities? To consider this matter, let us slightly shift α from R^2 and express the changes in energy and entropy up to the second order as follows

$$\Delta E = \frac{3}{16G_4R}\Delta\alpha\ , \qquad \Delta S = \frac{3\pi}{8G_4}\Delta\alpha + \frac{3\pi}{32G_4R^2}\Delta\alpha^2. \tag{4.2.59}$$

Substituting these expressions into the thermodynamic definition of the bounce action gives

$$\begin{aligned} B_{\text{singular}} &= B + \frac{\Delta E}{T} - \Delta S \\ &\simeq B + \frac{3\pi}{8G_4}\Delta\alpha - \frac{3\pi}{8G_4}\Delta\alpha - \frac{3\pi}{32G_4R^2}\Delta\alpha^2 \\ &= B - \frac{3\pi}{32G_4R^2}\Delta\alpha^2. \end{aligned} \tag{4.2.60}$$

Here, the first-order change in the energy is exactly canceled by the first-order change in the entropy, leaving only the second-order change in the entropy. This second-order change is always negative, indicating that shifts in the horizon position act as a factor that reduces the bounce action. In other words, while the energy increases, the entropy increases even more, reducing the free energy. This provides us with a thermodynamic interpretation of the enhancement of the vacuum decay in the presence of singularities.

4.3 Discussion and summary

In this chapter, we investigated the non-perturbative decay of five dimensional Kaluza-Klein spacetime using a singular instanton. The bounce action, which determines the decay rate, was found to be smaller than that of Witten's nonsingular solution, leading to an increased decay rate. This result implies that instantons with singularities may play a dominant role in decay in higher-dimensional theories with compactified spaces, potentially contributing significantly to discussions around the swampland conjectures. We also explored thermodynamic interpretations of the enhancement. Specifically, we found that the contributions from singularities increase the internal energy, but this is outweighed by an even greater increase in entropy, resulting in a net decrease in free energy and, thus, an enhancement of vacuum decay.

The origin of the increase in entropy merits further discussion. One possibility lies in the regularization of the singularity. As shown by the authors of [48], the contributions of singularities to the on-shell action do not depend on the specific regularization scheme, provided the spacetime is smoothly regularized. If the regularization parameter ϵ is kept finite rather than taking the $\epsilon \to 0$ limit, a variety of states with slightly different profiles near the singularity could emerge. These states may account for the entropy increase observed in this analysis.

Variants of the BoN solution have already been discussed within the framework of string theory [148, 149]. We anticipate that singular instantons will also significantly contribute to string theory contexts, which we plan to explore in future work. Furthermore, while

this paper focuses on gravitational transitions between two vacua without introducing scalar fields explicitly, including such fields is necessary for studying more realistic models. For guidance, the work presented in [150] may be particularly helpful, and attempting to generalize our approach to models with scalar fields would provide a deeper understanding of the role of singularities in vacuum decay.

To address the conical deficit from relaxing the smoothness condition, we employed a regularization method based on replacing the singular region with a smooth metric. However, it is known that singularities can also be resolved through codimension-two defects. For instance, the authors of [151] introduced end-of-the-world (ETW) branes at the singularity's tip, a concept supported by the cobordism conjecture [152].[5] They constructed a bounce solution by replacing the singularity with a brane, demonstrating that this approach promotes vacuum decay. Interestingly, their findings share several features with our regularization procedure, such as a negative contribution from the singularity that enhances vacuum decay. Both approaches recover Witten's result under the smoothness condition. However, in cases where the deficit angle is positive, their results differ from ours. We interpret this discrepancy as reflecting two distinct decay channels. The authors of [151] introduced a new physical object, adding its contribution to the Lagrangian, whereas we stayed within the framework of Einstein gravity. Thus, it is natural for the derived bounce actions to differ.

Besides the above discussion, Introducing negative tension defects typically requires adding source terms to the Lagrangian. In several gravitational theories coupled with scalar fields, configurations corresponding to negative tension ETW branes have been constructed [153,154]. Moreover, it has been shown that smooth cigar geometries in higher dimensions can lead to negative tension branes at the tip of the spacetime in the lower-dimensional viewpoint of Einstein-dilaton gravity when reduced to lower dimensions [155]. The authors of [155] demonstrated the emergence of negative tension branes in specific examples of AdS solitons. For the related study, see [156]. Nonetheless, constructing negative tension defects from a top-down perspective involves setups beyond pure gravity, indicating a fundamentally different decay channel from the one studied in this thesis.

Furthermore, revealing the quantum processes responsible for generating defects is another intriguing direction for future research. For example, the nucleation of Chiral Soliton Lattice (CSL) in QCD under strong magnetic fields or rapid rotation provides a promising direction [157, 158]. These domain walls, with negative energy due to topological interactions, form through quantum tunneling facilitated by interactions such as the Dzyaloshinskii-Moriya interaction. If a similar mechanism could apply in string compactifications, topological interactions with the background Ramond-Ramond flux might play an important role in domain wall generation. Investigating such mechanisms in the BoN scenario while incorporating additional elements into the Lagrangian is an exciting avenue for future exploration.

Finally, let us address the issue of negative modes around the classical solution. Following Witten's discussion, we assumed the existence of a single negative mode since we utilized almost the same solution. However, the presence of singularities may introduce additional negative modes. Previous studies [159, 160] have shown that gravitational instantons can exhibit multiple negative modes. Thus, a more careful analysis of negative modes is required to fully understand the stability of the solutions presented here. We

[5] We thank the authors of [151] for letting us know their study and sharing us a helpful comment.

intend to revisit this issue in future work.

Chapter 5

Conclusion

In this thesis, we considered the enhancement of the decay of higher-dimensional vacuum based on the specific models. Inhomogeneous phase transitions around some catalysis are universal phenomena in nature and can also occur in higher-dimensional theories. If such enhancement occurs, it is expected to provide more efficient decay channels in the string landscape. From this point of view, we focus on the two possibilities, Dp-branes and the singularities in instanton spacetime as specific objects particular to higher-dimensional theories, and show that they indeed enhance the vacuum decay by WKB analysis. Here, we summarize the contents of this thesis.

In Chap. 3, we realized a metastable state geometrically through D5-branes and anti D5-branes wrapped on a manifold with singularities and investigated the catalytic effect of D3-branes wrapped on the internal space. These D3-branes form bound states with domain wall D5-branes, which connect the false and true vacua, and the remnant of the D3-branes can be seen as magnetic fields on the D5-branes. We derived the life-time of these bound states at the 1-loop level and confirmed numerically that the instability increases and the life-time decreases as the magnetic field strength grows. To perform the analysis, we generalized the Gel'fand-Yaglom method, presenting a formulation of the functional determinant that can be applied even to non-canonical theories, such as the EFT on Dp-branes. Furthermore, we numerically demonstrated the breakdown of WKB analysis in regions of strong instability and, instead, utilized previous results of anharmonic oscillators to derive the life-time in the limit where the potential barrier vanishes. While it might intuitively seem that the critical life-time would go to zero in this scenario, we explicitly showed that the life-time takes a non-zero value. Additionally, we compared the critical life-time with the constraints imposed by the TCC. Our results confirm the existence of a parameter region that satisfies the TCC constraints under reasonable assumptions regarding the size of the compactified space.

In Chap. 4, we investigated the non-perturbative decay of higher-dimensional vacua mediated by singular instantons. Higher-dimensional vacua with compactified dimensions possess a decay channel through which the spacetime is entirely overwhelmed by the bubble of nothing. Here, We considered relaxing the smoothness condition imposed on the gravitational instanton mediating this decay and calculated the contribution from the singularity based on the conical deficit regularization. We confirmed that the contribution, given by a Bekenstein-Hawking-like formula, reduces the bounce action. This finding suggests that decay via singular instantons could play a dominant role in the decay of

higher-dimensional vacua. Additionally, we reconstructed the bounce action using thermodynamic functions. While the original instanton spacetime is singular, the regularized spacetime is smooth, allowing us to apply the black hole thermodynamics without issue. In the regularized spacetime, we calculated the ADM energy and the Bekenstein-Hawking entropy and derived the Helmholtz free energy. Dividing the free energy by the Hawking temperature, we confirmed that the reconstructed bounce action coincides with the previous calculations based on the definition of the EH action and the GHY action. Our analysis reveals the mechanism whereby, as α deviates from the point where the smoothness condition ($\sqrt{\alpha} = R$) is satisfied, both the energy and the entropy in the Euclidean spacetime increase, but the change in entropy is greater, resulting in a smaller bounce action.

These studies suggest further diversity in quantum transition phenomena within the string landscape. The model investigated in the first study was relatively simple, involving a bound state formed by D5-branes and D3-branes. However, in more realistic scenarios, the presence of other objects may also be considered. Exploring the catalytic effects of branes in stringy setups that include background fluxes or singularities in much detail is an important direction for future work. Furthermore, as discussed in this study, examining whether the swampland conditions can still be satisfied in such setups would be intriguing. In addition, as suggested by the second study, singular instantons may play a critical role in the decay of compactified spacetimes. While this study focused on the instability of the simplest higher-dimensional vacua, it would be worthwhile to investigate whether decay channels mediated by singular instantons also play a dominant role in the collapse of more complex vacua embedded in string theory. Although constructing instanton solutions in such cases would not be straightforward, it is anticipated that doing so could open new windows to string-theoretic model building.

Appendix A

Gravitational Correction to Brane Bubble

In Chap. 3, we realized the bound state between the domain wall D5-brane and D3-branes and investigated the magnetic field dependence of the life-time by the WKB analysis. Let us analyze this bound state from a different point of view. Once the bound state is formed, the remnants of the D3-branes can be considered a background magnetic field on the domain wall. This appears as a spherically symmetric, magnetically charged bubble to an observer in four dimensional spacetime. Due to the inherent nonlinearity of string theory, this brane bubble maintains finite radii, even at the probe level. In this chapter, we propose a new stabilization mechanism for brane bubbles in four dimensional spacetime. By incorporating a gravitational correction inspired by general relativity into the brane bubble, we examine its influence on the potential. Our analysis reveals that in parameter regions with significant gravitational effects, the potential value at the horizon becomes relatively higher than the potential minimum, effectively removing even non-perturbative instabilities. Furthermore, we identify the existence of over-extremal states, characterized by $(gQ)^2 \geq G_4 m^2$, in regions where the magnetic field strength is sufficiently large. However, in our model, gravitational corrections cannot completely stabilize such over-extremal bubbles. This appendix also explores the trade-off between stabilizing the bubble and achieving an over-extremal state. The research results described in this appendix are based on [3].

The remainder of this chapter is organized as follows: in Section A.1, we first review the weak gravity conjecture. In Section A.2, we add the gravitational correction to (3.3.25) and show the beyond probe level potential. In Section A.3, we investigate the stability of the brane shell under gravitational correction and discuss the stabilization mechanism. Finally, in Section A.4, we study the over-extremal property of the brane bubble using a numerical calculation.

A.1 Weak gravity conjecture

Weak Gravity Conjecture (WGC) [161] is one of the most well-investigated swampland conjectures, which gives a lower bound to the gauge coupling constant (see, e.g., [162, 163]

for reviews). The original statement is below:[1]

Weak gravity conjecture
there must exist at least one particle that satisfies the following inequality

$$(gQ)^2 \geq \frac{m^2}{2M_{\rm pl}^2} = G_4 m^2 \ . \tag{A.1.1}$$

for $U(1)$ gauge coupling in four dimensional effective theory.

We will refer to this constraint as a weak gravity condition. This is called the *weak gravity* conjecture because it can be interpreted as an expression for the Coulomb force being greater than the gravitation force when both sides r^{-2} are multiplied. Indeed,

$$\frac{(gQ)^2}{r^2} \geq G_4 \frac{m^2}{r^2}. \tag{A.1.2}$$

A particle that satisfies (A.1.1) (or (A.1.2)) is commonly referred to as *over-extremal*. In theories decoupled from gravity, this condition simplifies to a trivial inequality with the right-hand side equal to zero. However, the Newton constant cannot be zero when considering an effective theory coupled with gravity. Determining whether such a compact object can exist within the framework of quantum gravity, such as string theory, remains a significant and nontrivial question.

A.2 Brane bubble potential beyond probe level

Following [185, 186], we introduce a gravitational correction to the probe-level potential (3.3.25). The authors of [185, 186] assumed that the interior of the bubble corresponds to a stable AdS spacetime, while the exterior represents a metastable vacuum. Denoting the exterior of the shell by $+$ and the interior by $-$, the metric for each side can be written as

$$ds_\pm^2 = -f_\pm(r)dt^2 + \frac{dr^2}{f_\pm(r)} + r^2 d\Omega_2^2, \tag{A.2.1}$$

where $d\Omega_2^2$ is the standard two dimensional round metric.[2] In this setup, since the lapse function depends only on r, the Israel junction condition is given by [187]

$$\mathcal{T}(r) = \frac{2}{8\pi G_4}\frac{1}{r}\left(\sqrt{f_-(r)} - \sqrt{f_+(r)}\right), \tag{A.2.2}$$

[1] This statement implies that black holes lacking (super)symmetry protection are inevitably unstable and must decay. When applied to extremal black holes, it suggests the possibility of WGC states where quantum corrections reduce the mass-to-charge ratio to below unity. This phenomenon has been corroborated across various gravitational theories. For discussions in the context of Einstein-Maxwell theory, see [164–183], and for recent extension to gravitational theories coupled with nonlinear electrodynamics, refer to [184].

[2] The precise expression of a general spherically symmetric spacetime is given by

$$ds^2 = -e^{2\psi(r)}f(r)dt^2 + f^{-1}(r)dr^2 + r^2 d\Omega_2^2.$$

However, by solving the Einstein equation $\partial\psi/\partial r = 0$, we are free to fix ψ to zero. Thus, in solving the Einstein equation in the following sections, it is sufficient to focus on $f(r)$.

where $\mathcal{T}(r)$ represents the tension of the shell. Later, we clarify the relationship between this tension and the previously mentioned domain wall tension.

First, we must appropriately select the interior and exterior spacetimes to add a gravitational correction. In the brane setup discussed in section 3.3, we considered a configuration where the four dimensional spacetime is populated with (anti) D5-branes, serving as the energy reference. Therefore, when incorporating the correction, it is reasonable to treat the interior spacetime (the true vacuum) as the Minkowski vacuum, which has zero gravitational energy. This implies that $f_-(r) = 1$. On the other hand, outside the shell (the false vacuum), we must consider Einstein gravity coupled with a nonlinear electromagnetic Lagrangian. This requires careful consideration. The well-known nonlinear electromagnetic Lagrangian, often referred to also as the DBI Lagrangian, is expressed as follows [188, 189]

$$\begin{aligned}\mathcal{L}_{DBI} &= -\frac{1}{\gamma}\left[\sqrt{-\det\left(\eta_{\mu\nu}+\sqrt{\gamma}F_{\mu\nu}\right)}-\sqrt{-\det\left(\eta_{\mu\nu}\right)}\right] \\ &= -\frac{1}{\gamma}\left[\sqrt{1+\frac{\gamma}{2}F_{\mu\nu}F^{\mu\nu}-\frac{\gamma^2}{16}\left(F_{\mu\nu}\widetilde{F}^{\mu\nu}\right)^2}-1\right] ,\end{aligned} \tag{A.2.3}$$

where γ is a parameter determining the cutoff scale, which is called the Born-Infeld parameter. Also, $\widetilde{F}^{\mu\nu}$ is the dual tensor defined by the anti-symmetric tensor as $\widetilde{F}^{\mu\nu} = (1/2)\epsilon^{\mu\nu\alpha\beta}F_{\alpha\beta}$. When $F_{\mu\nu}$ is very small, this Lagrangian reduces to the ordinary Maxwell Lagrangian. However, since brane has non-zero energy when $F_{\mu\nu}$ is turned off, it should reduce to the Nambu-Goto Lagrangian when $F_{\mu\nu} \to 0$. Thus, we should adopt

$$\mathcal{L}'_{DBI} = -\frac{1}{\gamma}\sqrt{1+\frac{\gamma}{2}F_{\mu\nu}F^{\mu\nu}-\frac{\gamma^2}{16}\left(F_{\mu\nu}\widetilde{F}^{\mu\nu}\right)^2}, \tag{A.2.4}$$

in our case and consider coupling with the Einstein gravity outside the bubble.

The bubble potential consists of three components: the energy inside the bubble, the outside of the bubble, and the bubble itself. We must evaluate each factor to derive the bubble potential with gravitational corrections. As stated above, since the inside of the bubble can be considered as the Minkowski spacetime, the first one is obviously zero. For the second one, the energy-momentum tensor of the gravity coupled with (A.2.4) is [190, 191]

$$T_{\mu\nu} = -\Pi^{-1/2}\left(F_\mu{}^\alpha F_{\nu\alpha}-\gamma\mathcal{G}\widetilde{F}_\mu{}^\alpha F_{\nu\alpha}\right)-g_{\mu\nu}\mathcal{L} , \quad \Pi = 1+\frac{\gamma}{2}F_{\alpha\beta}F^{\alpha\beta}-\frac{\gamma^2}{16}\left(F_{\alpha\beta}\widetilde{F}^{\alpha\beta}\right)^2 , \tag{A.2.5}$$

where $\mathcal{G} = (1/2)F_{\mu\nu}\widetilde{F}^{\mu\nu}$. If we substitute (A.2.4) into this expression, we obtain

$$\begin{aligned}T_{\mu\nu} &= -\left(1+\frac{\gamma}{2}F_{\alpha\beta}F^{\alpha\beta}\right)^{-1/2}F_\mu{}^\alpha F_{\nu\alpha}+\frac{g_{\mu\nu}}{\gamma}\sqrt{1+\frac{\gamma}{2}F_{\alpha\beta}F^{\alpha\beta}} \\ &= -\left(1+\frac{\gamma}{2}F_{\alpha\beta}F^{\alpha\beta}\right)^{-1/2}\left\{F_\mu{}^\alpha F_{\nu\alpha}-\frac{g_{\mu\nu}}{\gamma}\left(1+\frac{\gamma}{2}F_{\alpha\beta}F^{\alpha\beta}\right)\right\} .\end{aligned} \tag{A.2.6}$$

We omitted $F\widetilde{F}$ term before the calculation because the electric field is absent in our setup. Since we are considering a spherically symmetric spacetime, it is plausible to impose the

ansatz below on the metric

$$ds^2 = -f(r)dt^2 + f^{-1}(r)dr^2 + r^2\left(d\theta^2 + \sin^2\theta d\phi^2\right). \tag{A.2.7}$$

Utilizing this metric for the calculation of the energy-momentum tensor above, we can determine the energy density of the spacetime as

$$\begin{aligned}
\rho_M &= T^0{}_0 \\
&= f^{-1}(r)\left(1+\frac{\gamma}{2}F_{\alpha\beta}F^{\alpha\beta}\right)^{-1/2}\left\{F_0{}^\alpha F_{0\alpha} + \frac{f(r)}{\gamma}\left(1+\frac{\gamma}{2}F_{\alpha\beta}F^{\alpha\beta}\right)\right\}. \\
&= \gamma^{-1}\sqrt{1+\frac{\gamma}{2}F_{\alpha\beta}F^{\alpha\beta}} \\
&= \gamma^{-1}\sqrt{1+\gamma\frac{q^2}{r^4}}.
\end{aligned} \tag{A.2.8}$$

In the last line, since the magnetic field exists only in r-direction, we used

$$F_{\mu\nu}F^{\mu\nu} = F_{23}F^{23} + F_{32}F^{32} = \frac{2q^2}{r^4}\ , \tag{A.2.9}$$

where $F_{23} = q\sin\theta$. At first glance, it might appear that we should integrate the energy density ρ_M from r to ∞. However, as mentioned earlier, we used the vacuum with supersymmetry restored as the energy reference on the string theory side. Therefore, the term $4\pi\int_0^\infty \rho_M(r)r^2\,dr$ should be subtracted as a background. That is,

$$\begin{aligned}
V_+ &= 4\pi\left(\int_r^\infty - \int_0^\infty\right)drr^2\rho_M(r) \\
&= -4\pi\int_0^r drr^2\rho_M(r) \\
&= -4\pi\gamma^{-1/2}rq_2F_1\left(-\frac{1}{2},\frac{1}{4},\frac{5}{4};-\frac{r^4}{\gamma q^2}\right)\ .
\end{aligned} \tag{A.2.10}$$

Next, let us evaluate the energy of the bubble itself. In our model, the bubble is made by the domain wall D5-brane, so we can derive the energy by multiplying the bubble tension by the surface area. This tension has a relation with the Euclidean action of the domain wall D5-brane in the following manner

$$\frac{S_{\rm DW}}{2} = \mathcal{T}(r)\int\sqrt{-h}d^3x, \tag{A.2.11}$$

where h is a metric determinant on the bubble. Note that the 1/2 factor on the LHS owes to the fact that the present discussion focuses on the single bubble in contrast to the discussion in Chap. 3. From this equation, we can relate the bubble tension with the domain wall potential as

$$4\pi\mathcal{T}(r)r^2dt = \frac{V_{\rm DW}}{2}dT = 2\pi T_{\rm DW}\sqrt{R^4+b_{\rm D3}^2}dT, \tag{A.2.12}$$

which implies the following relation

$$\mathcal{T}(r) = \frac{T_{\rm DW}}{2r^2}\sqrt{r^4+b_{\rm D3}^2}. \tag{A.2.13}$$

Using this expression, the junction condition shown in (A.2.2) becomes

$$\frac{T_{\mathrm{DW}}}{2r^2}\sqrt{r^4+b_{\mathrm{D3}}^2}=\frac{2}{8\pi G_4}\frac{1}{r}\left(\sqrt{f_-(r)}-\sqrt{f_+(r)}\right)\ . \tag{A.2.14}$$

We then obtain the contribution of the bubble by multiplying $\mathcal{T}$ by the surface area and $\frac{1}{2}(\sqrt{f_-}+\sqrt{f_+})$ as follows

$$V_{\mathrm{shell}}=4\pi r^2\mathcal{T}(r)\cdot\frac{1}{2}\left(\sqrt{f_-(r)}+\sqrt{f_+(r)}\right). \tag{A.2.15}$$

By combining the results of (A.2.10) and (A.2.15), the potential of the brane bubble is obtained as

$$\begin{aligned}V_{\mathrm{tot}}&=V_-+V_{\mathrm{shell}}+V_+\\&=4\pi r^2\mathcal{T}(r)\cdot\frac{1}{2}\left(\sqrt{f_-(r)}+\sqrt{f_+(r)}\right)-4\pi\gamma^{-1/2}rq_2F_1\left(-\frac{1}{2},\frac{1}{4},\frac{5}{4};-\frac{r^4}{\gamma q^2}\right).\end{aligned} \tag{A.2.16}$$

Here, comparing this expression with the probe-level potential (3.3.25), we can derive the following relationships for the parameters:

$$q=\gamma^{-1/2}b_{D3},\quad \gamma^{-1}=T_{D5}r_{NS}, \tag{A.2.17}$$

where r_{NS} represents the integrated value of the B field on the cycle, distinct from the coordinate. Finally, the total potential with the gravitational correction can be expressed in terms of b_{D3} and T_{D5} as

$$V_{\mathrm{tot}}=2\pi T_{\mathrm{DW}}\sqrt{r^4+b_{D3}^2}\cdot\frac{1}{2}\left(\sqrt{f_-(r)}+\sqrt{f_+(r)}\right)-4\pi T_{D5}r_{NS}b_{D3}r_2F_1\left(-\frac{1}{2},\frac{1}{4},\frac{5}{4};-\frac{r^4}{b_{D3}^2}\right). \tag{A.2.18}$$

In the next section, we will use (A.2.18) to examine the stability of the brane shell.

At the end of the section, we will determine the expression of $f_+(r)$. Introducing the mass function $m(r,t)$ as

$$f(r)=1-\frac{2G_4m(r,t)}{r}, \tag{A.2.19}$$

the Einstein equation for a spherically symmetric spacetime is given by [192, 193]

$$\frac{\partial m}{\partial r}=4\pi r^2\left(-T^0{}_0\right),\quad \frac{\partial m}{\partial t}=-4\pi r^2\left(-T^1{}_0\right). \tag{A.2.20}$$

Since we are considering a static spacetime, it is sufficient to solve the first equation to obtain the mass function. Substituting (A.2.8) into $T^0{}_0$, we get

$$\frac{\partial m}{\partial r}=-\frac{4\pi r^2}{\gamma}\sqrt{1+\gamma\frac{q^2}{r^4}}=-4\pi r^2T_{D5}r_{NS}\sqrt{1+\frac{b_{D3}^2}{r^4}}, \tag{A.2.21}$$

which gives the mass function as

$$m(r)=-4\pi T_{D5}r_{NS}\left(\int_r^\infty-\int_0^\infty\right)dr\sqrt{r^4+b_{D3}^2}=4\pi T_{D5}r_{NS}rb_{D32}F_1\left(-\frac{1}{2},\frac{1}{4},\frac{5}{4};-\frac{r^4}{b_{D3}^2}\right). \tag{A.2.22}$$

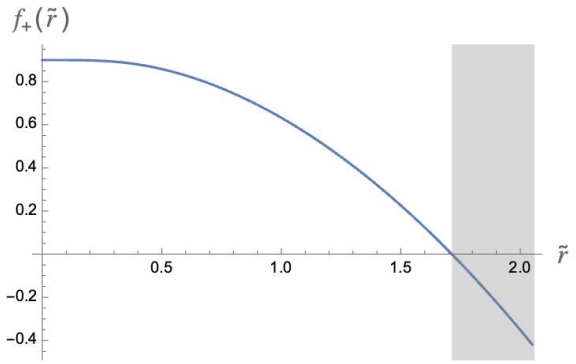

Figure A.1: Behavior of the lapse function for $\widetilde{b}_{D3} = 0.1$ and $\widetilde{G}_4 = 0.5$. The "cosmological horizon" exists at $\widetilde{r} = 1.7$. Tilde-added variables or constants are dimensionless quantities. The shaded region represents the outside the horizon. This Figure is a slightly modified version of the one used in [3].

Therefore, the expression for $f_+(r)$ is

$$f_+(r) = 1 - \frac{2G_4 m(r)}{r}\ , \quad m(r) = 4\pi T_{D5} r_{NS} b_{D3}^2 F_1\left(-\frac{1}{2}, \frac{1}{4}, \frac{5}{4}; -\frac{r^4}{b_{D3}^2}\right). \tag{A.2.23}$$

This function $f_+(r)$ is monotonically decreasing with respect to r, taking its maximum value at $r = 0$ and zero at $r = r_{\rm ch}$, as shown in Figure A.1. There is no physical spacetime in the region where r exceeds $r_{\rm ch}$; "cosmological horizon" exists outside the brane bubble. This is a crucial point when analyzing the stability of the shell in the next section. This horizon can exist if the maximum value of f_+ is positive, i.e.,

$$f_+(0) = 1 - 8\pi G_4 b_{D3} T_{D5} r_{NS} > 0. \tag{A.2.24}$$

The position of the horizon is determined by three factors: the brane tension, the Newton constant, and the magnetic field. The numerical value of the position can be found by solving $f_+(r_{\rm ch}) = 0$.

A.3 Stabilization mechanism

The fact that the shell has a finite radius means that there is a non-zero minimum value in the potential. For such a minimum to exist, there must be a value $r^\star$ that satisfies $\frac{\partial V_{\rm tot}}{\partial r^\star} = 0$ and $\partial^2 V_{\rm tot}/\partial r^{\star 2} > 0$. At this point, it is not possible to explicitly express $r^\star$ because f_+ is written in terms of a hypergeometric function. Therefore, we have no choice but to rely on numerical methods for practical calculations.

Here, we assume that a potential minimum $V(r_{\rm min})$ exists. At the probe level, the potential (3.3.25) is an unbounded potential like an anharmonic oscillator. However, when a gravitational effect is turned on, we should care about the contribution of the horizon, as noted in the previous section. The specific shape of the potential should ultimately be determined by the Newton constant and the magnetic field strength. To see the behavior

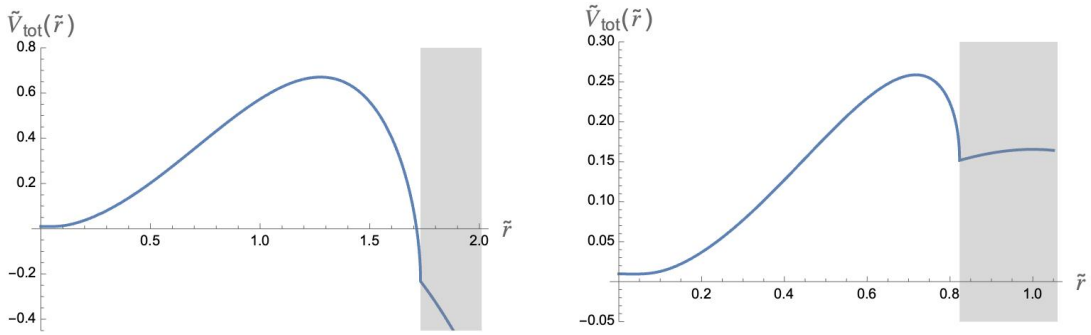

(a) Metastable potential for $\widetilde{b}_{D3} = 0.01$ and $\widetilde{G}_4 = 0.5$. The shell radius is estimated as $r_{\rm min} \approx 0.0037$.

(b) Stabilized potential for $\widetilde{b}_{D3} = 0.01$ and $\widetilde{G}_4 = 2.2$. The shell radius is estimated as $r_{\rm min} \approx 0.037$.

Figure A.2: Brane shell potentials for each parametrization. Shaded regions represent the outside of the horizon. This Figure is taken from [3].

of the potential in each parametrization, we introduce a dimensionless potential as follows

$$V_{\rm tot} = 2\pi T_{DW} c^2 \widetilde{V}_{\rm tot} \ , \tag{A.3.1}$$

$$\widetilde{V}_{\rm tot} = \sqrt{\tilde{r}^4 + \widetilde{b}_{D3}^2} \cdot \frac{1}{2}\left(1 + \sqrt{1 - \frac{2\widetilde{G}_4 \widetilde{m}(\tilde{r})}{\tilde{r}}}\right) - \widetilde{b}_{D3}\tilde{r}\,{}_2F_1\left(-\frac{1}{2}, \frac{1}{4}, \frac{5}{4}; -\frac{\tilde{r}^4}{\widetilde{b}_{D3}^2}\right), \tag{A.3.2}$$

where we defined dimensionless parameters as

$$r = c\tilde{r}, \quad b_{D3} = c^2 \widetilde{b}_{D3}^2, \quad c = T_{DW}/2T_{D5} r_{NS}, \tag{A.3.3}$$

as discussed in Section 3.3. In the derivation, we also introduced the dimensionless mass function and the dimensionless Newton constant as

$$m(r) = 2\pi T_{DW} c^2 \widetilde{m}(\tilde{r}), \quad \widetilde{m}(\tilde{r}) = \widetilde{b}_{D3}\tilde{r}\,{}_2F_1\left(-\frac{1}{2}, \frac{1}{4}, \frac{5}{4}; -\frac{\tilde{r}^4}{\widetilde{b}_{D3}^2}\right), \tag{A.3.4}$$

$$G_4 = c' \widetilde{G}_4, \quad c' = \frac{T_{D5} r_{NS}}{\pi T_{DW}^2}. \tag{A.3.5}$$

Now, we can numerically analyze the potential, and Figure A.2 shows the typical behavior of the potential. The left panel of Figure A.2 depicts a potential whose potential value at the horizon is lower than the minimum. When the potential is in this shape, the brane bubble is metastable and can decay through tunneling in a finite life-time. In contrast, the right panel shows a potential whose potential value at the horizon is larger than the minimum. In this case, the brane bubble is stabilized due to the gravity, and even non-perturbative instability is removed.

In summary, whether a system is stable or metastable is determined by whether the value of the potential in the horizon is greater or less than $V(r_{\rm min})$. That is,

$$V(r_{\rm min}) \geq V(r_{\rm ch}) \quad \text{metastable}, \tag{A.3.6}$$

$$V(r_{\rm min}) < V(r_{\rm ch}) \quad \text{stable}. \tag{A.3.7}$$

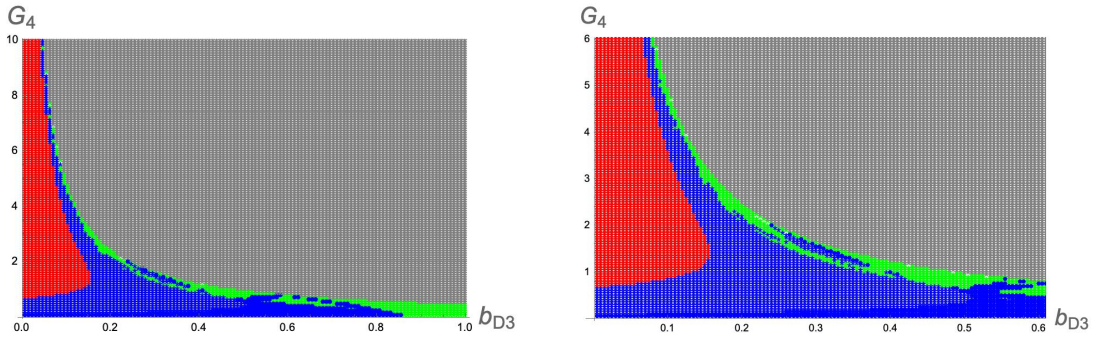

(a) (b)

Figure A.3: State diagram for brane bubble. The blue area is a metastable region, the red area is a region where the shell is stabilized, the green area is a region where the potential is monotonically decreasing, and there exists no minimum, and the gray area is a region where $f_+(r) < 0$ for all r and physical spacetime does not exist. The blue areas scattered among the green areas are numerical errors, and we cannot actually produce a (meta)stable bubble. These Figures are cited from [3].

While it is difficult to obtain an analytical expression of the potential minima, $V(r_{\rm min})$, a relatively simple expression can be given for the value of the potential in the horizon. Since $f_+(r_{\rm ch}) = 0$ holds at the horizon, the potential value is calculated from (A.2.18) as follows

$$V(r_{\rm ch}) = \pi T_{\rm DW}\sqrt{r_{\rm ch}^4 + b_{D3}^2} - 4\pi T_{D5} r_{NS}\int_0^{r_{\rm ch}} d\xi \sqrt{\xi^4 + b_{D3}^2}. \tag{A.3.8}$$

Using $f_+(r_{\rm ch}) = 0$, we can rewrite the second term of as

$$\begin{aligned} r_{\rm ch} &= 2G_4 \cdot 4\pi T_{D5} r_{NS}\int_0^{r_{\rm ch}} d\xi \sqrt{\xi^4 + b_{D3}^2} \\ &\longrightarrow 4\pi T_{D5} r_{NS}\int_0^{r_{\rm ch}} d\xi \sqrt{\xi^4 + b_{D3}^2} = \frac{r_{\rm ch}}{2G_4}. \end{aligned} \tag{A.3.9}$$

Then, the potential value in simpler form is

$$V(r_{\rm ch}) = \pi T_{\rm DW}\sqrt{r_{\rm ch}^4 + b_{D3}^2} - \frac{r_{\rm ch}}{2G_4}, \tag{A.3.10}$$

and we find that the simplest expression of the stability condition is

$$V(r_{\rm min}) \geq \pi T_{\rm DW}\sqrt{r_{\rm ch}^4 + b_{D3}^2} - \frac{r_{\rm ch}}{2G_4} \quad \text{metastable}, \tag{A.3.11}$$

$$V(r_{\rm min}) < \pi T_{\rm DW}\sqrt{r_{\rm ch}^4 + b_{D3}^2} - \frac{r_{\rm ch}}{2G_4} \quad \text{stable}. \tag{A.3.12}$$

In light of this condition, it is possible to determine numerically whether the bubble is stable for different magnetic field values and Newton constant, see the left panel of Figure A.3. As naively assumed, the greater the influence of gravity, the more stable the bubble becomes. In other words, a stable bubble is realized when the Newton constant

is sufficiently large. However, no stable state appears when the magnetic field strength is fixed at about 0.15, no matter how large the Newton constant is increased. This means that the bubble cannot be stabilized if the magnetic field is too strong. In addition, at the probe level, we could wrap as many D3-branes as we wanted. However, in the present discussion where gravity correction exists, the lapse function will always be negative if the magnetic field is too strong, and physical spacetime will no longer exist. As mentioned in 3.3.2, the magnetic field strength is proportional to the number of wrapped D3-branes. Therefore, this tendency suggests that there is an upper limit to the number of D3-branes that can be wrapped into the internal space. This was not confirmed in [186].

A.4 Over-extremality

It is not only a question of whether gravitational corrections stabilize the bubble but also whether the stabilized bubble is over-extremal regarding the Swampland problem. The over-extremality of compact objects is determined by the weak gravity condition (A.1.1) [161]. We can rewrite the condition as follows

$$\frac{G_4 m^2}{(gQ)^2} \leq 1 \ . \tag{A.4.1}$$

In the present discussion, we absorb the coupling constant to the definition of the charge as $gQ = q$. Moreover, we can rewrite this q by the magnetic field from D3-branes. Then, weak gravity condition becomes

$$\frac{G_4 m^2}{(gQ)^2} = \frac{G_4 m^2}{q^2} = \frac{G_4 m^2}{\gamma^{-1} b_{D3}^2} \leq 1 \ . \tag{A.4.2}$$

Here, m, which corresponds to the mass of the brane bubble, is calculated as the minimum value of the potential (A.2.18) [186] as

$$\partial_r V(r_{\rm min}) = 0 \ , \quad V(r_{\rm min}) = m \ . \tag{A.4.3}$$

The dimensionless version of (A.4.2) is given by

$$\frac{4\pi \widetilde{G}_4 \widetilde{m}}{\widetilde{b}_{D3}^2} \leq 1, \tag{A.4.4}$$

where we utilized the dimensionless parameters (A.3.1)-(A.3.5).

The right panel of Figure A.3 shows a magnified view of the region where G_4 and b_{D3} are small. The light blue region plotted with stars ($\star$) depicts non-extremal metastable states. In contrast, the deep blue region plotted with circles ($\bullet$) depicts over-extremal states. The whole red region is depicted by star symbols, so over-extremal states cannot be stabilized in our setup. This tendency is consistent with the difficulty of satisfying the weak gravity condition where the Newton constant is large.

Let us consider the properties of our constructed bubble from numerical results. We will focus on situations where we fix the dimensionless Newtonian constant and increase the magnetic field. We will assume that Newton's constant is an arbitrary value smaller than 1. As seen from Figure A.4, the bubble becomes over-extremal somewhere as the magnetic

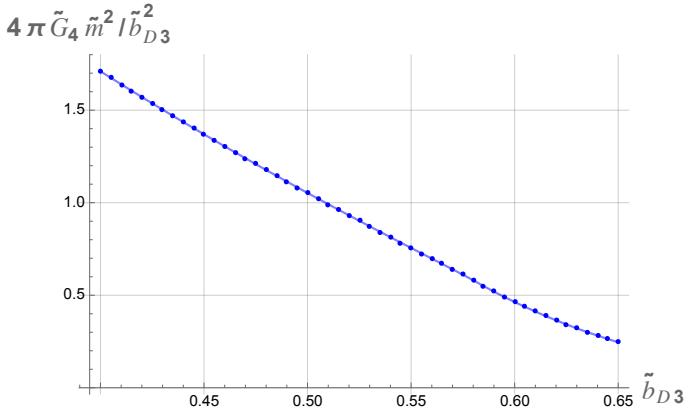

Figure A.4: Mass to charge ratio for a fixed Newton constant at $\widetilde{G}_4 = 0.5$. In this case, the brane bubble becomes over-extremal when the $\widetilde{b}_{D3}$ is larger than about 0.51. This Figure is cited from [3].

field increases. This behavior is easily assumed from the weak gravity conditioin(A.4.2) (or (A.4.4)). However, if the magnetic field becomes too strong, the potential minima disappear, and bubbles of finite size cannot exist. If the magnetic field is further enhanced from there, we now enter a region that cannot even be physically interpreted. In other words, to achieve an over-extremal state in the presence of gravity, there must be some upper limit to the value of the magnetic field. This upper bound characterizes at least the conditions for the existence of a metastable bubble, so numerically, it corresponds to the value of the magnetic field at the boundary between the blue and green regions.

A.5 Discussion

In this appendix, we focused on the bound state discussed in Chap. 3 and analyzed the stabilization mechanism and the over-extremality. Owing to the nonlinear properties of the DBI action, this brane bubble possesses a finite radius even before tunneling. By incorporating a gravitational correction through the junction condition, we examined the stability of the brane bubble and its over-extremality in the context of the weak gravity conjecture. While the gravitational correction does not alter the potential's intrinsic form, it introduces a "cosmological" horizon in the spacetime exterior of the bubble. The horizon's position is determined by the background magnetic field b_{D3} and the four dimensional Newton constant G_4. Through numerical analysis, we demonstrated that the gravitational correction stabilizes the brane shell at a finite radius, particularly when the Newton constant assumes sufficiently large values. Conversely, by fixing the Newton constant and increasing the magnetic field strength, we confirmed that the brane bubble can be an over-extremal state, satisfying the weak gravity condition in parameter regimes where the magnetic field is sufficiently strong.

Our model could not identify any configuration of the brane bubble that is fully stabilized and over-extremal when gravitational corrections are included. This suggests the existence of a trade-off: increasing the Newton constant promotes stability while increasing the magnetic field supports the weak gravity condition. This tension is evident from

the form of the weak gravity condition given in (A.1.1) (or (A.4.1)). In particular, within the framework of our model, excessively large values for both the Newton constant and the magnetic field lead to the disappearance of the potential minima as well as the physical spacetime itself. As a result, it is impossible to simultaneously increase both parameters to achieve stability and over-extremality. Investigating whether we can realize a completely stable and over-extremal state in a stringy model is a fascinating open question we aim to explore in future research.

Appendix B

Appendix for Chapter 2

B.1 Proportionality between zero mode and time derivative of bounce solution

In section 2.1.3, we simply assumed that the following relation between zero mode solution and bounce solution also holds for non-canonical systems.

$$q_0 = \frac{1}{\sqrt{N_0}} \frac{d\bar{q}}{dt}. \tag{B.1.1}$$

We show a proof here. As stated in section 2.1.3, we are free to choose the functions to be an eigenfunction of the fluctuation operator, which is determined by the second variation of the Euclidean action. Certainly, the zero mode function is not an exception. The second variation is given by

$$\begin{aligned}
\delta^2 S &= \int dt \left\{ \frac{\partial^2 L}{\partial q^2} (\delta q)^2 + 2 \frac{\partial^2 L}{\partial q \partial \dot{q}} \delta q \delta \dot{q} + \frac{\partial^2 L}{\partial \dot{q}^2} (\delta \dot{q})^2 \right\} \\
&= \int dt \left\{ -\frac{d}{dt} \frac{\partial^2 L}{\partial \dot{q}^2} \left(\frac{d}{dt} \delta q \right) \delta q - \frac{\partial^2 L}{\partial \dot{q}^2} \left(\frac{d^2}{dt^2} \delta q \right) \delta q \right. \\
&\qquad \left. + \frac{\partial^2 L}{\partial q^2} (\delta q)^2 - \frac{d}{dt} \frac{\partial^2 L}{\partial q \partial \dot{q}} (\delta q)^2 \right\} .
\end{aligned} \tag{B.1.2}$$

In the last equality, we did integrations by parts. As well as (3.4.9), if we define $P[q]$ and $Q[q]$ as

$$P[q] \equiv \frac{\partial^2 L}{\partial \dot{q}^2} , \quad Q[q] \equiv \frac{\partial^2 L}{\partial q^2} - \frac{d}{dt} \frac{\partial^2 L}{\partial q \partial \dot{q}} , \tag{B.1.3}$$

we find the zero mode equation as follows

$$\left[-\frac{d}{dt} \left(P[\bar{q}] \frac{d}{dt} \right) + Q[\bar{q}] \right] q_0 = 0 . \tag{B.1.4}$$

Since we are considering the fluctuations around the periodic configuration, the fluctuations should also satisfy the periodic B.C., that is,

$$q_0 \left(-\frac{\beta}{2} \right) = q_0 \left(\frac{\beta}{2} \right) , \quad \dot{q}_0 \left(-\frac{\beta}{2} \right) = \dot{q}_0 \left(\frac{\beta}{2} \right) . \tag{B.1.5}$$

Next, we examine a differential equation which the time derivative of the bounce solution obeys. The bounce solution is the classical solution, then satisfies

$$\left(\frac{d}{dt} \frac{\partial L}{\partial \dot{\bar{q}}} - \frac{\partial L}{\partial \bar{q}} \right) = 0 \ . \tag{B.1.6}$$

Taking another derivative with respect to t, we find

$$\left\{ -\frac{\partial^2 L}{\partial \dot{\bar{q}}^2} \frac{d^2}{dt^2} - \frac{d}{dt} \frac{\partial^2 L}{\partial \dot{\bar{q}}^2} \frac{d}{dt} + \frac{\partial^2 L}{\partial \bar{q}^2} - \frac{d}{dt} \frac{\partial^2 L}{\partial \bar{q} \partial \dot{\bar{q}}} \right\} \dot{\bar{q}} = 0 \ . \tag{B.1.7}$$

This is the same differential equation as (B.1.4). The bounce solution is the periodic configuration, and its time derivative is also periodic. Namely, $\dot{\bar{q}}$ satisfies (B.1.5). Therefore, $\dot{\bar{q}}$ is also a zero mode and proportional to q_0 with the normalization constant as (B.1.1).

Appendix C

Appendix for Chapter 3

C.1 Contour deformation and analytic continuation of spectral zeta function

As reviewed in Section 2.2, even in cases where the specific spectrum of the operator associated with a potential $V(x)$ is difficult to determine, the value of the determinant can be obtained by examining the boundary values of the zero mode function. However, since the original Gel'fand-Yaglom method was developed for problems for Schrödinger-type operators, certain extensions are needed to apply to general Sturm-Liouville operators.

The contour deformation method was developed to derive the functional determinant of general Sturm-Liouville operators based on the zeta function regularization [118,119]. This method involves considering complex integrals on the λ-plane, which requires $\zeta'(s)$ to be regular at $s = 0$. However, the spectral zeta function is regular only in the region $\mathrm{Re}(s) > 1/2$, necessitating analytic continuation to the region $\mathrm{Re}(s) < 0$. The authors of [120] successfully carried out this analytic continuation by applying the theory of asymptotic analysis, deriving a well-defined expression for the derivative of the spectral zeta function. This Section provides a brief review of the contour deformation method and the derivation of the analytically continued spectral zeta function.

Let us consider the following Strum-Liouville operator

$$T_{A,B} = \frac{1}{r(x)}\left[-\frac{d}{dx}\left(p(x)\frac{d}{dx}\right) + q(x)\right], \quad x \in (a,b)\ , \tag{C.1.1}$$

where $r(x) > 0$, $p(x) > 0$ over the finite interval (a, b). $r(x)$ is a weight function, and for the present problem, it is sufficient to fix $r(x) = 1$. If we write the eigenvalues of this operator as λ_n, we can define the spectral zeta function as

$$\zeta(s; T_{A,B}) \equiv \sum_n \lambda_n^{-s}\ . \tag{C.1.2}$$

The spectral zeta function is known to be written by the contour integral of the Fredholm trace, which has simple poles at the eigenvalues λ_n [194, Lemma 2.6.]

$$\zeta(s, T_{A,B}) = -\frac{1}{2\pi i}\oint_\gamma d\lambda \lambda^{-s}\left(\mathrm{tr}\left((T_{A,B} - \lambda I_{\mathcal{H}})^{-1}\right) + \lambda^{-1} m_0\right)\ . \tag{C.1.3}$$

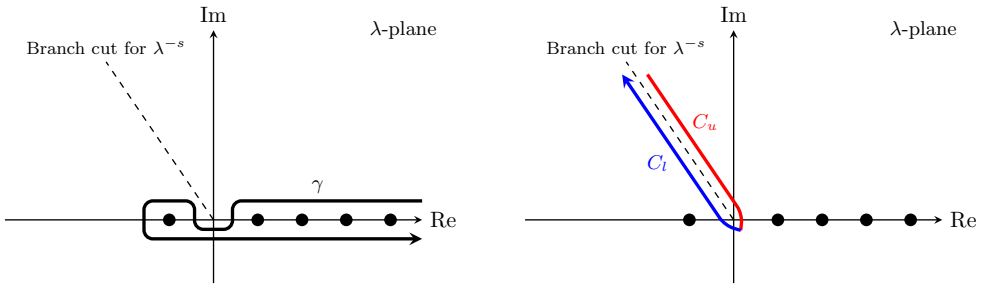

Figure C.1: The contours γ, C_u, and C_l are depicted on the complex λ-plane. The dashed lines indicate the branch cut of λ^{-s}, while the points marked on the real axis represent the eigenvalues of the differential operator $T_{A,B}$. While this Figure is cited from [1].

The second term in the integrand accounts for the subtraction of the contribution of zero modes, with m_0 denoting its multiplicity. The counterclockwise contour γ encircles the eigenvalues located at the real axis of the complex λ-plane and is deformed downward to bypass the origin, as illustrated in Figure C.1. See also original papers [118, 119].

For further discussion, we define characteristic functions by boundary conditions [195, Sect. 1.2], [196, Sect. 3.2]. These boundary conditions can be classified into two categories: *separated* or *coupled*.

1. *Separated boundary condition*
   Boundary conditions are called *separated* if the conditions at $x = a$ and $x = b$ are given separately as

$$\begin{aligned} g(a)\cos(\alpha) + g^{[1]}(a)\sin(\alpha) &= 0 \ , \\ g(b)\cos(\beta) - g^{[1]}(b)\sin(\beta) &= 0 \ , \end{aligned} \tag{C.1.4}$$

   where $g(x)$ is an eigenfunction of the Strum-Liouville operator (C.1.1). If we introduce the boundary value $U_{\alpha,\beta,i}(f)$ as follow

$$\begin{aligned} U_{\alpha,\beta,1}(f) &= f(a)\cos(\alpha) + f^{[1]}(a)\sin(\alpha) \ , \\ U_{\alpha,\beta,2}(f) &= f(b)\cos(\beta) - f^{[1]}(b)\sin(\beta) \ , \end{aligned} \tag{C.1.5}$$

   the characteristic function is defined by

$$F_{\alpha,\beta}(\lambda) = \det \begin{pmatrix} U_{\alpha,\beta,1}(\theta_\lambda) & U_{\alpha,\beta,1}(\phi_\lambda) \\ U_{\alpha,\beta,2}(\theta_\lambda) & U_{\alpha,\beta,2}(\phi_\lambda) \end{pmatrix} \ , \tag{C.1.6}$$

   where θ_λ and ϕ_λ are independent fundamental solutions, which satisfy the following boundary conditions

$$\theta_\lambda(a) = \phi_\lambda^{[1]}(a) = 1 \ , \quad \theta_\lambda^{[1]}(a) = \phi_\lambda(a) = 0 \ , \tag{C.1.7}$$

   where $g^{[1]}$ represents a pseudo-derivative of g, which is defined by $g^{[1]} = p(x)g'(x)$.

2. *Coupled boundary condition*
   Boundary conditions are called *coupled* if the boundary values at $x = a$ and $x = b$

satisfy the following equation

$$\begin{pmatrix} g(b) \\ g^{[1]}(b) \end{pmatrix} = e^{i\varphi} R \begin{pmatrix} g(a) \\ g^{[1]}(a) \end{pmatrix} \ , \tag{C.1.8}$$

where $\varphi \in [0, \pi)$, and $R \in SL(2, \mathbb{R})$. If we introduce the boundary value $V_{\varphi,R,i}(f)$ as

$$\begin{aligned} V_{\varphi,R,1}(f) &= f(b) - e^{i\varphi} R_{11} f(a) - e^{i\varphi} R_{12} f^{[1]}(a) \ , \\ V_{\varphi,R,2}(f) &= f^{[1]}(b) - e^{i\varphi} R_{21} f(a) - e^{i\varphi} R_{22} f^{[1]}(a) \ , \end{aligned} \tag{C.1.9}$$

the characteristic function is defined by

$$F_{\varphi,R}(\lambda) = \det \begin{pmatrix} V_{\varphi,R,1}(\theta_\lambda) & V_{\varphi,R,1}(\phi_\lambda) \\ V_{\varphi,R,2}(\theta_\lambda) & V_{\varphi,R,2}(\phi_\lambda) \end{pmatrix} \ . \tag{C.1.10}$$

By definition, the complex value λ^*, at which the characteristic function vanishes, corresponds to the eigenvalues of the original Sturm-Liouville problem.

The above characteristic functions can be related to a Fredholm determinant and a Fredholm trace [194, Thm.3.4.]. Since the periodic boundary condition, $\varphi = 0$, $R = I$, is significant for our purpose, we need only focus on $F_{\varphi,R}(\lambda)$ in the following discussion. Supposing λ_0 is one of the eigenvalues, then the Fredholm determinant can be rewritten as

$$\det_{L^2_r((a,b))} \left(I_{L^2_r((a,b))} - (\lambda - \lambda_0) \left(T_{\varphi,R} - \lambda_0 I_{L^2_r((a,b))} \right)^{-1} \right) = \frac{F_{\varphi,R}(\lambda)}{F_{\varphi,R}(\lambda_0)}, \quad \lambda \in \mathbb{C} \ . \tag{C.1.11}$$

For the Fredholm trace, in particular, we have

$$\mathrm{tr}_{L^2_r((a,b))} \left(\left(T_{\varphi,R} - \lambda I_{L^2_r((a,b))} \right)^{-1} \right) = -\frac{d}{d\lambda} \ln \left(F_{\varphi,R}(\lambda) \right) \ , \quad \lambda \in \rho(T_{\alpha,\beta}) \ . \tag{C.1.12}$$

Substituting this equation into (C.1.3), we can rewrite the integral representation for the spectral zeta function as

$$\zeta(s; T_{A,B}) = \frac{1}{2\pi i} \oint_\gamma d\lambda \lambda^{-s} \left(\frac{d}{d\lambda} \ln(F_{A,B}(\lambda)) - \lambda^{-1} m_0 \right) \ . \tag{C.1.13}$$

We can transform (C.1.13) into a simpler representation. Let us denote

$$R_\psi = \left\{ \lambda = te^{i\psi} | t \in [0, \infty) \right\} \ , \quad \psi \in (\pi/2, \pi) \tag{C.1.14}$$

as a branch cut of λ^{-s}. If the spectral zeta function is regular in the vicinity of $s = 0$, we are free to deform the integration path to sandwich the branch cut, as shown in Figure C.1. Then, the contour integral is replaced with the calculation of the discontinuity across the branch cut as follows.

$$\zeta(s; T_{A,B}) = e^{is(\pi-\psi)} \frac{\sin(\pi s)}{\pi} \int_0^\infty dt t^{-s} \frac{d}{dt} \ln \left(F_{A,B}(te^{i\psi}) t^{-m_0} e^{-im_0\psi} \right) \ . \tag{C.1.15}$$

To calculate the determinants, we need to take the derivative at $s = 0$ of the spectral zeta function, so we must pay attention to its regularity. We can determine the regular

region of the spectral zeta function (C.1.15) by analysis of the asymptotic behavior of $\ln(F_{A,B}(\lambda))$ in $\lambda \to 0$ and $\lambda \to \infty$. In the small λ region, the characteristic function $F_{A,B}(\lambda)$ can be expanded as

$$F_{A,B}(\lambda) = F_{m_0}\lambda^{m_0} + \sum_{n=m_0+1}^{\infty} F_n \lambda^n \ , \tag{C.1.16}$$

where m_0 represents the multiplicity of zero eigenvalues. Thus, in the limit $\lambda \to 0$, we find

$$\frac{d}{d\lambda}\ln(F_{A,B}(\lambda)\lambda^{-m_0}) \underset{\lambda\to 0}{=} O(1) \ . \tag{C.1.17}$$

On the other hand, in the large λ region, $F_{A,B}(\lambda)$ can be expanded as

$$\ln(F_{A,B}(\lambda)\lambda^{-m_0}) \underset{|\lambda|\to\infty,\ \mathrm{Im}(\lambda^{1/2})\geq 0}{=} -ic\lambda^{1/2} - \frac{k_0+1}{2}\ln(\lambda) + \ln\left(\frac{\Gamma_{k_0}}{2ic}\right) + \sum_{m=1}^{N}\Psi_m\lambda^{-m/2} \ . \tag{C.1.18}$$

Refer to [120, Sect.3.2] for a detailed discussion of the asymptotic analysis. Thus, in the limit $|\lambda| \to \infty$, we find

$$\frac{d}{d\lambda}\ln(F_{A,B}(\lambda)\lambda^{-m_0}) \underset{|\lambda|\to\infty,\ \mathrm{Im}(\lambda^{1/2})\geq 0}{=} O\left(\frac{1}{\sqrt{\lambda}}\right) \ . \tag{C.1.19}$$

Given the asymptotic behavior (C.1.17) and (C.1.19), we see that the contour deformation is only valid for $1/2 < s < 1$, not including $s = 0$.

To evaluate the derivative at $s = 0$, it is necessary to carry out an analytic continuation to the left of the abscissa of the boundary $s = 1/2$. This can be achieved by subtracting N terms from the asymptotic expansion (C.1.18) and subsequently re-adding them. Namely,

$$\zeta(s; T_{A,B}) = Z(s, A, B) + \sum_{j=-1}^{N} h_j(s, A, B) \ , \tag{C.1.20}$$

The explicit forms of $Z(s, A, B)$ and $h_j(s, A, B)$ are defined as

$$\begin{aligned} Z(s,A,B) =& e^{is(\pi-\psi)}\frac{\sin(\pi s)}{\pi}\int_0^\infty dt t^{-s}\frac{d}{dt}\left\{\ln\left(F_{A,B}(te^{i\psi})t^{-m_0}e^{-im_0\psi}\right)\right. \\ & -H(t-1)\left[-ic\lambda^{1/2}e^{i\psi/2} - \left[\frac{k_0+1}{2}+m_0\right]\ln(t)\right. \\ & \left.\left. -\left[\frac{k_0+1}{2}+m_0\right]i\psi + \ln\left(\frac{\Gamma_{k_0}}{2ic}\right) + \sum_{n=1}^{N}\Psi_n e^{in\psi/2}t^{-n/2}\right]\right\} \ , \end{aligned} \tag{C.1.21}$$

$$\begin{aligned} h_{-1}(s,A,B) &= -ie^{i\pi(\pi-\psi)}\frac{\sin(\pi s)}{\pi}\frac{ce^{i\psi/2}}{2s-1} \ , \\ h_0(s,A,B) &= -(k_0+1+2m_0)e^{is(\pi-\psi)}\frac{\sin(\pi s)}{2\pi s} \ , \\ h_n(s,A,B) &= -e^{is(\pi-\psi)}\frac{\sin(\pi s)}{\pi}\frac{n}{2s+n}e^{-in\psi/2}\Psi_n \ . \end{aligned} \tag{C.1.22}$$

where $H(s)$ is a step function. By this procedure, the regular region of the spectral zeta function is extended to $-(N+1)/2 < \mathrm{Re}(s) < 1$. As $N = 0$ suffices to encompass $s = 0$, the derivative of the spectral zeta function at $s = 0$ can be expressed using (C.1.20) as follows

$$\begin{aligned}\zeta'(0; L_{A,B}) &= Z'(0, A, B) + h'_{-1}(0, A, B) + h'_0(0, A, B) \\ &= i\pi n - \ln\left(2c\left|\frac{F_{m_0}}{\Gamma_{k_0}}\right|\right) \ . \end{aligned} \tag{C.1.23}$$

Appendix D

Appendix for Chapter 4

D.1 Notation

We summarize the notation for the geometric quantities in Chap. 4 here. Greek indices $(\alpha, \beta, \gamma, \cdots)$ represent five-metric, Latin indices $(i, j, k, \cdots)$ represent four-metric, and capital letters $(A, B, C, \cdots)$ represent three-metric. Ω_n is a n-dimensional angular coordinates, that is, $\Omega_n = (\theta_1, \theta_2, \theta_3, \cdots, \theta_{n-1}, \theta_n)$. When we refer to an arbitrary coordinate constant surface, we put the coordinate to Σ as a subscript. For example, Σ_ϕ represents a ϕ-constant surface. For other geometric quantities on surfaces, see the Table D.1. Moreover, we implicitly assume that unit vectors n^α and r^α face in the positive direction.

Table D.1: Geometric quantities of surfaces. This table is cited from [2].

Surface	arbitrary surface	Σ_ϕ	$\Sigma_r(\Sigma_\rho)$	$S_{\phi r}$
Unit normal vector	$\tilde{n}^\alpha$ (outward)	n^α	r^α	r^α
Subscript	$a, b, \cdots$	$a, b, \cdots = (r, \Omega_3)$	$i, j, \cdots = (\phi, \Omega_3)$	$A, B, \cdots = (\Omega_3)$
Coordinates	$\tilde{x}^a$	y^a	z^i	θ^A
Induced metric	$\tilde{g}_{ab}$	h_{ab}	γ_{ij}	σ_{AB}
Extrinsic curvature	$\mathcal{K}_{ab}$	K_{ab}	$\mathscr{K}_{ij}$	k_{AB}

D.2 Derivation of bounce action via ADM decomposition

In section 4.2.2, we evaluated the Euclidean action of $\mathscr{V} - \mathscr{B}$ by the definition of the gravitational action, while the authors of [48] utilized the Arnowitt-Deser-Misner (ADM) decomposition [141]. In this section, we also compute the Euclidean action $I_{\mathscr{V}-\mathscr{B}}$ via the ADM decomposition and show that our evaluation is consistent with the discussion in [48].

The gravitational action consists of the Einstein-Hilbert term and the Gibbons-Hawking-York term as follows

$$I_{\mathscr{V}-\mathscr{B}} = -\frac{1}{16\pi G_5}\int_{\mathscr{V}-\mathscr{B}} \mathcal{R}\sqrt{g}d^5x - \frac{1}{8\pi G_5}\oint_{\partial(\mathscr{V}-\mathscr{B})} (\mathcal{K} - \mathcal{K}_0)\sqrt{\tilde{g}}d^4\tilde{x}. \tag{D.2.1}$$

Just as we decompose Lorentzian spacetime by real time in the ordinary ADM decomposition, we can decompose the Euclidean action by the ϕ-constant hypersurface Σ_ϕ and we

find the following expression [141]

$$I_{\mathscr{V}-\mathscr{B}} = -\frac{1}{16\pi G_5}\int_0^{2\pi R} d\phi \left[\int_{\Sigma_\phi}\left({}^{(4)}\partial_\phi g_{ij}\pi^{ij} - N\mathcal{H} - N^i\mathcal{H}_i\right)N\sqrt{h}d^4y - 2\oint_{S_{\phi r}}(k-\mathscr{K}_0)N\sqrt{\sigma}d^3\theta\right]. \tag{D.2.2}$$

While We denote the non-dynamical term in the notation for the r-constant surface, we soon find that $\mathscr{K}_0$ coincide with k_0 by an explicit calculation. Here, $\mathcal{H}$ and $\mathcal{H}_i$ of the first term in (D.2.2) vanish due to the Hamiltonian and momentum constraint condition, $\mathcal{H} = \mathcal{H}_i = 0$. Also, ${}^{(4)}\partial_\phi g_{ij}\pi^{ij}$ also vanishes via the symmetry of spacetime with respect to ϕ direction. Thus, it suffices to focus on the boundary integral.[1] As mentioned in section 4.2.2, the non-singular manifold $\mathscr{V}-\mathscr{B}$ has two different boundary, the spatial boundary and the asymptotic boundary. Thus, the boundary integral in (D.2.2) will be decomposed into two parts, that is,

$$I_{\mathscr{V}-\mathscr{B}} = \frac{1}{8\pi G_5}\int_0^{2\pi R} d\phi \left\{\lim_{r_s\to\sqrt{\alpha}}\oint_{S_{\phi r_s}}(k-\mathscr{K}_0)N\sqrt{\sigma}d^3\theta - \lim_{r_\infty\to\infty}\oint_{S_{\phi r_\infty}}(k-\mathscr{K}_0)N\sqrt{\sigma}d^3\theta\right\}. \tag{D.2.3}$$

The trace of the extrinsic curvature for (ϕ, r)-constant surface is evaluated as follows

$$k = \frac{3\sqrt{f(r)}}{r}, \quad f(r) = 1 - \frac{\alpha}{r^2}. \tag{D.2.4}$$

$\mathscr{K}_0$, which is the trace of the extrinsic curvature of the surface embedded into flat spacetime, has already been derived as

$$\mathscr{K}_0 = \frac{3}{r}. \tag{4.1.18}$$

The volume element is

$$N\sqrt{\sigma} = \sqrt{f(r)}\; r^3\sin^2\theta_1\sin\theta_2, \tag{D.2.5}$$

then, substituting (D.2.4), (4.1.18) and (D.2.5) into (D.2.3), we obtain the Euclidean action as follows

$$\begin{aligned} I_{\mathscr{V}-\mathscr{B}} &= \frac{2\pi R}{8\pi G_5}\left\{\lim_{r_s\to\sqrt{\alpha}}\oint_{S_{\phi r_s}}\left(\frac{3\sqrt{f(r)}}{r} - \frac{3}{r}\right)\sqrt{f(r)}\; r^3\sin^2\theta_1\sin\theta_2 d^3\theta \right. \\ &\qquad \left. - \lim_{r_\infty\to\infty}\oint_{S_{\phi r_\infty}}\left(\frac{3\sqrt{f(r)}}{r} - \frac{3}{r}\right)\sqrt{f(r)}\; r^3\sin^2\theta_1\sin\theta_2 d^3\theta\right\} \\ &= \frac{3\cdot 2\pi^2}{8\pi G_4}\left\{\lim_{r_s\to\sqrt{\alpha}}\left(f(r) - \sqrt{f(r)}\right)r^2 - \lim_{r_\infty\to\infty}\left(f(r) - \sqrt{f(r)}\right)r^2\right\} \\ &= \frac{3\pi\alpha}{8G_4}. \end{aligned} \tag{D.2.6}$$

[1] See also section 4.2.5 for related discussions.

(D.2.6) successfully coincides with (4.2.15), which we derived by definition.

In the above calculation, the boundary integral yields a finite value, which seems to differ from the result in [48]. This apparent discrepancy arises from the fact that their analysis was based on a compact spacetime (de Sitter-Schwarzschild spacetime), whereas we considered a noncompact spacetime with an asymptotic boundary at spatial infinity. Consequently, Our results do not contradict their discussion.

Bibliography

[1] S. Tsukahara, *Life-time of metastable vacuum in string theory and trans-Planckian censorship conjecture*, *JHEP* **10** (2023) 109 [arXiv:2305.00781].

[2] Y. Ookouchi, R. Sato and S. Tsukahara, *Decay of Kaluza-Klein Vacuum via Singular Instanton*, arXiv:2404.13917.

[3] S. Tsukahara, *On Stabilization of Magnetically Charged Brane Shell and Over-extremality*, arXiv:2408.08798.

[4] ATLAS collaboration, *Observation of a new particle in the search for the Standard Model Higgs boson with the ATLAS detector at the LHC*, *Phys. Lett. B* **716** (2012) 1 [arXiv:1207.7214].

[5] CMS collaboration, *Observation of a New Boson at a Mass of 125 GeV with the CMS Experiment at the LHC*, *Phys. Lett. B* **716** (2012) 30 [arXiv:1207.7235].

[6] A.A. Starobinsky, *A New Type of Isotropic Cosmological Models Without Singularity*, *Phys. Lett. B* **91** (1980) 99.

[7] K. Sato, *First Order Phase Transition of a Vacuum and Expansion of the Universe*, *Mon. Not. Roy. Astron. Soc.* **195** (1981) 467.

[8] D. Kazanas, *Dynamics of the Universe and Spontaneous Symmetry Breaking*, *Astrophys. J. Lett.* **241** (1980) L59.

[9] A.H. Guth, *The Inflationary Universe: A Possible Solution to the Horizon and Flatness Problems*, *Phys. Rev. D* **23** (1981) 347.

[10] Planck collaboration, *Planck 2018 results. VI. Cosmological parameters*, *Astron. Astrophys.* **641** (2020) A6 [arXiv:1807.06209].

[11] A.D. Linde, *A New Inflationary Universe Scenario: A Possible Solution of the Horizon, Flatness, Homogeneity, Isotropy and Primordial Monopole Problems*, *Phys. Lett. B* **108** (1982) 389.

[12] A.D. Linde, *Chaotic Inflation*, *Phys. Lett. B* **129** (1983) 177.

[13] A. Albrecht and P.J. Steinhardt, *Cosmology for Grand Unified Theories with Radiatively Induced Symmetry Breaking*, *Phys. Rev. Lett.* **48** (1982) 1220.

[14] K. Freese, J.A. Frieman and A.V. Olinto, *Natural inflation with pseudo - Nambu-Goldstone bosons*, *Phys. Rev. Lett.* **65** (1990) 3233.

[15] A.D. Linde, *Hybrid inflation*, *Phys. Rev. D* **49** (1994) 748 [arXiv:astro-ph/9307002].

[16] D. Polarski and A.A. Starobinsky, *Spectra of perturbations produced by double inflation with an intermediate matter dominated stage*, *Nucl. Phys. B* **385** (1992) 623.

[17] E. Silverstein and D. Tong, *Scalar speed limits and cosmology: Acceleration from D-cceleration*, *Phys. Rev. D* **70** (2004) 103505 [arXiv:hep-th/0310221].

[18] J.B. Hartle and S.W. Hawking, *Wave Function of the Universe*, *Phys. Rev. D* **28** (1983) 2960.

[19] A. Vilenkin, *Creation of Universes from Nothing*, *Phys. Lett. B* **117** (1982) 25.

[20] T. Yoneya, *Connection of Dual Models to Electrodynamics and Gravidynamics*, *Prog. Theor. Phys.* **51** (1974) 1907.

[21] J. Scherk and J.H. Schwarz, *Dual Models for Nonhadrons*, *Nucl. Phys. B* **81** (1974) 118.

[22] G. Degrassi, S. Di Vita, J. Elias-Miro, J.R. Espinosa, G.F. Giudice, G. Isidori et al., *Higgs mass and vacuum stability in the Standard Model at NNLO*, *JHEP* **08** (2012) 098 [arXiv:1205.6497].

[23] S. Alekhin, A. Djouadi and S. Moch, *The top quark and Higgs boson masses and the stability of the electroweak vacuum*, *Phys. Lett. B* **716** (2012) 214 [arXiv:1207.0980].

[24] G. Isidori, G. Ridolfi and A. Strumia, *On the metastability of the standard model vacuum*, *Nucl. Phys. B* **609** (2001) 387 [arXiv:hep-ph/0104016].

[25] A. Andreassen, W. Frost and M.D. Schwartz, *Scale Invariant Instantons and the Complete Lifetime of the Standard Model*, *Phys. Rev. D* **97** (2018) 056006 [arXiv:1707.08124].

[26] S. Chigusa, T. Moroi and Y. Shoji, *State-of-the-Art Calculation of the Decay Rate of Electroweak Vacuum in the Standard Model*, *Phys. Rev. Lett.* **119** (2017) 211801 [arXiv:1707.09301].

[27] S. Chigusa, T. Moroi and Y. Shoji, *Decay Rate of Electroweak Vacuum in the Standard Model and Beyond*, *Phys. Rev. D* **97** (2018) 116012 [arXiv:1803.03902].

[28] P. Baratella, M. Nemevšek, Y. Shoji, K. Trailović and L. Ubaldi, *Revising the full one-loop gauge prefactor in electroweak vacuum stability*, arXiv:2406.05180.

[29] W. Lerche, D. Lust and A.N. Schellekens, *Chiral Four-Dimensional Heterotic Strings from Selfdual Lattices*, *Nucl. Phys. B* **287** (1987) 477.

[30] L. Susskind, *The Anthropic landscape of string theory*, arXiv:hep-th/0302219.

[31] S. Ashok and M.R. Douglas, *Counting flux vacua*, *JHEP* **01** (2004) 060 [arXiv:hep-th/0307049].

[32] J.D. Brown and C. Teitelboim, *Dynamical Neutralization of the Cosmological Constant*, *Phys. Lett. B* **195** (1987) 177.

[33] F.F. Gautason, B. Truijen and T. Van Riet, *The many faces of brane-flux annihilation*, *JHEP* **10** (2015) 152 [arXiv:1505.00159].

[34] E. Witten, *Instability of the Kaluza-Klein Vacuum*, *Nucl. Phys. B* **195** (1982) 481.

[35] P.J. Steinhardt, *Monopole and Vortex Dissociation and Decay of the False Vacuum*, *Nucl. Phys. B* **190** (1981) 583.

[36] P.J. Steinhardt, *Monopole Dissociation in the Early Universe*, *Phys. Rev. D* **24** (1981) 842.

[37] Y. Hosotani, *Impurities in the Early Universe*, *Phys. Rev. D* **27** (1983) 789.

[38] U.A. Yajnik, *PHASE TRANSITION INDUCED BY COSMIC STRINGS*, *Phys. Rev. D* **34** (1986) 1237.

[39] B. Kumar, M.B. Paranjape and U.A. Yajnik, *Fate of the false monopoles: Induced vacuum decay*, *Phys. Rev. D* **82** (2010) 025022 [arXiv:1006.0693].

[40] B.-H. Lee, W. Lee, R. MacKenzie, M.B. Paranjape, U.A. Yajnik and D.-h. Yeom, *Tunneling decay of false vortices*, *Phys. Rev. D* **88** (2013) 085031 [arXiv:1308.3501].

[41] E. Dupuis, Y. Gobeil, R. MacKenzie, L. Marleau, M.B. Paranjape and Y. Ung, *Tunneling decay of false kinks*, *Phys. Rev. D* **92** (2015) 025031 [arXiv:1506.05091].

[42] M. Haberichter, R. MacKenzie, M.B. Paranjape and Y. Ung, *Tunneling decay of false domain walls: the silence of the lambs*, *J. Math. Phys.* **57** (2016) 042303 [arXiv:1506.05838].

[43] E. Dupuis, Y. Gobeil, B.-H. Lee, W. Lee, R. MacKenzie, M.B. Paranjape et al., *Tunneling decay of false vortices with gravitation*, *JHEP* **11** (2017) 028 [arXiv:1709.03839].

[44] E. Dupuis, M. Haberichter, R. MacKenzie, M.B. Paranjape and U.A. Yajnik, *Vacuum Decay Induced by False Skyrmions*, *Phys. Rev. D* **99** (2019) 016016 [arXiv:1805.08038].

[45] N. Oshita, M. Yamada and M. Yamaguchi, *Compact objects as the catalysts for vacuum decays*, *Phys. Lett. B* **791** (2019) 149 [arXiv:1808.01382].

[46] M. Caneletti and I.G. Moss, *Seeding the decay of the false vacuum*, *Phys. Rev. D* **110** (2024) 105015 [arXiv:2408.12229].

[47] W.A. Hiscock, *CAN BLACK HOLES NUCLEATE VACUUM PHASE TRANSITIONS?*, *Phys. Rev. D* **35** (1987) 1161.

[48] R. Gregory, I.G. Moss and B. Withers, *Black holes as bubble nucleation sites*, *JHEP* **03** (2014) 081 [arXiv:1401.0017].

[49] P. Burda, R. Gregory and I. Moss, *Vacuum metastability with black holes*, *JHEP* **08** (2015) 114 [arXiv:1503.07331].

[50] P. Burda, R. Gregory and I. Moss, *Gravity and the stability of the Higgs vacuum*, *Phys. Rev. Lett.* **115** (2015) 071303 [arXiv:1501.04937].

[51] P. Burda, R. Gregory and I. Moss, *The fate of the Higgs vacuum*, *JHEP* **06** (2016) 025 [arXiv:1601.02152].

[52] C. Vafa, *The String landscape and the swampland*, arXiv:hep-th/0509212.

[53] H. Ooguri and C. Vafa, *On the Geometry of the String Landscape and the Swampland*, *Nucl. Phys. B* **766** (2007) 21 [arXiv:hep-th/0605264].

[54] H. Ooguri and C. Vafa, *Non-supersymmetric AdS and the Swampland*, *Adv. Theor. Math. Phys.* **21** (2017) 1787 [arXiv:1610.01533].

[55] G. Obied, H. Ooguri, L. Spodyneiko and C. Vafa, *De Sitter Space and the Swampland*, arXiv:1806.08362.

[56] S.K. Garg and C. Krishnan, *Bounds on Slow Roll and the de Sitter Swampland*, *JHEP* **11** (2019) 075 [arXiv:1807.05193].

[57] H. Ooguri, E. Palti, G. Shiu and C. Vafa, *Distance and de Sitter Conjectures on the Swampland*, *Phys. Lett. B* **788** (2019) 180 [arXiv:1810.05506].

[58] D. Lüst, E. Palti and C. Vafa, *AdS and the Swampland*, *Phys. Lett. B* **797** (2019) 134867 [arXiv:1906.05225].

[59] E. Palti, *The Swampland: Introduction and Review*, *Fortsch. Phys.* **67** (2019) 1900037 [arXiv:1903.06239].

[60] T.D. Brennan, F. Carta and C. Vafa, *The String Landscape, the Swampland, and the Missing Corner*, *PoS* **TASI2017** (2017) 015 [arXiv:1711.00864].

[61] U.H. Danielsson and T. Van Riet, *What if string theory has no de Sitter vacua?*, *Int. J. Mod. Phys. D* **27** (2018) 1830007 [arXiv:1804.01120].

[62] Y. Akrami, R. Kallosh, A. Linde and V. Vardanyan, *The Landscape, the Swampland and the Era of Precision Cosmology*, *Fortsch. Phys.* **67** (2019) 1800075 [arXiv:1808.09440].

[63] M. Graña and A. Herráez, *The Swampland Conjectures: A Bridge from Quantum Gravity to Particle Physics*, *Universe* **7** (2021) 273 [arXiv:2107.00087].

[64] M. van Beest, J. Calderón-Infante, D. Mirfendereski and I. Valenzuela, *Lectures on the Swampland Program in String Compactifications*, *Phys. Rept.* **989** (2022) 1 [arXiv:2102.01111].

[65] D. Harlow and H. Ooguri, *Constraints on Symmetries from Holography*, *Phys. Rev. Lett.* **122** (2019) 191601 [arXiv:1810.05337].

[66] H. Ooguri and Y. Wang, *Universal Bounds on CFT Distance Conjecture*, arXiv:2405.00674.

[67] A. Bedroya and C. Vafa, *Trans-Planckian Censorship and the Swampland*, *JHEP* **09** (2020) 123 [arXiv:1909.11063].

[68] A. Bedroya, R. Brandenberger, M. Loverde and C. Vafa, *Trans-Planckian Censorship and Inflationary Cosmology*, *Phys. Rev. D* **101** (2020) 103502 [arXiv:1909.11106].

[69] R. Brandenberger, *Trans-Planckian Censorship Conjecture and Early Universe Cosmology*, *LHEP* **2021** (2021) 198 [arXiv:2102.09641].

[70] G. Aldazabal, L.E. Ibanez, F. Quevedo and A.M. Uranga, *D-branes at singularities: A Bottom up approach to the string embedding of the standard model*, *JHEP* **08** (2000) 002 [arXiv:hep-th/0005067].

[71] G. Aldazabal, S. Franco, L.E. Ibanez, R. Rabadan and A.M. Uranga, *Intersecting brane worlds*, *JHEP* **02** (2001) 047 [arXiv:hep-ph/0011132].

[72] G. Aldazabal, S. Franco, L.E. Ibanez, R. Rabadan and A.M. Uranga, *$D = 4$ chiral string compactifications from intersecting branes*, *J. Math. Phys.* **42** (2001) 3103 [arXiv:hep-th/0011073].

[73] M. Cvetic, G. Shiu and A.M. Uranga, *Chiral four-dimensional N=1 supersymmetric type 2A orientifolds from intersecting D6 branes*, *Nucl. Phys. B* **615** (2001) 3 [arXiv:hep-th/0107166].

[74] M. Cvetic, G. Shiu and A.M. Uranga, *Three family supersymmetric standard - like models from intersecting brane worlds*, *Phys. Rev. Lett.* **87** (2001) 201801 [arXiv:hep-th/0107143].

[75] G.R. Dvali and S.H.H. Tye, *Brane inflation*, *Phys. Lett. B* **450** (1999) 72 [arXiv:hep-ph/9812483].

[76] C.P. Burgess, M. Majumdar, D. Nolte, F. Quevedo, G. Rajesh and R.-J. Zhang, *The Inflationary brane anti-brane universe*, *JHEP* **07** (2001) 047 [arXiv:hep-th/0105204].

[77] G.R. Dvali, Q. Shafi and S. Solganik, *D-brane inflation*, in *4th European Meeting From the Planck Scale to the Electroweak Scale*, 5, 2001 [arXiv:hep-th/0105203].

[78] G. Shiu and S.H.H. Tye, *Some aspects of brane inflation*, *Phys. Lett. B* **516** (2001) 421 [arXiv:hep-th/0106274].

[79] B. Kyae and Q. Shafi, *Branes and inflationary cosmology*, *Phys. Lett. B* **526** (2002) 379 [arXiv:hep-ph/0111101].

[80] L.E. Ibanez and A.M. Uranga, *String theory and particle physics: An introduction to string phenomenology*, Cambridge University Press (2, 2012).

[81] F. Quevedo, *Lectures on string/brane cosmology*, *Class. Quant. Grav.* **19** (2002) 5721 [arXiv:hep-th/0210292].

[82] R. Blumenhagen, M. Cvetic, P. Langacker and G. Shiu, *Toward realistic intersecting D-brane models*, *Ann. Rev. Nucl. Part. Sci.* **55** (2005) 71 [arXiv:hep-th/0502005].

[83] R. Blumenhagen, B. Kors, D. Lust and S. Stieberger, *Four-dimensional String Compactifications with D-Branes, Orientifolds and Fluxes*, *Phys. Rept.* **445** (2007) 1 [arXiv:hep-th/0610327].

[84] J. Polchinski, *String theory. Vol. 1: An introduction to the bosonic string*, Cambridge Monographs on Mathematical Physics, Cambridge University Press (12, 2007), 10.1017/CBO9780511816079.

[85] J. Polchinski, *String theory. Vol. 2: Superstring theory and beyond*, Cambridge Monographs on Mathematical Physics, Cambridge University Press (12, 2007), 10.1017/CBO9780511618123.

[86] B. Zwiebach, *A first course in string theory*, Cambridge University Press (7, 2006).

[87] A. Sen, *Tachyon condensation on the brane anti-brane system*, *JHEP* **08** (1998) 012 [arXiv:hep-th/9805170].

[88] A. Kasai and Y. Ookouchi, *Decay of False Vacuum via Fuzzy Monopole in String Theory*, *Phys. Rev. D* **91** (2015) 126002 [arXiv:1502.01544].

[89] A. Kasai, Y. Nakai and Y. Ookouchi, *Baryon as Impurity for Phase Transition in String Landscape*, *JHEP* **06** (2016) 029 [arXiv:1508.04608].

[90] Y. Nakai, Y. Ookouchi and N. Tanahashi, *Dyonic catalysis in the Kachru-Pearson-Verlinde vacuum decay*, *Phys. Rev. D* **100** (2019) 086013 [arXiv:1808.10235].

[91] F. Cachazo, K.A. Intriligator and C. Vafa, *A Large N duality via a geometric transition*, *Nucl. Phys. B* **603** (2001) 3 [arXiv:hep-th/0103067].

[92] C. Vafa, *Superstrings and topological strings at large N*, *J. Math. Phys.* **42** (2001) 2798 [arXiv:hep-th/0008142].

[93] M. Aganagic, C. Beem, J. Seo and C. Vafa, *Geometrically Induced Metastability and Holography*, *Nucl. Phys. B* **789** (2008) 382 [arXiv:hep-th/0610249].

[94] S.W. Hawking and N. Turok, *Open inflation without false vacua*, *Phys. Lett. B* **425** (1998) 25 [arXiv:hep-th/9802030].

[95] N. Turok and S.W. Hawking, *Open inflation, the four form and the cosmological constant*, *Phys. Lett. B* **432** (1998) 271 [arXiv:hep-th/9803156].

[96] W.G. Unruh, *On the Hawking - Turok solution to the open universe wave function*, arXiv:gr-qc/9803050.

[97] A. Vilenkin, *Singular instantons and creation of open universes*, *Phys. Rev. D* **57** (1998) 7069 [arXiv:hep-th/9803084].

[98] J. Garriga, *Open inflation and the singular boundary*, *Phys. Rev. D* **61** (2000) 047301 [arXiv:hep-th/9803210].

[99] J. Garriga, *Smooth 'creation' of an open universe in five-dimensions*, arXiv:hep-th/9804106.

[100] J. Garriga, X. Montes, M. Sasaki and T. Tanaka, *Spectrum of cosmological perturbations in the one bubble open universe*, *Nucl. Phys. B* **551** (1999) 317 [arXiv:astro-ph/9811257].

[101] M. Hashimoto, *Action of singular instantons of Hawking-Turok type*, *Phys. Rev. D* **63** (2001) 043510 [arXiv:hep-th/0005102].

[102] D.V. Fursaev and S.N. Solodukhin, *On the description of the Riemannian geometry in the presence of conical defects*, *Phys. Rev. D* **52** (1995) 2133 [arXiv:hep-th/9501127].

[103] S.R. Coleman, *The Fate of the False Vacuum. 1. Semiclassical Theory*, *Phys. Rev. D* **15** (1977) 2929.

[104] C.G. Callan, Jr. and S.R. Coleman, *The Fate of the False Vacuum. 2. First Quantum Corrections*, *Phys. Rev. D* **16** (1977) 1762.

[105] E.J. Weinberg, *Classical solutions in quantum field theory: Solitons and Instantons in High Energy Physics*, Cambridge Monographs on Mathematical Physics, Cambridge University Press (9, 2012), 10.1017/CBO9781139017787.

[106] M. Mariño, *Instantons and Large N: An Introduction to Non-Perturbative Methods in Quantum Field Theory*, Cambridge University Press (9, 2015).

[107] M. Paranjape, *The Theory and Applications of Instanton Calculations*, Oxford University Press (2018), 10.1017/9781009291248.

[108] F. Devoto, S. Devoto, L. Di Luzio and G. Ridolfi, *False vacuum decay: an introductory review*, *J. Phys. G* **49** (2022) 103001 [arXiv:2205.03140].

[109] L.D. Landau and E.M. Lifshitz, *Quantum mechanics: non-relativistic theory*, vol. 3, Elsevier (2013).

[110] K. Konishi and G. Paffuti, *Quantum mechanics: a new introduction*, OUP Oxford (2009).

[111] I.M. Gelfand and A.M. Yaglom, *Integration in functional spaces and it applications in quantum physics*, *J. Math. Phys.* **1** (1960) 48.

[112] L. Takhtadzh k an, *Quantum Mechanics for Mathematicians*, Graduate Studies in Mathematics, American Mathematical Society (2008).

[113] S.W. Hawking, *Zeta Function Regularization of Path Integrals in Curved Space-Time*, *Commun. Math. Phys.* **55** (1977) 133.

[114] A. Voros, *Spectral functions, special functions and the selberg zeta function*, *Communications in Mathematical Physics* **110** (1987) 439.

[115] J. Martin and R.H. Brandenberger, *The TransPlanckian problem of inflationary cosmology*, *Phys. Rev. D* **63** (2001) 123501 [arXiv:hep-th/0005209].

[116] J.M. Maldacena and C. Nunez, *Supergravity description of field theories on curved manifolds and a no go theorem*, *Int. J. Mod. Phys. A* **16** (2001) 822 [arXiv:hep-th/0007018].

[117] R.G. Leigh, *Dirac-Born-Infeld Action from Dirichlet Sigma Model*, *Mod. Phys. Lett. A* **4** (1989) 2767.

[118] K. Kirsten and A.J. McKane, *Functional determinants by contour integration methods*, *Annals Phys.* **308** (2003) 502 [arXiv:math-ph/0305010].

[119] K. Kirsten and A.J. McKane, *Functional determinants for general Sturm-Liouville problems*, *J. Phys. A* **37** (2004) 4649 [arXiv:math-ph/0403050].

[120] G. Fucci, F. Gesztesy, K. Kirsten and J. Stanfill, *Spectral zeta-Functions and zeta-Regularized Functional Determinants for Regular Sturm-Liouville Operators*, *Res. Math. Sci.* **8** (2021) 46 [arXiv:2101.12295].

[121] H. Kleinert and I. Mustapic, *Decay rates of metastable states in cubic potential by variational perturbation theory*, *Int. J. Mod. Phys. A* **11** (1996) 4383 [arXiv:quant-ph/9502027].

[122] F.J. Dyson, *Divergence of perturbation theory in quantum electrodynamics*, *Phys. Rev.* **85** (1952) 631.

[123] C.M. Bender and T.T. Wu, *Anharmonic oscillator*, *Phys. Rev.* **184** (1969) 1231.

[124] C.M. Bender and T.T. Wu, *Anharmonic oscillator. 2: A Study of perturbation theory in large order*, *Phys. Rev. D* **7** (1973) 1620.

[125] H. Kleinert, *Variational approach to tunneling. Beyond the semiclassical approximation of Langer and Lipatov: Perturbation coefficients to all orders*, *Phys. Lett. B* **300** (1993) 261.

[126] H. Kleinert, *Path integrals in quantum mechanics, statistics, polymer physics, and financial markets*, World scientific (2009).

[127] F.R. Tangherlini, *Schwarzschild field in n dimensions and the dimensionality of space problem*, *Nuovo Cim.* **27** (1963) 636.

[128] J.W. York, Jr., *Role of conformal three geometry in the dynamics of gravitation*, *Phys. Rev. Lett.* **28** (1972) 1082.

[129] G.W. Gibbons and S.W. Hawking, *Action Integrals and Partition Functions in Quantum Gravity*, *Phys. Rev. D* **15** (1977) 2752.

[130] F. Dowker, J.P. Gauntlett, G.W. Gibbons and G.T. Horowitz, *The Decay of magnetic fields in Kaluza-Klein theory*, *Phys. Rev. D* **52** (1995) 6929 [arXiv:hep-th/9507143].

[131] A.R. Brown, *Decay of hot Kaluza-Klein space*, *Phys. Rev. D* **90** (2014) 104017 [arXiv:1408.5903].

[132] W.A. Hiscock, *Exact Gravitational Field of a String*, *Phys. Rev. D* **31** (1985) 3288.

[133] J.R. Gott, III, *Gravitational lensing effects of vacuum strings: Exact solutions*, *Astrophys. J.* **288** (1985) 422.

[134] A. Adams, J. Polchinski and E. Silverstein, *Don't panic! Closed string tachyons in ALE space-times*, *JHEP* **10** (2001) 029 [arXiv:hep-th/0108075].

[135] N. Oshita and J. Yokoyama, *Creation of an inflationary universe out of a black hole*, *Phys. Lett. B* **785** (2018) 197 [arXiv:1601.03929].

[136] R. Gregory, I.G. Moss, N. Oshita and S. Patrick, *Hawking-Moss transition with a black hole seed*, *JHEP* **09** (2020) 135 [arXiv:2007.11428].

[137] J.W. York, Jr., *Black hole thermodynamics and the Euclidean Einstein action*, *Phys. Rev. D* **33** (1986) 2092.

[138] H.W. Braden, J.D. Brown, B.F. Whiting and J.W. York, Jr., *Charged black hole in a grand canonical ensemble*, *Phys. Rev. D* **42** (1990) 3376.

[139] F. Dowker, J.P. Gauntlett, G.W. Gibbons and G.T. Horowitz, *Nucleation of p-branes and fundamental strings*, *Phys. Rev. D* **53** (1996) 7115 [arXiv:hep-th/9512154].

[140] L.D. Landau and E.M. Lifshitz, *Statistical Physics, Part 1*, vol. 5 of *Course of Theoretical Physics*, Butterworth-Heinemann, Oxford (1980).

[141] S.W. Hawking and G.T. Horowitz, *The Gravitational Hamiltonian, action, entropy and surface terms*, *Class. Quant. Grav.* **13** (1996) 1487 [arXiv:gr-qc/9501014].

[142] J.D. Bekenstein, *Black holes and entropy*, *Phys. Rev. D* **7** (1973) 2333.

[143] J.D. Bekenstein, *Generalized second law of thermodynamics in black hole physics*, *Phys. Rev. D* **9** (1974) 3292.

[144] S.W. Hawking, *Particle Creation by Black Holes*, *Commun. Math. Phys.* **43** (1975) 199.

[145] R.M. Wald, *The thermodynamics of black holes*, *Living Rev. Rel.* **4** (2001) 6 [arXiv:gr-qc/9912119].

[146] J.D. Brown and J.W. York, Jr., *The Microcanonical functional integral. 1. The Gravitational field*, *Phys. Rev. D* **47** (1993) 1420 [arXiv:gr-qc/9209014].

[147] J.D. Brown and J.W. York, Jr., *Quasilocal energy and conserved charges derived from the gravitational action*, *Phys. Rev. D* **47** (1993) 1407 [arXiv:gr-qc/9209012].

[148] G.T. Horowitz, J. Orgera and J. Polchinski, *Nonperturbative Instability of AdS(5) x S**5/Z(k)*, *Phys. Rev. D* **77** (2008) 024004 [arXiv:0709.4262].

[149] H. Ooguri and L. Spodyneiko, *New Kaluza-Klein instantons and the decay of AdS vacua*, *Phys. Rev. D* **96** (2017) 026016 [arXiv:1703.03105].

[150] J.J. Blanco-Pillado, J.R. Espinosa, J. Huertas and K. Sousa, *Bubbles of nothing: the tunneling potential approach*, *JCAP* **03** (2024) 029 [arXiv:2312.00133].

[151] B. Friedrich, A. Hebecker and J. Walcher, *Cobordism and bubbles of anything in the string landscape*, *JHEP* **02** (2024) 127 [arXiv:2310.06021].

[152] J. McNamara and C. Vafa, *Cobordism Classes and the Swampland*, arXiv:1909.10355.

[153] R. Blumenhagen, C. Kneissl and C. Wang, *Dynamical Cobordism Conjecture: solutions for end-of-the-world branes*, *JHEP* **05** (2023) 123 [arXiv:2303.03423].

[154] R. Angius, A. Makridou and A.M. Uranga, *Intersecting end of the world branes*, *JHEP* **03** (2024) 110 [arXiv:2312.16286].

[155] S. Sugimoto and Y.-k. Suzuki, *End of the world branes from dimensional reduction*, *JHEP* **03** (2024) 165 [arXiv:2312.07891].

[156] M. Delgado, *The bubble of nothing under T-duality*, *JHEP* **05** (2024) 333 [arXiv:2312.09291].

[157] T. Higaki, K. Kamada and K. Nishimura, *Formation of a chiral soliton lattice*, *Phys. Rev. D* **106** (2022) 096022 [arXiv:2207.00212].

[158] M. Eto and M. Nitta, *Quantum nucleation of topological solitons*, *JHEP* **09** (2022) 077 [arXiv:2207.00211].

[159] H. Lee and E.J. Weinberg, *Negative modes of Coleman-De Luccia bounces*, *Phys. Rev. D* **90** (2014) 124002 [arXiv:1408.6547].

[160] R. Gregory, K.M. Marshall, F. Michel and I.G. Moss, *Negative modes of Coleman–De Luccia and black hole bubbles*, *Phys. Rev. D* **98** (2018) 085017 [arXiv:1808.02305].

[161] N. Arkani-Hamed, L. Motl, A. Nicolis and C. Vafa, *The String landscape, black holes and gravity as the weakest force*, *JHEP* **06** (2007) 060 [arXiv:hep-th/0601001].

[162] E. Palti, *A Brief Introduction to the Weak Gravity Conjecture*, *LHEP* **2020** (2020) 176.

[163] D. Harlow, B. Heidenreich, M. Reece and T. Rudelius, *Weak gravity conjecture*, *Rev. Mod. Phys.* **95** (2023) 035003 [arXiv:2201.08380].

[164] M. Natsuume, *Higher order correction to the GHS string black hole*, *Phys. Rev. D* **50** (1994) 3949 [arXiv:hep-th/9406079].

[165] Y. Kats, L. Motl and M. Padi, *Higher-order corrections to mass-charge relation of extremal black holes*, *JHEP* **12** (2007) 068 [arXiv:hep-th/0606100].

[166] C. Cheung, J. Liu and G.N. Remmen, *Proof of the Weak Gravity Conjecture from Black Hole Entropy*, *JHEP* **10** (2018) 004 [arXiv:1801.08546].

[167] Y. Hamada, T. Noumi and G. Shiu, *Weak Gravity Conjecture from Unitarity and Causality*, *Phys. Rev. Lett.* **123** (2019) 051601 [arXiv:1810.03637].

[168] B. Bellazzini, M. Lewandowski and J. Serra, *Positivity of Amplitudes, Weak Gravity Conjecture, and Modified Gravity*, *Phys. Rev. Lett.* **123** (2019) 251103 [arXiv:1902.03250].

[169] A.M. Charles, *The Weak Gravity Conjecture, RG Flows, and Supersymmetry*, arXiv:1906.07734.

[170] C.R.T. Jones and B. McPeak, *The Black Hole Weak Gravity Conjecture with Multiple Charges*, *JHEP* **06** (2020) 140 [arXiv:1908.10452].

[171] G.J. Loges, T. Noumi and G. Shiu, *Thermodynamics of 4D Dilatonic Black Holes and the Weak Gravity Conjecture*, *Phys. Rev. D* **102** (2020) 046010 [arXiv:1909.01352].

[172] G. Goon and R. Penco, *Universal Relation between Corrections to Entropy and Extremality*, *Phys. Rev. Lett.* **124** (2020) 101103 [arXiv:1909.05254].

[173] P.A. Cano, T. Ortín and P.F. Ramirez, *On the extremality bound of stringy black holes*, *JHEP* **02** (2020) 175 [arXiv:1909.08530].

[174] P.A. Cano, S. Chimento, R. Linares, T. Ortín and P.F. Ramírez, α' *corrections of Reissner-Nordström black holes*, *JHEP* **02** (2020) 031 [arXiv:1910.14324].

[175] S. Cremonini, C.R.T. Jones, J.T. Liu and B. McPeak, *Higher-Derivative Corrections to Entropy and the Weak Gravity Conjecture in Anti-de Sitter Space*, *JHEP* **09** (2020) 003 [arXiv:1912.11161].

[176] Q. Chen, W. Hong and J. Tao, *Universal thermodynamic extremality relations for charged AdS black hole surrounded by quintessence*, arXiv:2005.00747.

[177] G.J. Loges, T. Noumi and G. Shiu, *Duality and Supersymmetry Constraints on the Weak Gravity Conjecture*, *JHEP* **11** (2020) 008 [arXiv:2006.06696].

[178] N. Bobev, A.M. Charles, K. Hristov and V. Reys, *Higher-derivative supergravity, AdS_4 holography, and black holes*, *JHEP* **08** (2021) 173 [arXiv:2106.04581].

[179] N. Arkani-Hamed, Y.-t. Huang, J.-Y. Liu and G.N. Remmen, *Causality, unitarity, and the weak gravity conjecture*, *JHEP* **03** (2022) 083 [arXiv:2109.13937].

[180] L. Ma, Y. Pang and H. Lü, *α'-corrections to near extremal dyonic strings and weak gravity conjecture*, *JHEP* **01** (2022) 157 [arXiv:2110.03129].

[181] S. Cremonini, C.R.T. Jones, J.T. Liu, B. McPeak and Y. Tang, *Repulsive black holes and higher-derivatives*, *JHEP* **03** (2022) 013 [arXiv:2110.10178].

[182] L. Aalsma, *Corrections to extremal black holes from Iyer-Wald formalism*, *Phys. Rev. D* **105** (2022) 066022 [arXiv:2111.04201].

[183] T. Noumi and H. Satake, *Higher derivative corrections to black brane thermodynamics and the weak gravity conjecture*, *JHEP* **12** (2022) 130 [arXiv:2210.02894].

[184] Y. Abe, T. Noumi and K. Yoshimura, *Black hole extremality in nonlinear electrodynamics: a lesson for weak gravity and Festina Lente bounds*, *JHEP* **09** (2023) 024 [arXiv:2305.17062].

[185] U.H. Danielsson, G. Dibitetto and S. Giri, *Black holes as bubbles of AdS*, *JHEP* **10** (2017) 171 [arXiv:1705.10172].

[186] U. Danielsson, V. Van Hemelryck and T. Van Riet, *Over-extremal brane shells from string theory?*, *Class. Quant. Grav.* **39** (2022) 235001 [arXiv:2206.04506].

[187] W. Israel, *Singular hypersurfaces and thin shells in general relativity*, *Nuovo Cim. B* **44S10** (1966) 1.

[188] M. Born and L. Infeld, *Foundations of the new field theory*, *Proc. Roy. Soc. Lond. A* **144** (1934) 425.

[189] P.A.M. Dirac, *An Extensible model of the electron*, *Proc. Roy. Soc. Lond. A* **268** (1962) 57.

[190] K.A. Bronnikov, *Regular magnetic black holes and monopoles from nonlinear electrodynamics*, *Phys. Rev. D* **63** (2001) 044005 [arXiv:gr-qc/0006014].

[191] S.I. Kruglov, *Born–Infeld-type electrodynamics and magnetic black holes*, *Annals Phys.* **383** (2017) 550 [arXiv:1707.04495].

[192] R.M. Wald, *General Relativity*, Chicago Univ. Pr., Chicago, USA (1984), 10.7208/chicago/9780226870373.001.0001.

[193] E. Poisson, *A Relativist's Toolkit: The Mathematics of Black-Hole Mechanics*, Cambridge University Press (12, 2009), 10.1017/CBO9780511606601.

[194] F. Gesztesy and K. Kirsten, *Effective computation of traces, determinants, and ζ-functions for Sturm–Liouville operators*, *J. Funct. Anal.* **276** (2019) 520 [arXiv:1712.00928].

[195] M.A. Naimark, *Linear differential operators. Part I: Elementary theory of linear differential operators*, Frederick Ungar Publishing Company (1967).

[196] A. Zettl, *Sturm-liouville theory*, no. 121, American Mathematical Soc. (2012).